AN ABSTRACT OF THE DISSERTATION OF

Claire L. Phillips for the degree of Doctor of Philosophy in Forest Science presented on October 23, 2009
Title: Distinguishing Biological and Physical Controls on Soil Respiration

Abstract approved:

_____

Barbara J. Bond

Soil respiration, or the combined CO_2 emissions from roots and soil microorganisms, constitutes one of the largest losses of carbon (C) from terrestrial ecosystems. The major drivers of soil respiration, which include soil moisture, temperature, and substrate quality, have been known for some time. Nevertheless, correlations between these drivers and soil respiration vary substantially by site, and there is a lack of mechanistic principles that would allow prediction of soil respiration rates across sites and through time. Here I present three studies that attempted to characterize and differentiate biological and physical mechanisms controlling soil respiration. The purpose of the first study was to quantify the proportion of soil respiration derived from ectomycorrhizal (EcM) fungal mats, which can form dense aggregations of hyphae near the surface of forest soils. By comparing respiration rates on mats with neighboring non-mat soils, I estimated that approximately 10% of soil respiration was derived from EcM mats in an old-growth Douglas fir forest site. Seasonally, mat contributions correlated with soil moisture, which may be due to a physiological response of EcM fungi, but it also likely related to moisture impacts on

CO_2 flux contributions in deep soil below where EcM mats tend to colonize. In the second study I examined diel patterns of soil respiration, and used a gas diffusion model to develop a theoretical basis for why respiration is often lagged several hours from soil temperature. This study demonstrated that soil heat and gas transport can cause complex diel patterns in soil respiration, which must be accounted for to correctly interpret the impacts of temperature and other forcing factors on soil respiration. Finally, the third study examined the carbon isotopic composition of soil respiration ($\delta^{13}CO_2$), and whether $\delta^{13}CO_2$ is influenced by recent plant photosynthates, as has been suggested previously, or instead by microbial or gas-transport effects. I ruled out microbial effects as a possible influence on moisture-related $\delta^{13}CO_2$ dynamics, but showed that gas-transport likely influenced measurements of $\delta^{13}CO_2$ at high and low-moisture. Collectively, an important conclusion from these studies is that analysis of soil gradients, including gradients in environmental conditions, biological activity, and soil physical properties across the soil profile, helps to explain the dynamics of CO_2 fluxes from the soil surface. By examining respiration as a product of processes occurring across soil profiles, in contrast to treating soil as a flat surface or a homogenous medium, more mechanistic and universal relationships become apparent.

Distinguishing Biological and Physical Controls on Soil Respiration

by
Claire L. Phillips

A DISSERTATION

submitted to

Oregon State University

in partial fulfillment of
the requirements for the
degree of

Doctor of Philosophy

Presented October 23, 2009
Commencement June 2010

Doctor of Philosophy dissertation of Claire L. Phillips presented on October 23, 2009.

APPROVED:

Major Professor, representing Forest Science

Head of the Department of Forest Ecosystems and Society

Dean of the Graduate School

I understand that my dissertation will become part of the permanent collection of Oregon State University libraries. My signature below authorizes release of my thesis to any reader upon request.

Claire L. Phillips, Author

ACKNOWLEDGEMENTS

First and foremost, I thank my major professor, Barbara J. Bond for her unconditional support and confidence in me. The freedom she allowed me coupled with her faith in me has helped me to find my voice.

They say it takes a village to raise a child, and apparently it also takes a village to graduate a Ph.D. student. So many people have rallied to support me. I thank my committee members, Chris Anderson, Darius Adams, Dave Myrold, and Steve Perakis for their guidance, patience, and generosity in seeing me through this process. With great fondness I also thank my late committee member, Elizabeth Sulzman, who guided me towards the path of studying soil respiration.

To the many professors and other experts who made time for me, so much of my learning was through conversations with you. I thank the fungal experts: Dan Luoma, Efren Cezares, Jane Smith, Doni McKay, Paul Rygiewicz; the soil gurus: Kermit Cormack, Bruce Caldwell, Mark G. Johnson, Markus Kleber, James Irvine, and Jon Martin; and the isotope wizards: Alan Mix, Bill Rugh, and Renee Brooks.

A few people really helped when I hit road-blocks in my research. Both Jillian Gregg and Doni McKay stepped in with great ideas and access to equipment and other resources. Dave Risk and Nick Nickerson seemed to appear on a stairway from heaven at the 2007 AGU fall meeting. They understand the physical aspects of soil respiration better than anyone I know, and their angel dust glitters throughout the pages of this document.

I thank the members of the Bond Lab who showed me the way: Adam Kennedy, Holly Barnard, Zac Kayler, Mark Hauck, and Tom Pypker. A number of undergraduates assisted me and also became good friends, special thanks to Julie Pedersen, Michele Noble, Priscilla Woolverton, and Shane Easter. Many thanks to friends in the FES and CSS departments who made graduate school a wonderful experience. Special thanks to Laurel Kluber for helping to make the mycorrhizae project happen.

I thank all of my funders: the Richardson Family Fellowship, Elizabeth Sulzman's Airshed grant, Barb Bond's Spaniol Chair funds, the Dick and Doris Waring travel grant, the Northwest Scientific Association Graduate Research fellowship, the H&M Fowells fellowship, and the College of Forestry fellowship.

Finally, my father started this all when he said, "Of all my children, you will be a scholar one day." I thank my family for all their understanding and encouragement. Thank you to my husband, Chad Hanson, for everything you are and everything you do.

CONTRIBUTION OF AUTHORS

Chapter 2: Laurel Kluber assisted with experimental design and identification of mat taxa. Julia Pedersen assisted with data collection and analysis of CO_2 profiles. All authors provided comments to improve the manuscript.

Chapter 3: Nick Nickerson designed the basic model, taught me how to implement and validate it, and assisted with editing of the manuscript. Dave Risk and Barbara Bond assisted with editing of the manuscript.

Chapter 4: Nick Nickerson and Dave Risk assisted with the modeling components of the study. Zachary Kayler and Alan Mix assisted with experimental design and isotope analysis. Chris Andersen assisted with experimental design and provided access to the EPA ISIRF facility. Barbara Bond assisted with experimental design. All authors assisted with editing of the manuscript.

TABLE OF CONTENTS

Page

TABLE OF CONTENTS (Continued)

Page

TABLE OF CONTENTS (Continued)

Page

LIST OF FIGURES

LIST OF FIGURES (Continued)

Figure Page

LIST OF TABLES

DISTINGUISHING BIOLOGICAL AND PHYSICAL CONTROLS ON SOIL RESPIRATION

CHAPTER ONE: GENERAL INTRODUCTION

The study of soil respiration by many accounts has been fairly slow to advance. For example, respiration is widely represented using simple temperature relationships that have been modified little since the 1800s (Davidson *et al.*, 2006a). The basic drivers of soil respiration, including temperature, moisture, oxygen, and substrate supply, have been known for many decades (Hillel, 1998). Yet there are several indications that common ways of describing soil respiration are insufficient. Representing respiration as a function of moisture and temperature produces estimates of temperature and moisture sensitivity that vary greatly by site (Hibbard *et al.*, 2005), suggesting these are overly simplistic representations that miss important modulating variables. A recent comparison of the Biome-BGC model against ground measurements demonstrated substantial errors in its ability to predict soil respiration, which far exceeded errors for other components of the forest carbon cycle (Mitchell *et al.*, in press). Soil respiration patterns from different studies differ so widely that there is little consensus around the effects of major environmental variables, such as vegetation type, successional status, and site quality (Rustad *et al.*, 2001; Ryan & Law, 2005).

At the same time, because soil respiration is a large and variable CO_2 flux from terrestrial ecosystems, demand grows for better information and more universal predictive principles. On a global basis, soil respiration emits eight to ten times more CO_2 to the atmosphere than all fossil fuel emissions (Schlesinger & Andrews, 2000). Furthermore, in forest ecosystems, intersite and interannual comparisons indicate that

variability in respiration is a major determinant of forest carbon balance (Savage & Davidson, 2001; Valentini *et al.*, 2000). In many cases soil respiration is the largest pathway for respiratory losses from forests (Jassal *et al.*, 2007; Law *et al.*, 1999). Therefore, under changing climate regimes, the carbon storage capacity of ecosystems is likely to depend substantially on the response of soil respiration.

Part of the challenge in advancing more universal descriptions of soil respiration is that several different analysis approaches offer conclusions that are difficult to reconcile. For example, simple empirical models have been quite successful at describing temporal dynamics of respiration with few explanatory variables. Using multiple regression, most of the variability in soil respiration can be explained by temperature alone, and including soil moisture as an explanatory variable often accounts for much of the residual variability (Hibbard *et al.*, 2005; Martin & Bolstad, 2005) However, a number of other studies have also demonstrated close linkages between soil respiration and photosynthesis (Bahn *et al.*, 2009; Campbell *et al.*, 2004; Högberg *et al.*, 2001; Irvine *et al.*, 2008). These studies demonstrate the important role of canopy processes in addition to soil conditions, particularly for explaining autotrophic (root and rhizosphere) components of soil respiration. A third successful form of analysis has been a purely physics-based approach, describing soil surface fluxes with principles of gas diffusion, and more recently, advective processes. At the spatial scale of a single soil profile or pedon, fluxes modeled from physical processes have compared quite well

with soil surface flux measurements (Massman & Frank, 2006; Pumpanen *et al.*, 2003; Risk *et al.*, 2002; Tang *et al.*, 2003)

How is it possible that such disparate approaches to describing soil respiration have found strong evidence in their support? Part of the answer must be that multiple processes are correlated with each other. For example, temperature affects respiration rates both directly by impacting enzyme kinetics, and indirectly through influences on substrate supply, soil moisture, and rates of gas diffusion (Davidson *et al.*, 2006a). Empirical models demonstrate that temperature is important, but new work needs to address just *how* temperature and other environmental variables influence soil respiration.

The overarching goal of this dissertation was to tease apart some of the multiple influences that moisture and temperature can have on soil respiration. In particular, I was interested in separating soil physical and biological responses to these forcing factors. An approach I used throughout this dissertation was to analyze types of datasets that previously have been used to assess biological responses to temperature or moisture, and to consider how soil gas transport effects might alter those interpretations.

In Chapter Two, I examined how much a particular component of the soil biota contributes to forest soil respiration. Ectomycorrhizal (EcM) fungi, which form symbioses with plant roots, are thought to contribute a substantial proportion of forest soil respiration, but their intimate associations with roots generally make their contributions difficult to quantify *in situ*. Taking advantage of an EcM genus that forms

dense hyphal mats near the soil surface, I quantified EcM mat respiration by comparing surface flux rates from adjacent mat and non-mat soils. The patchy nature of EcM mats make them useful experimental subjects, but the fact that they only colonize near the soil surface potentially complicates interpretation of their contributions, because surface flux rates incorporate CO_2 produced throughout the soil profile. A component of this study examined whether moisture-related variation in EcM mat contributions was a physiological response of EcM fungi, or was instead due to physical effects of moisture, which impacts how easily CO_2 diffuses from deeper soils underlying EcM mats.

In Chapter Three, I examined whether diel oscillations in soil respiration are associated with physical transport processes or other biological or environmental influences. Many recent studies have found sinusoidal variations in soil respiration rates over the course of a day, but peak soil respiration rates are often offset by several hours from peak soil temperatures. Both biological and physical explanations have been suggested for these lags, and there is currently no consensus on their causes or how such data should be analyzed to interpret respiration temperature sensitivity. In this study I employed a one-dimensional soil CO_2 and heat transport model to demonstrate a theoretical basis for lags between surface flux and soil temperatures, and to examine the influence of soil properties and environment on lag times.

In Chapter Four, I examined moisture effects on the carbon isotopic composition of soil respiration ($\delta^{13}CO_2$), and tested whether moisture-related variation is due to changes in the $\delta^{13}C$ of newly-assimilated carbon, as has been previously suggested, or is

instead related 1) to gas-transport effects, or 2) to soil microbial responses to moisture. I performed greenhouse experiments to examine moisture effects on plant- and microbial-respired $\delta^{13}CO_2$, and modeled the experimental systems to examine potential gas-transport effects.

In Chapter Five, I offer some general conclusions on all three studies.

Bahn M, Schmitt M, Siegwolf R, Richter A, Brüggemann N (2009) Does photosynthesis affect grassland soil-respired CO_2 and its carbon isotope composition on a diurnal timescale? *New Phytologist,* **182**, 451-460.

Campbell JL, Sun OJ, Law BE (2004) Supply-Side Controls on Soil Respiration Among Oregon Forests *Global Change Biology,* **10**, 1857-1869.

Davidson EA, Janssens IA, Luo Y (2006) On the variability of respiration in terrestrial ecosystems: moving beyond Q_{10}. *Global Change Biology,* **12**, 154-164.

Hibbard KA, Law BE, Reichstein M, Sulzman J (2005) An analysis of soil respiration across northern hemisphere temperate ecosystems. *Biogeochemistry,* **73**, 29.

Hillel D (1998) *Environmental Soil Physics*, San Diego, Academic Press.

Högberg P, Nordgern A, Buchmann N *et al.* (2001) Large-scale forest girdling shows that current photosynthesis drives soil respiration. *Nature,* **411**, 789-792.

Irvine J, Law B, Martin J, Vickers D (2008) Interannual variation in soil CO_2 efflux and the response of root respiration to climate and canopy gas exchange in mature ponderosa pine. *Global Change Biology,* **14**, 2848-2859.

Jassal RS, Black TA, Cai T, Morgenstern K, Li Z, Gaumont-Guay D, Nesic Z (2007) Components of ecosystem respiration and an estimate of net primary productivity of an intermediate-aged Douglas-fir stand. *Agricultural and Forest Meteorology,* **144**, 44-57.

Law BE, Ryan MG, Anthoni PM (1999) Seasonal and annual respiration of a ponderosa pine ecosystem. *Global Change Biology,* **5**, 169-182.

Martin JG, Bolstad PV (2005) Annual soil respiration in broadleaf forests of northern Wisconsin: influence of moisture and site biological, chemical, and physical characteristics. *Biogeochemistry,* **73**, 149.

Massman WJ, Frank JM (2006) Advective transport of CO2 in permeable media induced by atmospheric pressure fluctuations: 2. Observational evidence under snowpacks. *J. Geophys. Res.,* **111**.

Mitchell SR, Beven KJ, Freer JE (in press) Multiple sources of predictive uncertainty in modeled estimates of net ecosystem CO_2 exchange. *Ecological Modeling*.

Pumpanen J, Ilvesniemi H, Hari P (2003) A Process-Based Model for Predicting Soil Carbon Dioxide Efflux and Concentration. *Soil Sci Soc Am J,* **67**, 402-413.

Risk D, Kellman L, Beltrami H (2002) Carbon dioxide in soil profiles: production and temperature dependence. *Geophysical Research Letters,* **29**.

Rustad LE, Campbell JL, Marion GM *et al.* (2001) A meta-analysis of the response of soil respiraiton, net nitrogen mineralization, and aboveground plant growth to expeirmental ecosystem warming. *Oecologia,* **126**, 543-562.

Ryan MG, Law BE (2005) Interpreting, measuring, and modeling soil respiration. *Biogeochemistry,* **73**, 3.

Savage KE, Davidson EA (2001) Interannual Variation of Soil Respiraiton in Two New England Forests. *Global Biogeochemical Cycles,* **15**, 337-350.

Schlesinger WH, Andrews JA (2000) Soil respiration and the global carbon cycle. *Biogeochemistry,* **48**, 7-20.

Tang J, Baldocchi DD, Qi Y, Xu L (2003) Assessing soil CO_2 efflux using continuous measurements of CO_2 profiles in soils with small solid-state sensors. *Agricultural and Forest Meteorology*, **118**, 207.

Valentini R, Matteucci G, Dolman AJ (2000) Respiration as the main determinant of carbon balance in European forests. *Nature,* **404**, 861-864.

CHAPTER TWO: CONTRIBUTIONS OF ECTOMYCORRHIZAL FUNGAL MATS TO FOREST SOIL RESPIRATION

Claire L. Phillips, Laurel Kluber, Julia Pedersen, and Barbara J. Bond

ABSTRACT

Ectomycorrhizal (EcM) fungi are a prominent and ubiquitous feature of forest soils, forming symbioses with many tree species, yet there are few studies quantifying their impacts on forest carbon cycles. A subset of EcM fungi form dense, perennial aggregations of hyphae, which have elevated respiration rates compared with neighboring non-mat soils. These mats are a focus of EcM activity and thereby a natural observatory for examining how EcM fungi impact soil carbon cycling. In order to constrain estimates of the contributions of EcM fungi to forest soil respiration, we quantified the proportion of total soil respiration that was derived from EcM mat soils in an old-growth Douglas-fir forest in western Oregon. One dominant genus of mat-forming fungi, *Piloderma*, covered 56.6% of the soil surface area. *Piloderma* mats were monitored for respiration rates over two growing seasons and found to have on average ~16% higher respiration than non-mat soil. Differences in mat and non-mat respiration were most likely due to microbial activity, and were not related to root biomass or other soil properties. We estimated *Piloderma* mats were responsible for approximately 9.6% of total soil respiration, and 32-40% of rhizosphere respiration in this old-growth forest stand.

INTRODUCTION

Soil flux measurements integrate plant and microbial processes that differ in function and environmental sensitivity (Carbone & Vargas, 2008; Trumbore, 2006).

Increasingly, researchers are quantifying both autotrophic and heterotrophic components of soil respiration to assess these distinct processes (Bond-Lamberty *et al.*, 2004; Subke *et al.*, 2006). However, the convenient operational definition of "autotrophic" soil respiration pools together fluxes from roots and microbial symbionts, and does not capture differences in activity between these two types of biota that may critically impact carbon and associated nutrient cycles. In forest ecosystems in particular, respiration by ectomycorrhizal (EcM) fungi is thought to be a major component of soil respiration, perhaps accounting for as much as 25% of soil flux (Heinemeyer *et al.*, 2007). Quantifying respiration from EcM fungi *in situ* is a tremendous challenge because of their intimate associations with roots, but several taxa of EcM fungi form mats, or dense aggregations of hyphae, where they locally dominate the soil, allowing EcM activity to be detected readily. Several mat-forming taxa are common in mature forests of the Pacific Northwest, and our goal was to utilize their abundance to quantify EcM mat contributions to total soil respiration.

The EcM symbiosis is critical for growth of many tree taxa (Read & Perez-Moreno, 2003), and EcM fungi are a ubiquitous feature of forest soils. EcM fungi use carbohydrates supplied by plant hosts to mobilize nutrients from soil, and translocate nutrients back to the host. Laboratory studies with tree seedlings have shown allocation to EcM fungi accounts for 1% to 21% of net primary production (reviewed by Hobbie, 2006), and extraradical EcM mycelia have been estimated to constitute as much as one-third of microbial biomass in a coniferous forest (Högberg & Högberg, 2002).

Although the functions performed by EcM fungi are critical for forest productivity, EcM respiration is rarely quantified directly. More often, the pooled respiration from roots, their mycorrhizal symbionts, and free-living rhizosphere microbes is measured, which is termed "rhizosphere respiration" (Carbone *et al.*, 2007; Irvine *et al.*, 2005), "autotrophic soil respiration" (Tang & Baldocchi, 2005), or even "root respiration" (Bhupinderpal-Singh *et al.*, 2003; Ekblad *et al.*, 2005). Roots and EcM fungi have qualitatively and quantitatively different functions in soil, and there are reasons to expect substantively different outcomes for forest carbon balance depending on the relative activity of EcM fungi versus roots.

For example, EcM fungi are likely to turn over plant-derived carbon more rapidly than roots. EcM fungi secrete high levels of extracellular enzymes, and several studies have found bacterial communities associated with EcM hyphae, indicating secretions may become rapidly consumed by free-living microorganisms in the soil (Garbaye, 1994; Warmink *et al.*, 2009). EcM roots are also associated with lower pH and higher levels of mineral weathering than non-mycorrhizal roots due to secretions of organic acids (Hoffland *et al.*, 2004). Although non-mycorrhizal roots secrete many of these compounds as well, concentrations of extracellular enzymes are generally correlated with levels of EcM fungal biomass (Simard *et al.*, 2002).

EcM fungi also have the ability to decompose soil organic matter through extracellular enzymatic activity (Read & Perez-Moreno, 2003; Talbot *et al.*, 2008). The traditional view of mycorrhizal fungi is that they receive C primarily from their host

plants. EcM fungi, however, are capable of mobilizing and assimilating low-molecular weight organic compounds such as amino acids. EcM fungi produce extracellular enzymes that can decompose a range of organic compounds, and in laboratory cultures they can metabolize as their sole C source relatively large and recalcitrant compounds such as chitin, cellulose, and polyphenols (Cairney & Chambers, 1999; topic reviewed by Read & Perez-Moreno, 2003; Trojanowski *et al.*, 1984). Although the decomposer behavior of EcM fungi is likely limited in comparison to obligate saprotrophs (Read *et al.*, 2004), it nevertheless has important implications for forest carbon balance. Rather than only turning over recently assimilated plant carbon, EcM fungi can mobilize older and more stabilized soil carbon, potentially reducing the carbon storage potential of forest soils.

The magnitude of respiration from EcM fungi is also important to quantify because EcM fungi may differ from roots and other soil organisms in response to environmental change. Although respiration of EcM fungi can be strongly influenced by the availability of carbon from plant hosts (Heinemeyer *et al.*, 2006), EcM activity may become uncoupled from plants for periods due to unique life cycles and environmental tolerances. For example, EcM fungi in temperate forests can produce high levels of extracellular enzymes during the winter, when photosynthesis rates decline (reviewed in Talbot *et al*. 2008). EcM fungi also often produce sporocarps during a narrow seasonal time window (Selosse *et al.*, 2001), and the phenology of these events as well as soil

resource availability are thought to influence fungal growth and respiration rates (Heinemeyer *et al.*, 2007; Olsson *et al.*, 2002; Vargas & Allen, 2008a).

To constrain estimates of the contributions of EcM fungi to soil respiration, we took advantage of the natural observatory provided by mat-forming EcM fungi. Mat-forming EcM fungi have a nearly global distribution and can be found in forests ranging from boreal to semi-tropical (Castellano, 1988), although much of the past research on mats has been conducted on several genera in western Oregon, in a series of studies spanning nearly thirty years. These studies have shown that in mat-colonized organic soils, fungal hyphae can constitute up to 50% of dry weight (Ingham *et al.*, 1991). Mat-colonized soils also have altered biological and chemical properties, including elevated enzymatic activity (Griffiths *et al.*, 1994; Griffiths & Caldwell, 1992), higher levels of dissolved organic carbon, including organic acids (Cromack *et al.*, 1979), higher levels of microbial diversity (Cromack *et al.*, 1988), faster rates of litter decomposition (Entry *et al.*, 1991) and elevated respiration rates in laboratory incubations (Griffiths *et al.*, 1990). In forest stands where mats are abundant they are hypothesized to be important participants in nutrient and carbon cycles (Griffiths & Caldwell, 1992).

We quantified EcM mat respiration in an old-growth Douglas-fir forest in the western Cascades of Oregon, by comparing respiration rates from soils colonized by mats with neighboring uncolonized soils. To our knowledge, the only other study to attempt *in situ* respiration measurements of EcM fungi was the study by Heinemeyer *et al*. (2007), which used mesh exclosures to exclude either roots or fungal mycelia. Their

study demonstrated that as much as 25% of soil respiration came from EcM hyphae in an early seral, lodgepole pine forest. Our work provides estimates of EcM contributions at the other extreme of forest development, allowing us to begin assessing the generality of previous findings.

Our approach depended on utilizing natural spatial variability in hyphal abundance, in contrast to physically separating EcM fungi from roots or surrounding soil. This approach required two important assumptions be met, which we systematically tested as part of the study. The first assumption was that the only difference between mat and non-mat soils that might influence respiration was fungal biomass. We tested this by comparing root biomass, substrate quality, pH, moisture, and soil physical characteristics to determine whether other variables differed between the soil types. The second assumption was that CO_2 contributions from deep soil, underlying the area mats tend to colonize, did not have an important influence on respiration measurements. We tested this by measuring soil CO_2 profiles and vertically partitioning CO_2 production by genetic soil horizons.

After satisfying both assumptions, we used respiration measurements and percent cover estimates of mat soil to address the following questions: (1) What proportion of total surface efflux is derived from EcM fungal mats? and (2) To what extent do EcM mat contributions vary seasonally, and in response to moisture or temperature?

MATERIALS AND METHODS

Site description

A 0.1ha study site was located at the HJ Andrews Experimental Forest in the western Cascades of Oregon, part of the Willamette National Forest (44º13”25’N, 122º15”30’W, 484m above sea level), and has also been included in previous EcM mat studies (Dunham *et al.*, 2007). The surrounding forest was ~450 years old, dominated by Douglas-fir (*Psuedotsuga menziesii*) and western hemlock (*Tsuga heterophylla*), both hosts for mat-forming EcM species, and Western redcedar (*Thuja plicata*), a host for arbuscular mycorrhizal fungi, which do not form mats. The understory plants included vine maple, salal, red huckleberry, sword fern, and sorrel (*Acer circinatum, Gaultheria shallon, Vaccinium parvifolium, Polystichum munitum, Oxalis oregano*), and the forest floor was covered with a layer of bryophytes. Fallen logs in advanced stages of decay were common. The soil has strong andic properties and is classified as coarse loamy mixed mesic Typic Hapludands (Dixon, 2003), with an average O-horizon depth of 6cm.

This region experiences a Mediterranean climate, with cool, moist winters and warm, dry summers. At this elevation snow accumulation is generally minimal; however, the winter during which the study was performed experienced record snow levels, with snow persisting from late December 2007-April 2008.

Identification of fungal mats

For the purposes of this study, mats were defined as dense profusions of rhizomorphs that aggregate humus or soil, are associated with obvious EcM root tips, and are uniform in structure and appearance for a depth of at least 2cm and an area at least 12cm in diameter. This definition is adapted from the criteria of Dunham *et al.* (2007), which was developed with input from Griffiths and Cromack to be consistent with earlier EcM mat studies. Using molecular techniques, Dunham *et al*. surveyed mat-forming EcM fungal species at HJ Andrews, and demonstrated that two genera occur commonly in old-growth stands, accounting for over 80% of the mats that were found. These two genera, *Piloderma* and *Ramaria,* are easily recognized and distinguished by their morphology and preferred soil type. *Piloderma* mats are characterized by stringy white or yellow rhizomorphs that permeate the organic soil horizon (Figure 1). *Ramaria* mats generally resemble ash, with a white or pale grey, powdery, hydrophobic appearance, and they colonize mineral soil. Dunham also found that mats were generally dominated by a single species.

For the initial phases of this study we categorized mats as either *Piloderma*-like or *Ramaria*-like, based on growth habit and morphology. In cover surveys we determined that *Ramaria* mats were uncommon at our site (Table 1), so we examined respiration rates only on *Piloderma*-like mats and non-mat areas.

After establishing permanent measurement locations for respiration, we used terminal restriction fragment length polymorphism analysis (T-RFLP) to confirm the initial identification of *Piloderma* mats. In June 2008, we sampled ~10g of organic soil

adjacent to each respiration measurement area, and after respiration measurements were completed in November 2008 we resampled the entire measurement area (~100g). Repeated sampling allowed us to assess whether *Piloderma* persisted as the dominant genus over time.

T-RFLP analysis uses restriction enzymes to cleave fungal DNA at specific nucleotide sequences near the terminus of DNA strands, producing fragments of various lengths that are characteristic of unique fungal genera or species. We assessed the presence of *Piloderma* by comparing T-RFLP patterns from soil extracts to those of known *Piloderma* isolates. Detailed methods of extraction and analysis are described by Blanchard (2008). Soil samples were kept cold on ice in the field and frozen at -80ºC upon returning to the lab. Three grams of frozen soil were ground with mortar and pestle to homogenize, and 0.25g of ground soil was used to extract DNA with the MOBio PowerSoil™ DNA isolation kit (MoBio Laboratories, Carlsbad, CA). We amplified fungal DNA using ITS1-F and ITS4 rDNA primers, with the forward primers fluorescently labeled with 5'-6-FAM (6-carboxyfluorescein). PCR products were cleaned to remove excess primer and nucleotides, and then digested with Hinf1 restriction endonucleases. The restriction products were submitted to OSU Center for Genome Research and Biocomputing for analysis. Sizes and relative abundances of the T-RFLP fragments were quantified using Genotyper® version 3.7 software (Applied Biosystems, Inc., Foster City, CA).

First assumption: Mat and non-mat soils only differ in fungal biomass

At the outset of the study in July 2007, we randomly chose 10 *Piloderma* mat and 5 non-mat soils (not paired) for one time respiration measurements, and then destructively cored the soils to measure root biomass, substrate quality as indicated by %C and %N, soil pH, moisture, and litter depth. In addition, we performed t-RFLP analysis to confirm the identity of the mat soils, and removed one mat soil that did not produce a characteristic *Piloderma* T-RFLP pattern.

Soil cores 8cm in diameter were removed directly underneath respiration collars in 4 depth increments: the entire O-horizon, 0-10cm, 10-20cm, and 20-35cm below the mineral soil surface. Fine root (<2mm diameter) and total root biomass were determined by wet sieving soils through 1mm sieves, and picking roots by hand. We measured total soil C and N by drying 1g of organic soil and 5g of mineral soil at 65°C for 48 hours, grinding soils to fine powder on a roller mill, and analyzing 3-10mg subsamples on a Costech ECS-4010 elemental combustion analyzer (Costech Analytical, Valencia, CA, USA) against an atropine standard.

Second assumption: CO_2 production from deep soil does not substantially impact surface measurements

Surface flux measurements incorporate CO_2 produced throughout the soil profile, whereas *Piloderma* mat activity is localized in the O-horizon. Davidson *et al*. (2006b) showed that in a temperate hardwood forest, the O-horizon contributed 40-48% of CO_2 flux from soil surface on an annual basis. This indicates that for our study, mat

and non-mat organic soils should have a major influence on surface flux rates, but spatial variation in deeper soil contributions may also potentially influence our results. To test this, we vertically partitioned CO_2 production at our site following the approach of Davidson *et al.* (2006b), in which CO_2 fluxes at the interfaces of each horizon are modeled according to Fick's first law of diffusion:

$$F = D_s \frac{dC}{dz} \quad (1)$$

where F is CO_2 efflux (μmol $m^{-2}s^{-1}$), D_s is the effective CO_2 diffusivity in soil ($m^2 s^{-1}$), C is CO_2 mole concentration, and z is depth.

We established two small soil pits in the study area (approximately 15 × 100 × 80cm deep), one in an extensive mat area and the other in an extensive non-mat area, to measure CO_2 concentrations profiles for dC/dz, and soil moisture and temperature to calculate D_s (Figure 2.2).

To sample soil CO_2, we inserted 30mL buffer volumes ("gas wells") constructed from PVC pipe into the intact profile wall at five depths: the O-A interface (5-7.5cm), the A-Bw interface (15-17cm), an indistinct boundary between Bw1-Bw2 (25-27.5cm), the Bw2-C interface (45-47.5cm), and within the C-horizon at 80cm. The buffer volumes were connected to the soil surface by 4.5mm diameter stainless steel tubing, which were sealed at the surface with Swagelok fittings containing acetyl-butyl septa. Duplicate profiles were installed in each pit about 1m apart with moisture and temperature sensors centered between, and the pits were back-filled. We calculated

dC/dz from the derivative of third order polynomials fitted to the concentration profiles (Figure 2.3).

Gas samples were collected by first drawing and discarding the tubing volume with a syringe, and then collecting 12mL samples into Exetainer™ vials (Labco, UK), which were pre-flushed with N_2 and evacuated with a handpump. Exetainers were capped with silicone adhesive and analyzed within 24-48 hours in the laboratory using a LiCor-6252 infrared gas analyzer (LI-COR Biosciences, Lincoln, NE, USA) configured for injection of small volumes (Davidson & Trumbore, 1995). A calibration curve was created by injecting standard gases to translate peak height to CO_2 concentration. The combined standard uncertainties of the measurements, which include sampling and instrument uncertainties (NIST guidelines, Taylor & Kuyatt, 1994), was determined based on replicate analyses to be 3.8% of CO_2 concentration.

To calculate D_s, we used the relationship described by Moldrup *et al*. (1999), which relates D_s to air-filled pore space and soil texture parameters. We removed soil samples from the pits for textural and bulk density analysis, and determined air-filled pore space from volumetric moisture measurements made with CS-615 TDR probes (Campbell Scientific, Logan, Utah, USA), using a site-specific calibration calculated by comparing voltage and water content of repacked soil columns. Diffusivity was also corrected for soil temperature, which was measured with type T thermocouple wire. Data were logged hourly with a Campbell Scientific CR-10x datalogger and AM416 multiplexer.

We quantified production in each horizon as the difference between fluxes leaving and entering that horizon. For the O-horizon, production was estimated as the difference between surface flux and the incoming flux from the A-horizon. Production from the C horizon and below was estimated as the flux of CO_2 from the top of the C horizon. Production values were calculated six times over the course of the study (Figure 2.3). We used Monte Carlo simulations to calculate uncertainties for production values. The component uncertainties of measured data were determined when possible from the standard deviation of repeated measures. For non-replicated measures (% OM and soil texture), uncertainty was assumed to be 5%, and for bulk density we used a conservative uncertainty estimate of 10%.

Percent Cover

To measure the percent cover of mat and non-mat soils, we mapped the 20m x 50m study area into $1m^2$ numbered quadrats, and randomly chose 50 quadrats to search intensively for mats. We pulled back the bryophyte layer, exposing the organic soil surface to look for *Piloderma* mats, and then gently lifted the organic soil to look for *Ramaria* mats at the mineral soil surface. We determined average mat width, length, and depth from 3-5 individual measurements in each dimension, and approximated the projected areas of mats by multiplying the average width and length. We also quantified the area within quadrats occupied by large roots or downed logs that prevented colonization of the organic horizon, and thus determined two values for mat cover: the

percentage of exposed soil available to be colonized by mats, and the percentage of the entire surveyed area (Table 2.1). When quadrats were entirely occupied by large trees or fallen logs, we quantified the area as occupied by coarse plant material, and also randomly selected another quadrat to search for mats.

Respiration measurements

We chose locations for respiration measurements where mat soils were within 1m proximity of non-mat soils, to compare the soil types in similar microenvironments. To minimize potential new colonization in non-mat areas over the course of the experiment, we required that non-mat areas had no visible hyphae for an area at least 15cm in diameter. Similarly, to avoid potential recession of EcM mats, mat soils had to be at least 15cm in diameter and at least 2cm thick, with only a single morphotype present (i.e. no *Piloderma*-type mat directly above a *Ramaria*-type mat).

Soil surface flux rates were measured with a portable gas exchange system and soil flux chamber (Li-Cor model 6400 and 6400-19, respectively, LI-COR Biosciences, Lincoln, NE, USA). To provide an interface between the soil and the respiration chamber, soil collars constructed from schedule 40 PVC pipe were inserted 1-2cm into the organic horizon. Each individual respiration measurement covered 80.3cm^2 of ground surface. Any potential severing of roots or hyphae appeared to be minimal because rhizomorphs were generally most concentrated below this depth, and the soil humus also tended to compress under the collar rims. Soil collars were installed 48

hours prior to initial measurements and left in place for the duration of the study. Bryophytes and small green plants growing inside the collars were removed, and a plug of unrooted bryophytes was replaced in the collar between measurements to mimic surrounding ground cover.

To check that mat soils remained rhizomorphic and non-mat soils did not become rhizomorphic over the course of the study, we probed the O-horizon just outside permanently installed soil respiration collars approximately every 2 months to detect rhizomorphs.

Soil temperature and moisture were measured coincident with respiration measurements. Temperature at 10cm depth was measured by inserting a probe adjacent to the respiration collars. We measured gravimetric water content in the O-horizon, and at 5 and 15cm below the mineral soil surface, by collecting soil cores from five small coring fields established across the study area, and associating each soil collar with moisture values from the nearest coring field.

Data analysis

We tested the assumption that mat and non-mat soils have similar chemical and biological characteristics, aside from fungal biomass, by performing t-tests for each of the measured soil properties (by individual layer as well as volume-weighted profile averages). We also examined whether any of the soil properties correlated with

respiration rates, which we measured prior to coring, by analyzing individual linear regressions.

Our first research question asked: what proportion of total surface efflux is derived from EcM fungal mats? To answer this we calculated the percent difference in respiration rate between mat and non-mat pairs, which we refer to as "mat contributions". We scaled-up mat contributions to whole study area in order to account for the patchiness of mats, by multiplying average mat contributions by the percent cover of mats.

Our second question asked: to what extent do EcM mat contributions vary seasonally, and in response to moisture or temperature? We studied seasonal variability in mat respiration by examining correlations with soil temperature and moisture. Soil respiration is often described as an exponential function of temperature and moisture (Martin & Bolstad, 2005):

$$F = \alpha e^{\beta_1 T + \beta_2 M} \tag{2}$$

where F is surface flux, T is soil temperature, and M is soil moisture. To linearize this equation we took the natural logarithm of each side

$$\ln F = \ln \alpha + \beta_1 T + \beta_2 M \tag{3}$$

and then calculated the difference between neighboring mat (F_m) and non-mat soils (F_{nm}) as follows:

$$\ln R_m = \ln\left(\frac{F_m}{F_{nm}}\right) = \ln F_m - \ln F_{nm} \tag{4}$$

where R_m is the ratio of mat and non-mat fluxes. This is related to the average temperature (T_{ave}) and average O-horizon moisture (M_{ave}) for each neighboring mat and non-mat pair as follows:

$$\ln R_m = \ln \alpha + \beta_1 T_{ave} + \beta_2 M_{ave} \quad (5)$$

We analyzed Eq.4 using a statistical linear mixed effects model, with temperature and moisture as fixed effects, pair location as a random effect, and an expanded error term to account for repeated measures, using a linear spatial correlation matrix for the variance-covariance structure. All analyses were performed with S-PLUS v.8.

RESULTS

EcM mat cover and identification

Piloderma-like mats occupied approximately 42% of the surveyed area and *Ramaria*-like mats occupied another 1.9%, demonstrating almost half of the forest floor in this old-growth stand contained EcM mats (Table 2.1). Trees, coarse roots, and coarse woody debris that prevented mat colonization also occupied about 23% of the soil surface. Of the soil surface that was available for mat colonization, almost 57% was occupied by *Piloderma*-like mats, and 2.6% of the exposed mineral soil surface was occupied by *Ramaria*-like mats.

Table 2.1. Percent of soil surface occupied by coarse plant material, *Ramaria*-like and *Piloderma*-like fungal mats, and non-mat soil.

	Tree boles, roots, and CWD	EcM Mats		Non mat
		Ramaria	*Piloderma*	
Total area	22.8%	1.9%	42.2%	33.2%
Exposed soil	--	2.6%	56.6%	40.9%

All of the 12 *Piloderma* mats selected for long-term respiration measurements had characteristic *Piloderma* T-RFLP patterns in both the June and November samples, except for two mats that had became non-mat-like during the winter and contained almost no visible rhizomorphs by the time we sampled in June 2008. The T-RFLP results confirmed our ability to recognize *Piloderma* based on morphology. We also found two of the non-mat soils contained *Piloderma* DNA, although they did not contain sufficient visible rhizomorphs to be considered mats.

Visually, most of the mats maintained a stable density of rhizomorphs throughout the study, but in a few locations we observed changes in rhizomorph density, particularly in the second growing season when we had to cull data for three pairs in which the mat soil became too weakly rhizomorphic to be considered mats, and also for two pairs in which the non-mat soils became colonized. For each mat and non-mat pair, we included data only for date ranges where we had positive visual confirmation of the soil condition.

First assumption: Mat and non-mat soils only differ in fungal biomass

Of the suite of soil properties we examined, we found no differences between mat and non-mat soils in moisture, fine root biomass, total root biomass, %C, %N, C:N ratio, or litter depth. We found mat soils had marginally more acidic organic horizons than non-mat soil, although the difference was not significant (pH = 4.58 vs. 5.48, p = 0.063). None of these properties, however, correlated significantly with respiration when analyzed individually. These findings indicate that our first assumption was met, and that mat and non-mat soils did not have obvious differences in soil qualities other than fungal biomass.

Second assumption: CO_2 production from deep soil does not substantially impact surface flux measurements

We measured soil profiles in both mat and non-mat areas of the study site, and found subsurface CO_2 profiles (Figure 2.3) and surface flux rates (Figure 2.4) had similar patterns in the two areas, therefore we will describe results from both areas together. Using a Fickian approach to partition CO_2 fluxes, we calculated that contributions from the O-horizon ranged from as much as 93% in May, when snow had just melted and the ground was essentially saturated, to 37% in August, when the soil was extremely dry (4-6% water content at the O/A interface). Across all sampling dates, O-horizon contributions averaged 73% (95% CI = 61-85%). Calculated contributions

from the A-horizon were small (Figure 2.4), and we even calculated a CO_2 sink in this horizon in early October of both years, when the O-horizon had regained more moisture than underlying mineral soil (Figure 2.6). CO_2 concentrations were more variable on these dates, however, and the errors associated with the resulting negative production values were particularly large.

Overall, these partitioning results indicate that when soils were moist, the majority of CO_2 production originates from depths where *Piloderma* colonizes, and our assumption that contributions from sub-mat soil depths are minor was met. Under dry conditions the late summer, however, it appears our assumption may not have been met, as CO_2 contributions from mineral soil exceeded the contributions of the O-horizon. This finding has implications for our ability to quantify mat contributions during late summer, and also for correlations between soil moisture and mat contributions, which we discuss later.

EcM mat versus non-mat respiration

The average difference in surface flux between mat and neighboring non-mat soils was significantly greater than zero on most, but not all, sampling days (Figure 2.5B). Differences between mat and non-mat soils were more consistently high during the first growing season, and surface flux from *Piloderma* mats was on average 17% higher than from non-mat soil (95% CI=10-25%).

In the second year *Piloderma* mat respiration was on average 16% higher than non-mat soil (95% CI=7-27%), although variability between sampling dates was much greater. A notable spike in mat contributions occurred in early June, 2008 (Figure 2.5B). Mat surface flux averaged almost 40% higher than non-mat surface flux on this date, with smaller variance than on any other sampling event. The spike in respiration was brief; when we sampled again only two weeks later mat contributions were statistically not different from zero. Average mat contributions were also high in November 2008, but with greater variability between pairs.

Environmental controls on mat contributions

We examined seasonal variability in mat contributions in response to soil temperature and moisture. We found surface flux rates from both mat and non-mat soils correlated strongly with soil temperature; however, the difference between these values did not show a relationship with soil temperature (Figure 2.7).

In contrast, moisture content of the O-horizon did correlate significantly with mat contributions (Figure 2.8, $P = 0.0001$). For every 10% increase in soil moisture, mat contributions increase by 8% (95% CI = 3.6-13.9%). The second summer of our study was substantially drier than the first summer (Figure 2.6), and these drier conditions were associated with lower respiration rates and mat contributions (Figure 2.5).

DISCUSSION

Tests of assumptions

Our tests of assumptions provide strong evidence that differences in respiration between mat and non-mat soils was due primarily to activity of EcM fungi and other microbes associated with mats, in contrast to other potential explanatory variables. Mat and non-mat soils did not differ significantly in soil properties that could potentially influence respiration rates, such as %C, %N, litter depth, and soil moisture. Most notably, root biomass was similar in mat and non-mat soils, indicating that differences in surface flux rates were not likely due to root respiration. This finding of similar root biomass in the two soil types is consistent with previous EcM mat studies (Griffiths *et al.*, 1990). At our site, the similarity in root biomass may be due in part to western redcedar occupying non-mat soils, which is a host for non mat-forming arbuscular mycorrhizae.

We did find slightly higher pH in non-mat soils, which is also consistent with previous work that shows EcM mat soils have higher levels of organic acids than non-mat soils (Griffiths *et al.*, 1994). Lower pH in mat soil solution may also be a result of higher CO_2 concentrations increasing dissolved carbonic acid; however, we did not find a significant correlation between soil pH and respiration.

Our analysis of CO_2 production within the soil profile indicated that during most times of the year, surface flux measurements are an excellent approach for measuring EcM mat contributions. During times when soils were high to moderately moist, the O-horizon contributed a large proportion (48-93%) of total surface flux. During the late

summer prior to fall rains, however, contributions from deeper soil horizons were more substantial, and spatial variability in deep production may have influenced calculations of mat contributions. Comparisons of mat and non-mat surface fluxes showed mat contributions were, indeed, smaller under dry soil conditions (Figure 2.8). This trend may be related to biological responses of EcM fungi, or may instead be related to physical effects of moisture on gas transport from mineral soil horizons, an issue we discuss more below in the section on environmental controls.

Contributions of EcM mats to total soil respiration

This study demonstrated significant differences in respiration between EcM mats and neighboring non-mat soils on most sampling dates, and indicates that in areas where mats are abundant, they are likely to make important contributions to soil respiration. To assess how much *Piloderma* mats may have contributed to soil respiration across our whole study site, we multiplied the percent cover of mats (56.6%) by average mat contributions from each year of the study. We estimated that *Piloderma* mats contributed on average 9.6% (95% CI= 10-14%) to total soil respiration between July-December 2007, and 9.1% (95% CI= 4-15%) between May-December 2008.

This value for total mat contributions across the site represents an under estimate and a low-end constraint for the amount of soil respiration contributed by *Piloderma*, and EcM hyphae in general. Diffuse mycelia of *Piloderma* and other EcM fungal taxa are present throughout the soil and contribute to the flux measured from non-mat soils.

EcM taxa vary in growth habits, with some forming dispersed mycelia, and still others forming smooth mantles around root tips with few external mycelia extending into soil. Significant levels of metabolic activity are likely to occur within these structures that our study did not account for.

Despite significant mat contributions to total soil respiration, the differences we observed between mat and non-mat respiration were much smaller than was demonstrated in a previous lab incubation study (Griffiths *et al.*, 1990). Over two years of monthly samples, Griffiths *et al*. consistently found respiration rates three to 11 times higher in mats compared with neighboring non-mats. These soils were cored in the field and incubated in the lab, and therefore the disturbance created by severing hyphae may have contributed to higher mat respiration. Because we measured fluxes *in situ,* CO_2 contributions from deeper soil horizons also make our measurements less sensitive to differences occurring only in the organic horizon.

Environmental controls on EcM mat contributions

We found seasonal variations in CO_2 production by *Piloderma* mats corresponded with soil moisture, but not with temperature. Heinemeyer *et al*. (2007) arrived at the same conclusion in their field study of EcM hyphal respiration. However, an important question raised by our vertical partitioning calculations is whether moisture actually enhanced mat metabolism, or whether moisture decreased the relative

contributions of CO_2 from deeper soil horizons, which improved our ability to detect differences between mat and non-mat soil when soils were wet.

To test this, we examined the relationship between CO_2 production and soil moisture for each genetic horizon (Figure 2.9), and found production had more significant negative correlations with moisture in the Bw and C-horizons than in the O- and A-horizons. This indicates that deep soil CO_2 production was more sensitive to moisture than shallow soil CO_2 production, and moisture-related variation in mat contributions may have resulted more from changes in deep production than shallow production.

There are several mechanisms that can explain reduced fluxes from deep soil horizons under wet conditions. Soil water may have increased CO_2 storage in the profile, and also restricted movement of CO_2 in the gas phase. Effective gas diffusivity decreases as soil moisture increases, limiting the ability of CO_2 to diffuse through soil to the surface. Another possibility is that oxygen became limited at depth under wet conditions, restricting rates of aerobic respiration.

In contrast to our field results, Griffiths *et al*. (1991) performed lab incubations of mat and non-mat soils and found no relationship between soil moisture and respiration. This indicates that moisture conditions in the immediate environment of EcM mats may have weak direct effects on mat respiration. The comparison of lab and field results suggests seasonal changes in EcM contributions may be related more to changes in vertical partitioning of soil flux than to moisture tolerances of EcM fungi.

EcM mat respiration as a component of rhizosphere respiration

We compared our estimates of *Piloderma* mat contributions to estimates of total rhizosphere contributions (root + EcM fungi) in an area of similar-aged forest less than 1km from our study area (44ºN 14”0’N, 122º13’0”W, 531m elevation), part of the Detritus Input and Removal Treatments (DIRT) experiment (Sulzman *et al.*, 2005). From 2001-2003, Sulzman *et al.* compared respiration rates from root-free trenched plots and untreated control plots, and estimated that approximately ¼ of total soil respiration came from rhizosphere respiration. If we assume that rhizosphere respiration similarly accounted for ¼ of total soil respiration in our study area, this suggests *Piloderma* mat respiration may have accounted for almost 40% of rhizosphere respiration. A more conservative estimate that considers only the wet year of their study, which was most similar to the conditions we encountered, suggests that EcM mats may have contributed 32% of rhizosphere respiration in this old-growth Douglas-fir forest.

Previous studies have also indicated a large EcM fungal component of rhizosphere respiration. Using a mass balance approach, Fahey *et al.* (2005) estimated 17% of rhizosphere respiration was from mycorrhizal fungi and rhizodeposition, although the authors acknowledged this estimate had high uncertainty. Heinemeyer *et al.* (2007) found that EcM hyphal respiration was about 70% of rhizosphere respiration, using mesh of varying sizes to exclude fungal hyphae or roots. The variability among these estimates is not unlike the variability seen in estimates of total rhizosphere respiration, which varies with forest type as well as with estimation technique (Bond-

Lamberty *et al.*, 2004; Subke *et al.*, 2006). Despite the range in values, our results contribute to a growing consensus that EcM respiration is a substantial component of rhizospheric respiration, and indicates EcM contributions are significant both in early and late seral forests.

EcM fungal respiration and seral development

Although this study demonstrated EcM respiration can be substantial in old-growth forest, too few studies have been performed to assess the extent to which EcM respiration changes with forest age. Large aggregations of mat-forming fungi may be more commonly associated with late-seral forests, as indicated by several studies that have shown *Piloderma*-like and *Ramaria*-like EcM fungi associated with large trees and older stands (Dunham *et al.*, 2007; Griffiths *et al.*, 1996; Smith *et al.*, 2000). Other work also suggests that overall EcM abundance increases as stands develop, due in part to a preference by some species for organic matter accumulation (reviewed by Erland & Taylor, 2002). However, non-mat forming EcM taxa associated with younger trees appear to have high carbon demands as well, as indicated by the field study by Heinemeyer *et al*. (2007) and a number of lab studies with tree seedlings (Reid *et al.*, 1983; Rygiewicz & Andersen, 1994).

Future research should investigate whether EcM carbon demands increase as stands age, because such a relationship may help to explain age-related declines in stand productivity. The percentage of gross primary production allocated belowground has

been show to increase with stand age and to contribute to declines in aboveground wood production (Ryan *et al.*, 2004). This observation would be consistent with increased carbon demands from EcM symbionts.

CONCLUSIONS

This study demonstrates EcM mats contribute a significant CO_2 flux in old-growth forest, and may account for as much as 9.6% of total soil respiration and 32-40% of rhizosphere respiration. Comparisons of mat and non-mat soil properties show that elevated respiration on mat soils is not likely a result of root respiration or other soil characteristics, but of activity from EcM fungi and associated microbes. In addition to biological activity, physical processes may impact the contributions of EcM mats on total soil respiration. The spatial location of EcM mats close to the soil surface appears to increase their proportional contribution when soils are wet. To better represent the distinct functions and activity of different soil biota, soil respiration models may need to be adapted to better account for the carbon demands of EcM fungi, as well as their spatial growth habits.

ACKNOWLEDGEMENTS

Bruce Caldwell and Dave Myrold provided advice on experimental design and helpful feedback on the manuscript. Doni McKay and Jane Smith assisted with T-RFLP analysis. Thanks to Shane Easter, Priscilla Woolverton, and Michele Noble for

assistance with lab and field work. Funding was provided by the Northwest Scientific Association Graduate Research Fellowship. We conducted this research at HJ Andrews Experimental Forest, which is funded by the National Science Foundation's Long-Term Ecological Research Program (DEB 08-23380), US Forest Service Pacific Northwest Research Station, and Oregon State University.

REFERENCES

Bhupinderpal-Singh A, Nordgren A, Ottosson Löfvenius M, Högberg MN, Mellander P-E, Högberg P (2003) Tree root and soil heterotrophic respiration as revealed by girdling of boreal Scots pine forest: extending observations beyond the first year. *Plant, Cell, and Environment*, **26**, 1287-1296.

Blanchard JH (2008) Episodic dynamics of microbial communities associated with the birth and death of ectomycorrhizal mats in old-growth Douglas-fir stands. Unpublished M.S. Oregon State University, Corvallis, 52 pp.

Bond-Lamberty B, Wang C, Gower ST (2004) A Global Relationship Between the Heterotrophic and Autotrophic Components of Soil Respiration? *Global Change Biology*, **10**, 1756-1766.

Cairney JWG, Chambers SM (eds) (1999) *Ectomycorrhizal Fungi: Key Genera in Profile*, Berlin, Springer.

Carbone MS, Czimczik CI, McDuffee KE, Trumbore SE (2007) Allocation and residence time of photosynthetic products in a boreal forest using a low-level ^{14}C pulse-chase labeling technique. *Global Change Biology*, **13**, 466-477.

Carbone MS, Vargas R (2008) Automated soil respiration measurements: new information, opportunities and challenges. *New Phytologist*, **177**, 295-297.

Castellano MA (1988) The taxonomy of the genus *Hysterangium* (Basidiomycotina, Hysterangiaceae) with notes on its ecology. Unpublished Ph.D. Oregon State University, Corvallis, OR, 238 pp.

Cromack K, Fichter BL, Moldenke AM, Entry JA, Ingham ER (1988) Interactions between soil animals and ectomycorrhizal fungal mats. *Agriculture, Ecosystems & Environment*, **24**, 161-168.

Cromack K, Sollins P, Graustein WC *et al.* (1979) Calcium oxalate accumulation and soil weathering in mats of the hypogeous fungus *Hysterangium crassum*. *Soil Biology & Biochemistry*, **11**, 463-468.

Davidson EA, Savage KE, Trumbore SE, Borken W (2006) Vertical partitioning of CO2 production within a temperate forest soil. *Global Change Biology*, **12**, 944-956.

Davidson EA, Trumbore SE (1995) Gas diffusivity and production of CO_2 in deep soils of the eastern Amazon. *Tellus B,* **47**, 550-565.

Dixon JJ (2003) Applying GIS to soil-geomorphic landscape mapping in the Lookout Creek valley, Western Cascades, Oregon. Unpublished M.S. Oregon State University, Corvallis.

Dunham SM, Larsson K-H, Spatafora JW (2007) Diversity and community structure of mat-forming ectomycorrhizal fungi in old growth and rotation age Douglas-fir forests fo the HJ Andrews Experimental Forest, Oregon, USA. *Mycorrhiza,* **17**, 633-645.

Ekblad A, Boström B, Holm A, Comstdet D (2005) Forest soil respiration rate and $\delta^{13}C$ is regulated by recent above ground weather conditions. *Oecologia,* **143**, 136-142.

Entry JA, Rose CL, Cromack K (1991) Litter decomposition and nutrient release in ectomycorrhizal mat soils of a Douglas fir ecosystem. *Soil Biology & Biochemistry*, **23**, 285-290.

Erland S, Taylor AFS (2002) Diveristy of ecto-mycorrhizal fungal communities in relation to the abiotic environment. In: *Mycorrhizal Ecology.* (eds Van Der Heijden Mga, Sanders Ir) pp Page. Berlin, Springer-Verlag.

Fahey T, Tierney G, Fitzhugh R, Wilson G, Siccama T (2005) Soil respiration and soil carbon balance in a northern hardwood forest ecosystem. *Canadian Journal of Forest Research*, **35**, 244-253.

Garbaye J (1994) Helper bacteria: a new dimension to the mycorrhizal symbiosis. *New Phytologist,* **128**, 197-210.

Griffiths RP, Baham JE, Caldwell BA (1994) Soil solution chemistry of ectomycorrhizal mats in forest soil. *Soil Biology & Biochemistry,* **26**, 331-337.

Griffiths RP, Bradshaw GA, Marks B, Lienkaemper GW (1996) Spatial distribution of ectomycorrhizal mats in coniferous forests of the Pacific Northwest, USA. *Plant and Soil,* **180**, 147-158.

Griffiths RP, Caldwell BA (1992) Mycorrhizal mat communities in forest soils. In: *Mycorrhizae in ecosystems.* (eds Read Dj, Lewis Dh, Fitter Ah, Alexander Ij) pp Page. Cambridge, Cambridge University Press.

Griffiths RP, Caldwell BA, Cromack Jr K, Morita RY (1990) Douglas-fir forest soils colonized by ectomycorrhizal mats. I. Seasonal variation in nitrogen chemistry and nitrogen cycle transformation rates. *Canadian Journal of Forest Research,* **20**, 211-218.

Heinemeyer A, Hartley IP, Evans SP, Carreira de la Fuentes JA, Ineson P (2007) Forest soil CO_2 flux: uncovering the contribution and environmental responses of ectomycorrhizas. *Global Change Biology,* **13**, 1786-1797.

Heinemeyer A, Ineson P, Ostle N, Fitter AH (2006) Respiration of the External Mycelium in the Arbuscular Mycorrhizal Symbiosis Shows Strong Dependence on Recent Photosynthates and Acclimation to Temperature. *New Phytologist,* **171**, 159-170.

Hobbie EA (2006) Carbon Allocation to Ectomycorrhizal Fungi Correlates with Belowground Allocation in Culture Studies. *Ecology,* **87**, 563-569.

Hoffland E, Kuyper TW, Wallander H *et al.* (2004) The role of fungi in weathering. *Frontiers in Ecology and the Environment,* **2**, 258-264.

Högberg MN, Högberg P (2002) Extramatrical Ectomycorrhizal Mycelium Contributes One-Third of Microbial Biomass and Produces, Together with Associated Roots, Half the Dissolved Organic Carbon in a Forest Soil. *New Phytologist,* **154**, 791-795.

Ingham ER, Griffiths RP, Cromack K, Entry JA (1991) Comparison of Direct vs Fumigation Incubation Microbial Biomass Estimates from Ectomycorrhizal Mat and Non-mat Soils. *Soil Biology and Biochemistry,* **23**, 465-471.

Irvine J, Law BE, Kurpius MR (2005) Coupling of canopy gas exchange with root and rhizosphere respiration in a semi-arid forest. *Biogeochemistry,* **73**, 271.

Martin JG, Bolstad PV (2005) Annual soil respiration in broadleaf forests of northern Wisconsin: influence of moisture and site biological, chemical, and physical characteristics. *Biogeochemistry,* **73**, 149.

Moldrup P, Olesen T, Yamaguchi T, SchjÃ¸nning P, Rolston DE (1999) Modeling Diffusion and Reaction in Soils: Ix. the Buckingham-Burdine-Campbell Equation for Gas Diffusivity in Undisturbed Soil. *Soil Science,* **164**, 542-551.

Olsson PA, KJakobsen I, Wallander H (2002) Foraging and resource allocation strategies of mycorrhizal fungi in a patchy environment. In: *Mycorrhizal Ecology.* (eds Van Der Heijden Mga, Sanders Ir) pp Page. Berlin, Spring-Verlag.

Read DJ, Leake JR, Perez-Moreno J (2004) Mycorrhizal fungi as drivers of ecosystem processes in heathland and boreal forest biomes. *Canadian Journal of Botany,* **82**, 1243-1263.

Read DJ, Perez-Moreno J (2003) Mycorrhizas and Nutrient Cycling in Ecosystems--A Journey Towards Relevance? *New Phytologist,* **157**, 475-492.

Reid CPP, Kidd FA, Ekwebelam SA (1983) Nitrogen nutrition, photosynthesis and carbon allocation in ectomycorrhizal pine. *Plant and Soil,* **71**, 415-432.

Ryan MG, Binkley D, Fownes JH, Giardina CP, Senock RS (2004) An experimental test of the causes of forest growth decline with stand age. *Ecological Monographs,* **74**, 393-414.

Rygiewicz PT, Andersen CP (1994) Mycorrhizae alter quality and quantity of carbon allocated below ground. *Nature,* **369**, 58-60.

Selosse M-A, Martin F, Le Tacon F (2001) Intraspecific variation in fruiting phenology in an ectomycorrhizal *Lacarria* population under Douglas fir. *Mycological Research,* **105**, 524-531.

Simard SW, Jones MD, Durall DM (2002) Carbon and Nutrient Fluxes Within and Between Mycorrhizal Palnts. In: *Mycorrhizal Ecology.* (eds Van Der Heijden Mga, Sanders Ir) pp Page. Berlin, Springer-Verlag.

Smith JE, Molina R, Huso M, Larsen MJ (2000) Occurrence of *Piloderma fallax* in young, rotation-age, and old-growth stands of Douglas-fir (*Pseudotsuga menziesii*) in the Cascade Range of Oregon , U.S.A. *Canadian Journal of Botany,* **78**, 995-1001.

Subke J-A, Inglima I, Francesca Cotrufo M (2006) Trends and methodological impacts in soil CO_2 efflux partitioning: A metaanalytical review. *Global Change Biology,* **12**, 921-943.

Sulzman EW, Brant JB, Bowden RD, Lajtha K (2005) Contribution of aboveground litter, belowground litter, and rhizosphere respiration to total soil CO_2 efflux in an old growth coniferous forest. *Biogeochemistry,* **73**, 231-256.

Talbot JM, Allison SD, Treseder KK (2008) Decomposers in Disguise: Mycorrhizal Fungi as Regulators on Soil C Dynamics in Ecosystems Under Global Change. *Functional Ecology*, **22**, 955-963.

Tang J, Baldocchi DD (2005) Spatial and temporal variation in soil respiration in an oak-grass savanna ecosystem in California and its partitioning into autotrophic and heterotrophic components. *Biogeochemistry,* **73**, 183.

Taylor BN, Kuyatt CE (1994) NIST Technical Note 1297: Guidelines for Evaluating and Expressing the Uncertainty of NIST Measurement Results. *National Institute of Standards and Technology, US Dept of Commerce, Technology Administration*.

Trojanowski J, Haider K, Hüttermann A (1984) Decomposition of ^{14}C-labelled lignin, holocellulose and lignocellulose by mycorrhizal fungi. *Archives of Microbiology,* **139**, 202-206.

Trumbore SE (2006) Carbon respired by terrestrial ecosystems--recent progress and challenges. *Global Change Biology,* **12**, 141-153.

Vargas R, Allen MF (2008) Dynamics of Fine Root, Fungal Rhizomorphs, and Soil Respiration in a Mixed Temperate Forest: Integrating Sensors and Observations. *Vadose Zone Journal,* **7**, 1055-1064.

Warmink JA, Nazir R, van Elsas JD (2009) Univeral and species-specific bacterial 'fungiphiles' in the mycospheres of different basidiomycetous fungi. *Environmental Microbiology,* **11**, 300-312.

Figure 2.1. Photograph of a *Piloderma*-like mat. A) *Piloderma* mat colonizing the O-horizon, B) close-up of rhizomorphic growth habit.

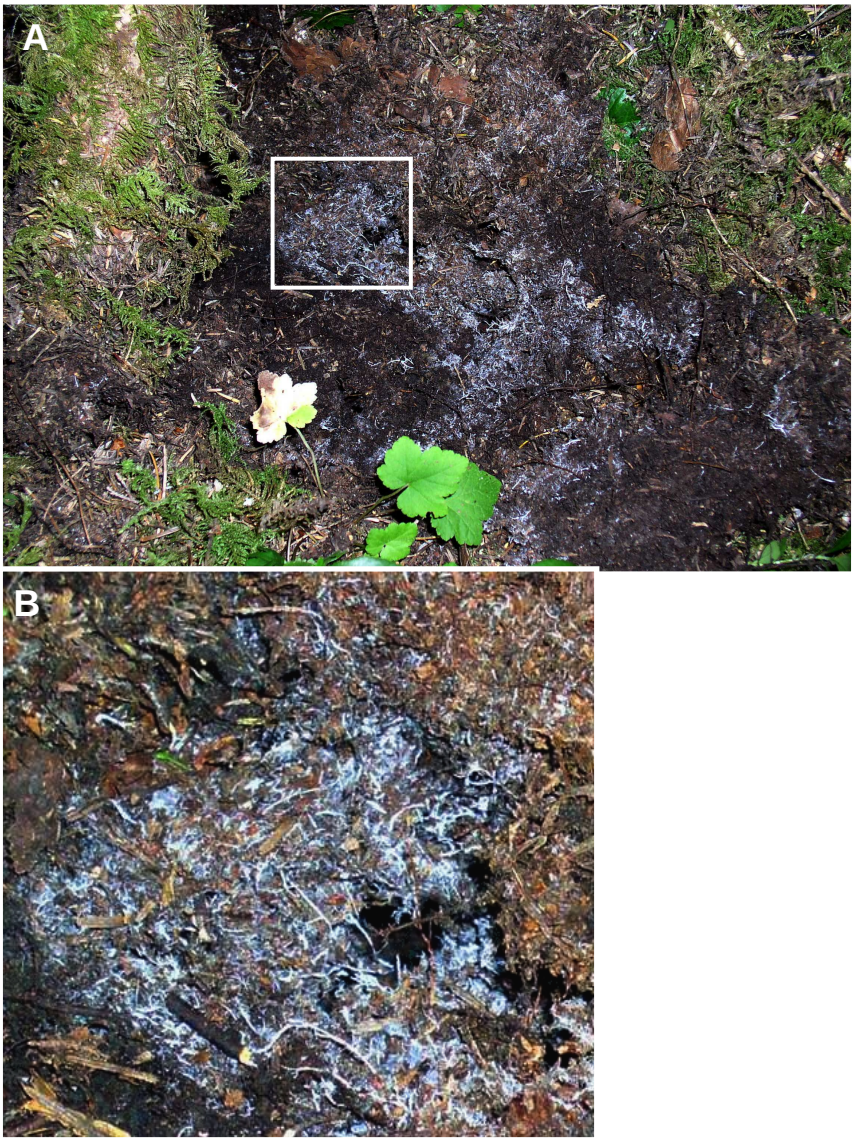

Figure 2.2. Schematic of instrumentation used for vertically partitioning soil CO_2 production.

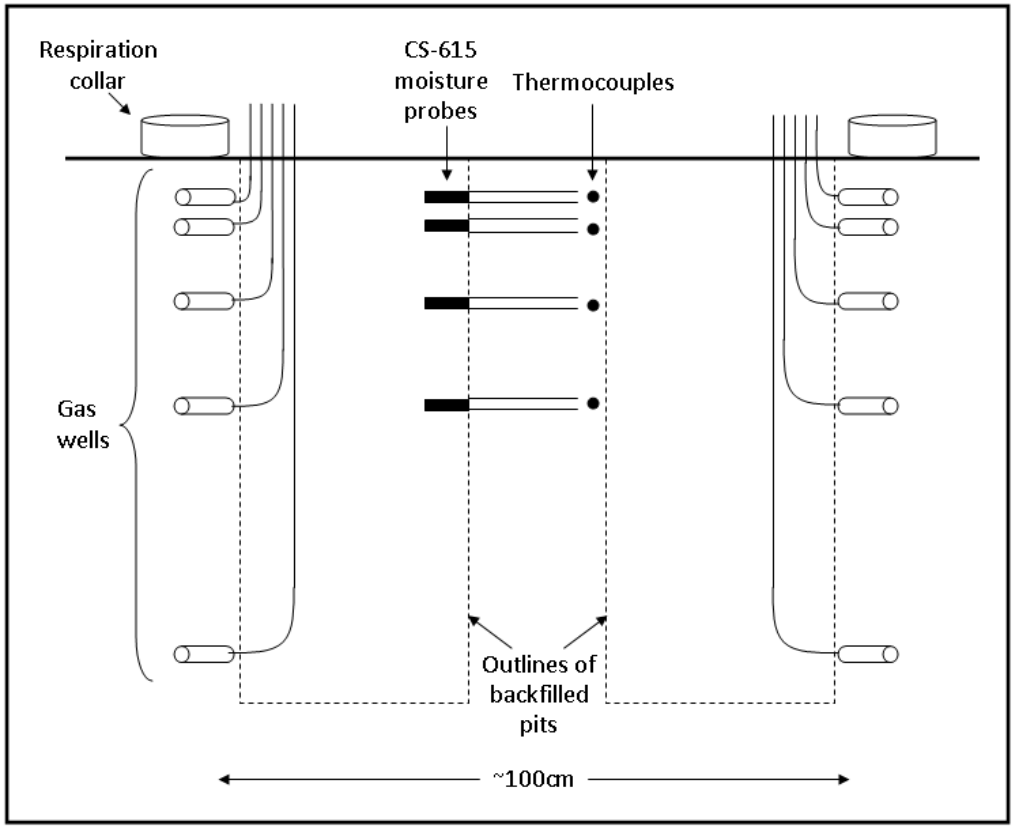

Figure 2.3. Example of soil CO_2 profiles fit with a third-order polynomial, from October 2007. Symbols denote duplicate gas wells at each depth, located approximately 1m apart.

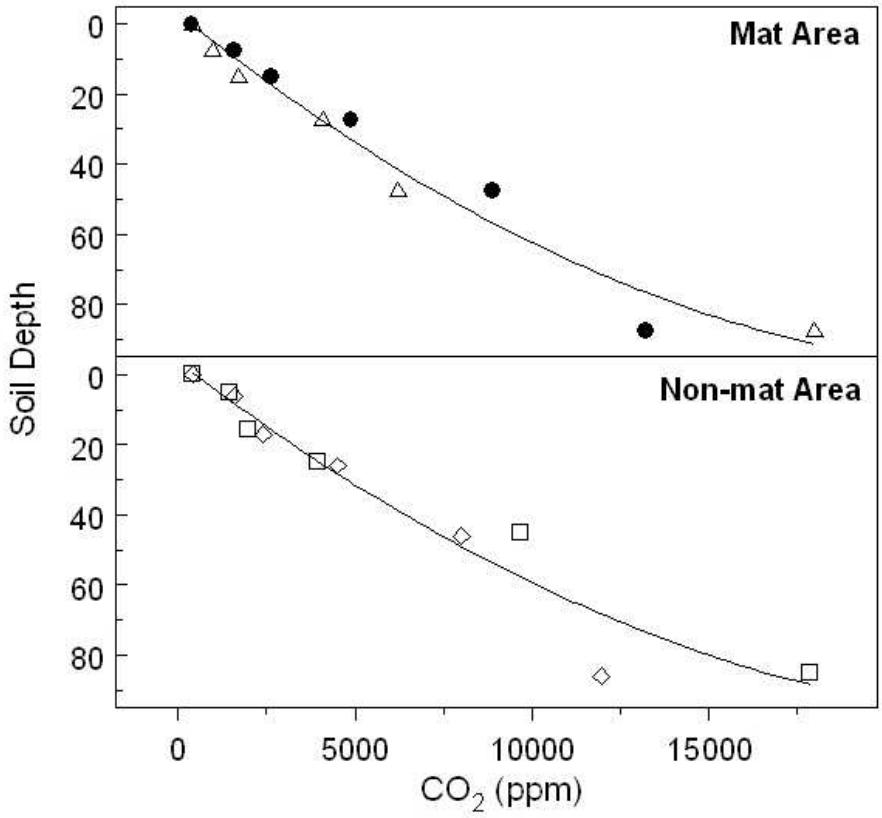

Figure 2.4. Vertical partitioning of soil respiration over time. Measured surface CO_2 flux (●) and calculated CO_2 production in the O (▲), A (■), Bw1 (♦), and Bw2 and C horizons (▼). Duplicate CO_2 profiles and surface flux rates were averaged for each area. Error bars represent the propagated uncertainty from Monte Carlo simulations.

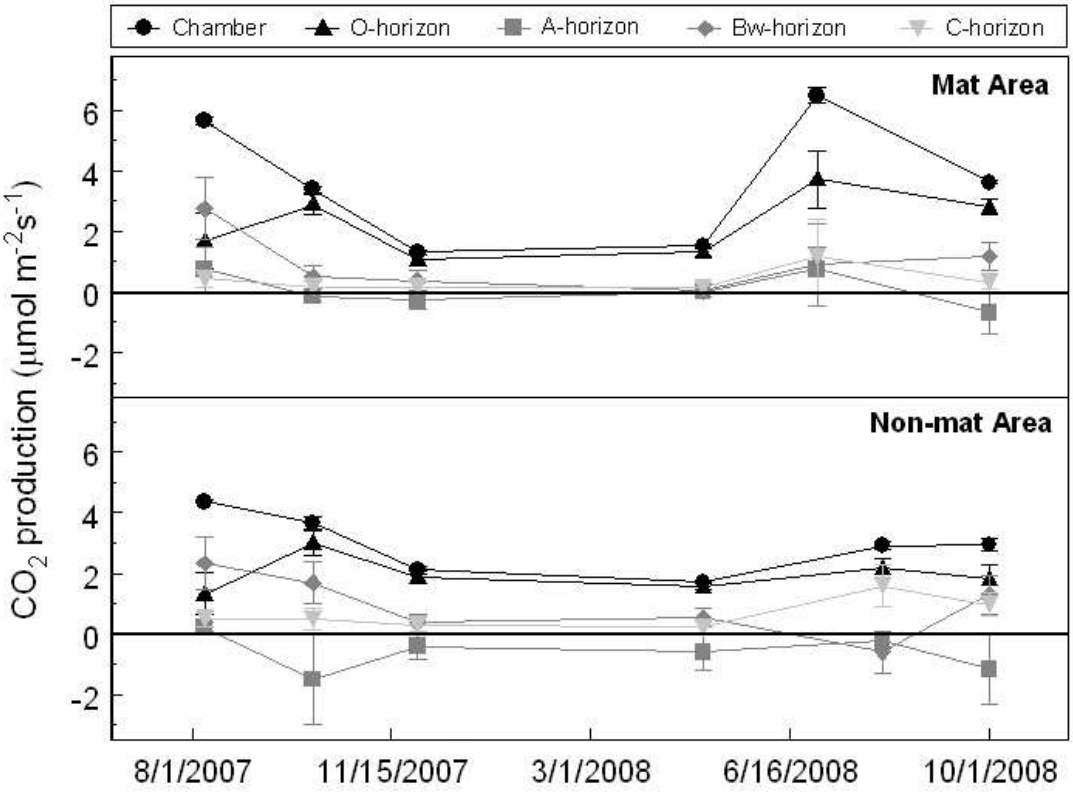

Figure 2.5. Time series of soil respiration and calculated mat contributions. A) Average respiration from mat (●) and non-mat soils (▲).B) Percent difference between mat and neighboring non-mat surface flux. Error bars are standard error.

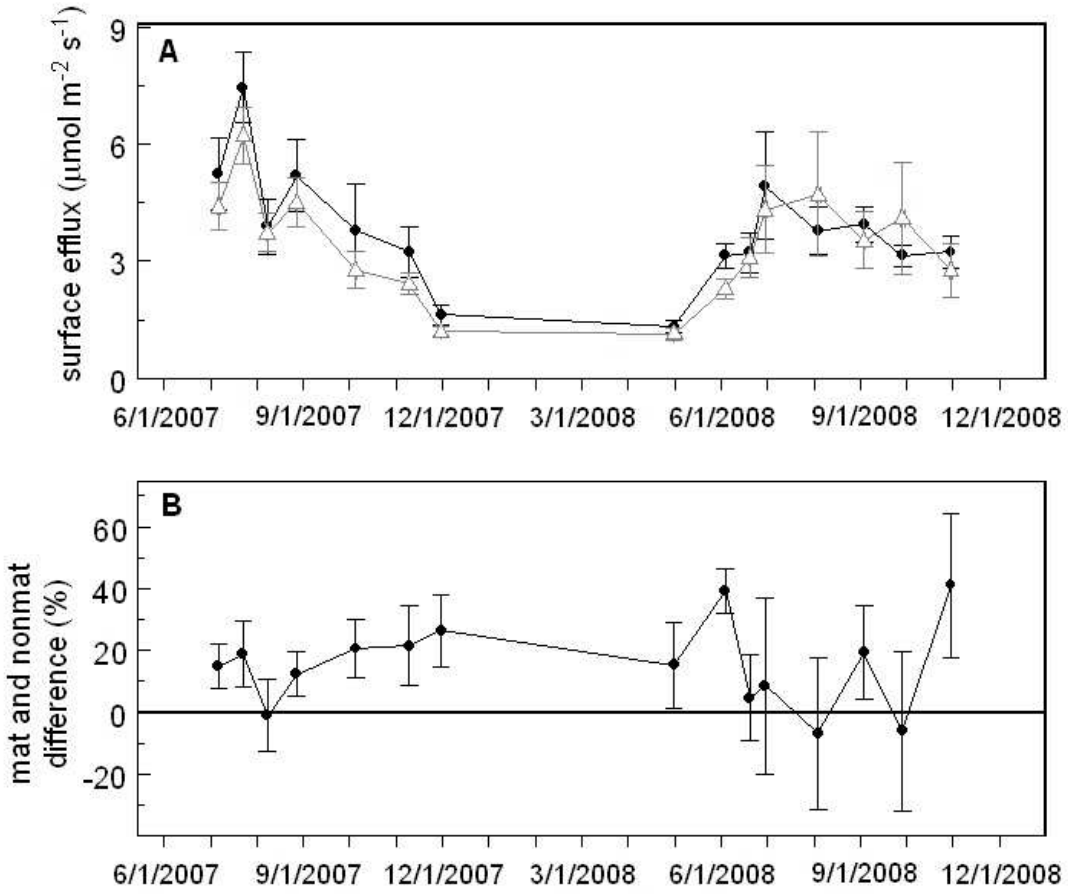

Figure 2.6. Time series of precipitation, soil moisture, and soil temperature. A) Soil temperature at 10cm depth (black) and precipitation (grey) from headquarters weather station (430m above sea level). B) Soil moisture sampled at study site. O-horizon gravimetric water content (●), and volumetric water content at 5cm (▲) and 15cm ( ) below mineral soil surface (gravimetric water content × bulk density). Error bars are standard deviation, n=5.

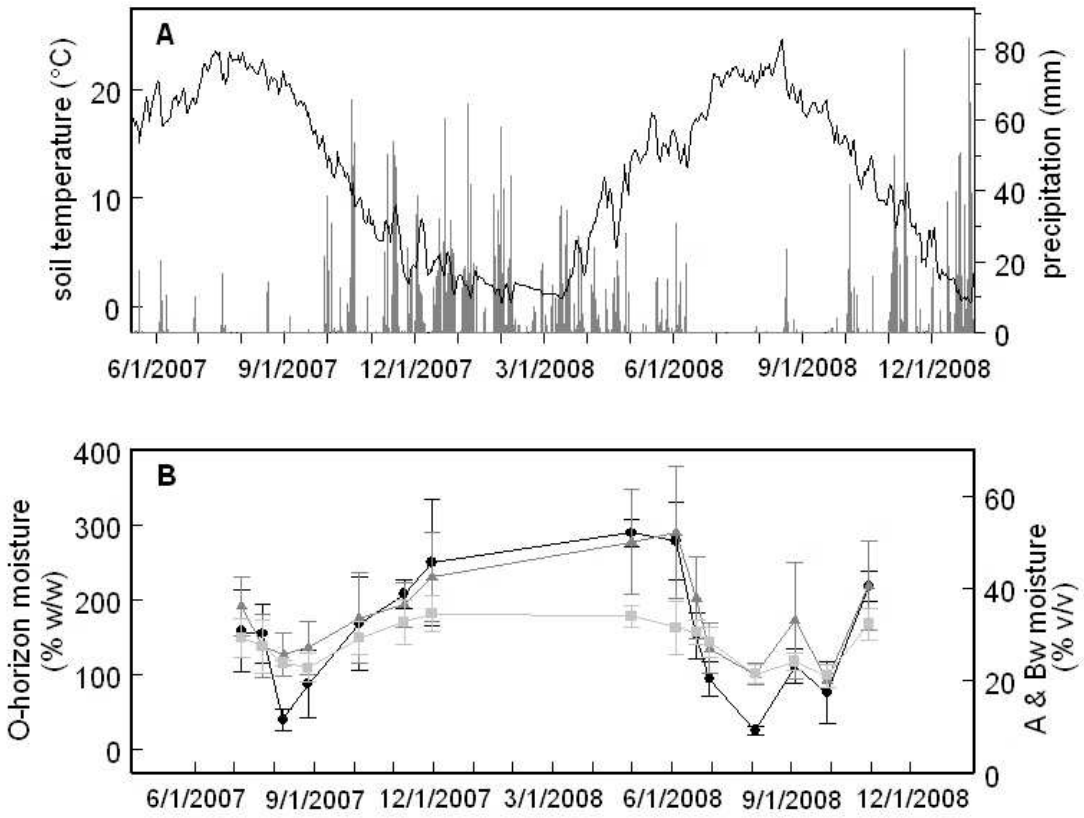

Figure 2.7. Relationship between soil temperature (10cm) and soil surface flux for mat soil (crosses), non-mat soil (squares), and the difference between mats and neighboring non-mats (circles). Soil efflux was ln-transformed from units of μmol CO_2 m^{-2} s^{-1}.

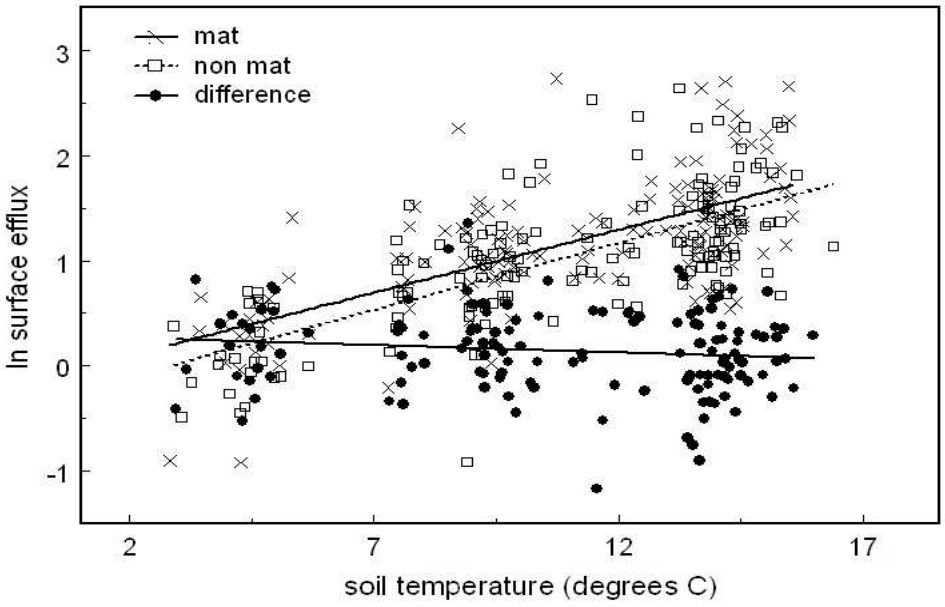

Figure 2.8. Relationship between O-horizon moisture and the difference between mat and neighboring non-mat surface flux. Surface efflux was ln-transformed from units of μmol CO_2 $m^{-2}s^{-1}$.

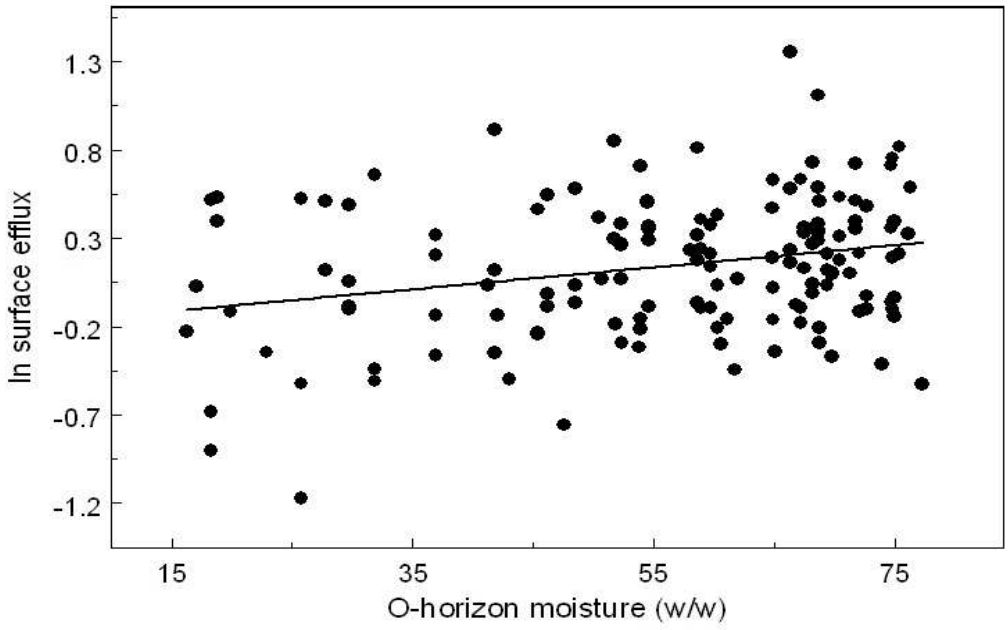

Figure 2.9.Effect of soil moisture on production from each genetic soil horizon. Water content measured at the bottom of the O-horizon (top panel), and at the top of the other genetic horizons.

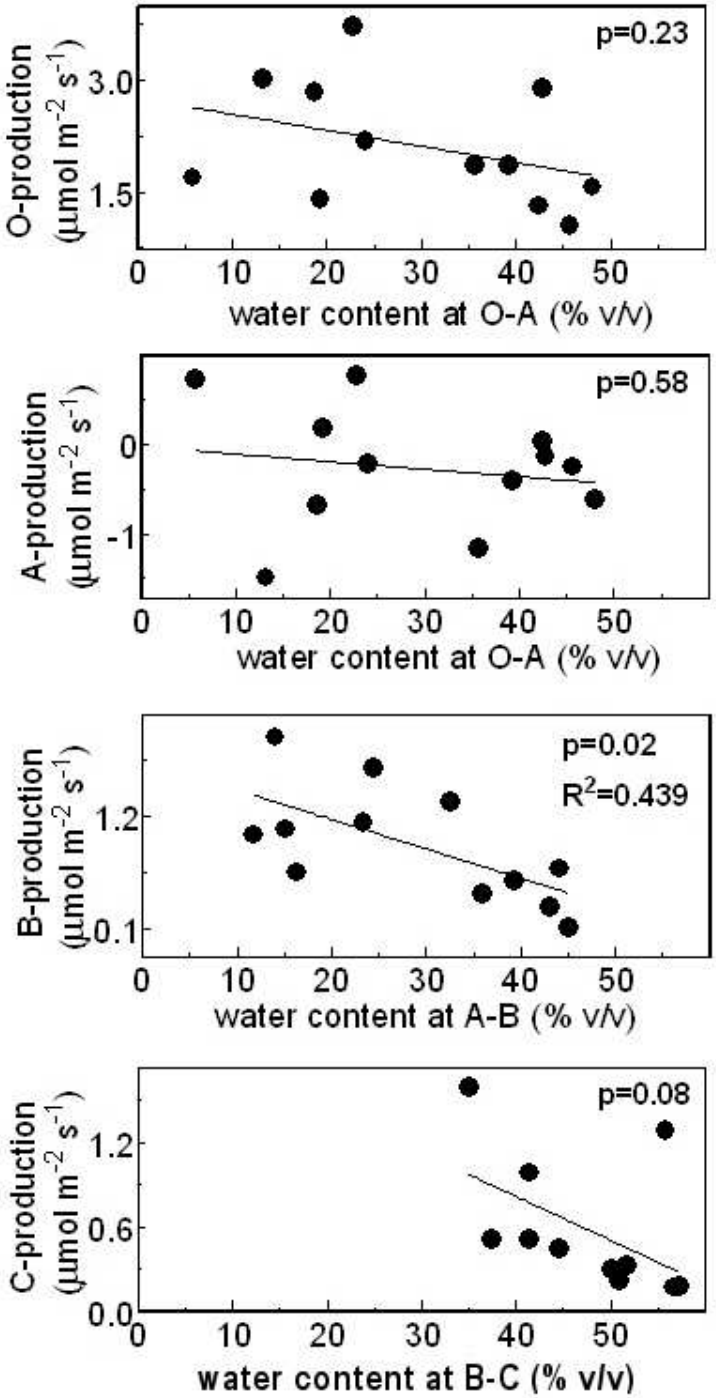

CHAPTER THREE: INTERPRETING DIEL HYSTERESIS OF SOIL RESPIRATION

Claire L. Phillips, Nick Nickerson, David Risk, Barbara J. Bond

Submitted to *Global Change Biology*
111 River Street
Hoboken, NJ 07030-5774

ABSTRACT

Increasing use of automated soil respiration chambers in recent years has demonstrated complex diel relationships between soil respiration and temperature that are not apparent from less frequent measurements. Soil surface flux is often lagged from soil temperature by several hours, which results in semi-elliptical hysteresis loops when surface flux is plotted as a function of soil temperature. Both biological and physical explanations have been suggested for hysteresis patterns, and there is currently no consensus on their causes or how such data should be analyzed to interpret respiration temperature sensitivity. In this study we employed a one-dimensional soil CO_2 and heat transport model to demonstrate a theoretical basis for lags between surface flux and soil temperatures, and to examine the influence of soil properties and environment on lag times and hysteresis patterns. Using numerical simulations, we demonstrated that diel phase lags between surface flux and soil temperature are a result of heat and CO_2 transport processes. Other factors that vary on a diel basis, such a carbon substrate supply and atmospheric CO_2 concentrations, can modify lag times and hysteresis patterns to varying degrees, but are not required to explain the existence of hysteresis between surface flux and soil temperature. Physical transport processes are especially sensitive to soil moisture, and physical effects of soil moisture on respiration dynamics may easily be confounded with biological effects. Consideration of heat and CO_2 transport processes is a requirement to correctly interpret diel soil respiration patterns.

INTRODUCTION

Soil respiration, which is often the largest flux of CO_2 leaving terrestrial ecosystems (Gaumont-Guay *et al.*, 2009; Jassal *et al.*, 2007; Ryan & Law, 2005), is likely to be an important determinant of ecosystem carbon balance under future climate scenarios. The temperature sensitivity of soil respiration is one of the more basic characteristics that ecologists would like to quantify in order to predict fluxes in changing environments. However, regressions between soil respiration and temperature often have relationships that do not agree with theoretical models, such as the commonly used Arrhenius or van't Hoff type expressions (see Davidson *et al.*, 2006a for a detailed discussion). Models based on simple reaction kinetics do not capture the biological and physical complexities of soil systems, including heat and gas transport dynamics (Davidson *et al.*, 2006b; Pavelka *et al.*, 2007; Pumpanen *et al.*, 2003; Risk *et al.*, 2002). While there is much agreement that more sophisticated, mechanistic models are required to describe and predict soil respiration, many suggestions have focused on improving descriptions of biological production (Carbone & Vargas, 2008; Trumbore, 2006), and the complexities of soil physical processes have not received the same level of attention.

In recent years, automated soil respiration chambers have gained widespread use, providing temporally-dense datasets that reveal complex relationships between soil respiration and temperature that are not apparent with less frequent survey measurements. Many researchers with automated chamber data have observed diel

hysteresis, evidenced by semi-elliptical shapes in regression plots of soil temperature and soil respiration (Figure 3.1A). These ellipses result from phase lags between the diel signals of soil temperature and soil respiration (Figure 3.1B), but there is no consensus on what causes phase lags, or how best to analyze lagged data in order to determine the temperature sensitivity of soil respiration (Gaumont-Guay *et al.*, 2009; Graf *et al.*, 2008; Pavelka *et al.*, 2007).

Two main lines of reasoning have been proposed to explain the origins of phase lags. The first is the covariate argument, that environmental factors which oscillate out of phase with soil temperature, such as carbon supply from recent photosynthate, modify CO_2 production (Riveros-Iregui *et al.*, 2007; Tang *et al.*, 2005; Vargas & Allen, 2008b). The second is the heat transport argument, that soil temperature measured at an arbitrary depth is out of sync with surface efflux, due to shifts in the phase and amplitude of soil temperature with depth (Graf *et al.*, 2008; Pavelka *et al.*, 2007). This argument is based on the fact that soil CO_2 production in an integrated response a to non-uniform temperature profile, so temperatures measured at discrete soil depths are likely to differ in both magnitude and phase from the average temperature forcing soil CO_2 production. The covariate and heat-transport explanations are not mutually exclusive, and both factors are likely to play important roles in diel soil respiration dynamics. An additional factor that has not been discussed extensively is that gas diffusion through soil imposes a lag between the time of CO_2 production at depth and release from the soil surface.

Lag times between soil respiration and temperature, and the semi-elliptical forms produced when these variables are plotted against each other, have been shown to vary seasonally with soil moisture (Carbone *et al.*, 2008; Riveros-Iregui *et al.*, 2007; Tang *et al.*, 2005; Vargas & Allen, 2008b). All of the processes mentioned above—substrate supply, heat transport, and CO_2 diffusion—are influenced by soil moisture and can provide partial explanations for seasonal changes in diel hysteresis. However, environmental influences other than moisture may be important as well, as hysteresis patterns can change day-to-day under conditions where soil moisture is fairly constant (Figure 3.1A).

These dynamic patterns complicate the goal of measuring the temperature sensitivity of respiration *in-situ*. Determining the temperature response of surface flux requires first disentangling the effects of temperature from other diel environmental drivers, and second, relating surface flux rates to non-uniform CO_2 production and temperature profiles. In this study we aimed to provide a conceptual framework and a modeling tool for analyzing diel soil respiration patterns. Using basic principles of gas diffusion and heat transport, we modeled the expected lag times and hysteresis patterns between soil temperature and surface flux due to physical transport processes. First, we examined how predicted hysteresis patterns changed as a function of temperature at different soil depths. Second, we performed sensitivity analyses to determine the impacts of variations in soil physical and environmental factors on lag times. We continued by simulating increasingly complex and realistic field scenarios, including

simultaneous changes in temperature and other environmental variables with diel periodicity such as atmospheric CO_2 and carbon substrate supply. These simulations show how hysteresis patterns between soil surface flux and temperature can take shape in response to both physical and biological drivers.

METHODS

Model Description

We modified the 1-dimensional soil CO_2 transport model described by Nickerson and Risk (2009c) so that it had the following functionality: 1) a CO_2 transport component governed by Fick's First law of diffusion, 2) a heat transport component that shifts and dampens oscillating air temperatures with increasing soil depth, and 3) a simple CO_2 production function that adjusts production rate in each soil layer by the depth and temperature of the layer.

The modeled environment assumes a well-mixed atmospheric boundary layer and a soil profile of length L (m) that is divided into 100 uniform layers. Each layer has specific values for total porosity, volumetric water content, and air-filled porosity. Air-filled porosity is used in turn to calculate both gas diffusivity (D_{CO2}) and thermal diffusivity (D_T), based on empirical relationships from the literature (details below). D_{CO2} and D_T, along with CO_2 and temperature gradients, determine the rate of heat and CO_2 transport, respectively. For the purposes of these instructive simulations soil

physical properties and diffusivities were assumed to be constant throughout the soil profile.

The CO_2 transport component of the model allows gas exchange between neighboring soil layers following concentration gradients. Flux rates between layers are determined with the discrete, one-dimensional form of Fick's First Law:

$$F_{ij} = -D_{ij} \frac{\Delta C_{ij}}{\Delta z_{ij}} \quad (1)$$

where D_{ij} is the effective CO_2 diffusion coefficient between two soil layers (layer *i* and layer *j*), ΔC_{ij} is the difference in layer CO_2 concentrations (μmol m^{-3}) and z_{ij} is the difference in the depths (m) of the two layers. Temperature-corrections for diffusivity are calculated for each layer at each model time step as follows:

$$D_i = D_0 \left(\frac{T_i}{T_0} \right)^{1.75} \quad (2)$$

where D_0 is soil diffusivity at reference temperature T_0 (273K), and T_i is the ambient temperature (K) of layer *i*.

At each model time step (1s) a new CO_2 concentration in each layer (C_i) is calculated as function of the layer depth:

$$C_i(z,t) = \frac{C_i(z,t-1)\theta \cdot L/N + F(z-1) - F(z) + \gamma(z)}{\theta \cdot L/N} \quad (3)$$

where $C_i(z, t\text{-}1)$ is the layer concentration at the previous time step, θ is the soil air-filled pore space, $F(z\text{-}1)$ is the flux from the layer below, $F(z)$ is the flux leaving the

layer, $\gamma(z)$ is layer CO_2 production (μmol m^{-3} s^{-1}), L is the total depth of the soil column and N is the total number of soil layers.

Unless otherwise noted, biological CO_2 production decreases with soil depth according to the following exponential function:

$$\gamma(z) = \frac{\Gamma}{\sum_{z=0}^{L} \exp\left(\frac{-z}{d_p}\right)} \exp\left(\frac{-z}{d_p}\right) \quad (4)$$

where Γ is total soil production (μmol m^{-3} s^{-1}), z is the layer depth, and d_p is the exponential folding layer, or the layer at which the proportion of total soil production remaining is 1/e (0.37). By manipulating d_P, CO_2 production can be confined mostly to shallow soil layers, or spread more evenly across the soil profile.

A basal value for total soil CO_2 production (Γ_0), representing production at the average temperature of the atmosphere and profile (T_{ave}), is defined by the user and partitioned with equation 3 to give layer-specific basal production ($\gamma(z, T_{ave})$). At each time step, layer production is adjusted in response to the current layer soil temperature $T(z, T)$ using a modified van't Hoff relationship.

$$\gamma(z, T) = \gamma(z, T_{ave}) \times Q_{10}^{((T(z,t)-T_{ave})/10)} \quad (5)$$

The heat transport component models air and soil temperature as sinusoidal curves (Hillel, 1998), where soil temperature is shifted and damped from the air temperature curve as a function of depth.

$$T(0,t) = T_{ave} + A_0 \sin(\omega t) \quad (6)$$

$$T(z,t) = T_{ave} + A_0[\sin(\omega t - z/d_T)]e^{-z/d_T} \quad (7)$$

$T(0,t)$ is the temperature at the soil surface (z=0), A_0 is the amplitude of the surface temperature fluctuation (1/2 of the total daily range), and ω is the radial frequency, which converts time to radians. For a sine wave oscillating on a period of 1day (86,400s), ω = 2π/86,400. The constant d_T is the thermal damping depth, and is defined as the depth at which temperature amplitude decreases to the fraction 1/e. Thermal damping depth (m) is related to thermal diffusivity (D_T) as follows:

$$d_T = \sqrt{2D_T/\omega} \quad (8)$$

One should note that the two parameters in the heat transport equations that vary with environment are diel air temperature amplitude (A_0), and thermal diffusivity (D_T).

Model Implementation

To examine the consequences of heat transport and CO_2 diffusion on diel hysteresis patterns of surface CO_2 flux, we defined a set of default soil physical and environmental conditions (Table 3.1), based on measurements of a sandy loam soil from the HJ Andrews Experimental Forest in the western Cascades of Oregon, USA (44.2ºN, 122.2ºW). Further description of the site and soil is provided by Pypker *et al*. (2008). Default environmental conditions are characteristic of early summer. For sensitivity analyses, we varied each of these parameters across a large range of realistic values. Soil depth was modeled as 100cm for all scenarios.

Realistic values for D_{CO2} at different soil moisture contents were modeled using the relationship described by Moldrup *et al*. (2000), which expresses soil gas diffusivity as a function of air-filled porosity and soil moisture release characteristics:

$$D_P = D_0 \times (2\ _{100}{}^3 + 0.04\ _{100}) \left(\frac{}{100} \right)^{2+3/b} \qquad (9)$$

D_P is soil gas diffusivity, D_0 is gas diffusivity in free air (1.39×10^{-5} m^2s^{-1} for CO_2 at 273K and 1atm) , ε is the ambient air-filled porosity, ε_{100} is the air-filled porosity at -100cm H_2O tension (~10kPa), and *b* is the slope from a log plot relating volumetric water content to soil water potential. We used coefficients determined from twelve intact soil cores taken from the HJ Andrews Experimental Forest. Moisture-release coefficients were determined by treating cores on pressure plates at pressures ranging from 10-150kPa.

Table 3.1. Default parameters for model simulations. Deviations from these values are noted in text or figures.

Parameter	Default value
soil porosity	0.65 (v/v)
air-filled porosity (Θ)	0.30 (v/v)
thermal diffusivity (D_T)	6.41×10^{-7} m^2 s^{-1}
gas diffusivity (D_{CO2})	1.29×10^{-6} m^2 s^{-1}
production exponential folding depth (d_P)	10cm
atmospheric CO_2	385 ppm
average air and soil temperature (T_{ave})	15˚C
air temperature amplitude (A_0)	7.5˚C
Q_{10}	2
total basal CO_2 production (Γ_0)	1.5 μmol m^{-2} s^{-1}

To parameterize D_T at different moisture levels, we used a published dataset for a sandy-loam soil of D_T measurements from intact soil cores across air-filled porosities ranging 0-0.60 (Ochsner *et al.*, 2001). To interpolate between measured porosities we fit the data with a 2nd order polynomial.

Simulations were initiated with a spin-up period for modeled CO_2 flux to stabilize. The spin-up period was deemed sufficiently long when daily maximum soil surface flux values were constant for at least five consecutive model days. To minimize spin-up time, simulations were initialized with the steady-state solution proposed by Cerling (1984) for a uniform profile. The model was solved by Euler integration with a computation time step for all simulations of 1s, and model output was recorded every 300s.

Two synthetic tests were conducted to examine the performance of the CO_2 transport component under steady-state and transient conditions. The steady-state test served to assess numerical errors associated with discretizing the soil profile into layers. This test entailed modeling uniform production profiles across a range of gas diffusivities, and comparing the modeled concentration profiles to Cerling's steady-state solution. We found soil concentration errors due to discretization to be less the 0.5% across all diffusivity levels. The transient test examined time lag errors related to iterating the model in discrete time steps. We varied CO_2 concentration at the upper boundary layer (atmosphere) as a sinusoidal wave, and compared the phase lags between peak CO_2 concentrations in the atmosphere and soil with the theoretical phase lag described by Beltrami (1996):

$$\delta = \frac{z}{2}\sqrt{\frac{\tau}{\pi \cdot D_{CO2}}} \qquad (10)$$

where δ is the phase lag (seconds), z is soil depth (m), τ is the period over which atmospheric CO_2 oscillates (1 day or 86,400s), and D_{CO2} is the effective CO_2 diffusivity of soil (m^2s^{-1}).

RESULTS AND DISCUSSION

Relationship between the depth of soil temperature measurements and hysteresis

Modeling results showed that hysteresis patterns for surface flux and soil temperature changed with soil depth, due to the attenuation and phase shift of soil temperature oscillations with increasing depth (Figure 3.2). Both the rotational direction of hysteresis loops and their orientation varied depending on the lag time between surface flux and temperature. For example, for the exponential production profile modeled in Figure 2, most production occurred close to the soil surface and soil respiration was most closely synchronized with soil temperature at 5cm depth (lag time $\leq$ 5 minutes). At 5cm depth and above, temperature peaked before surface flux, resulting in clockwise hysteresis loops, and at deeper depths soil temperature peaked after surface efflux, resulting in counter-clockwise hysteresis loops (see arrows in Figure 3.2).

Lag time also determined the orientation, or the principle axes, of the hysteresis loops, which in turn impacted the slopes of least mean square fits to the data. This phenomenon is described in detail by (Smerdon *et al.*, 2009), and similarly, others have observed that the apparent temperature sensitivity of soil respiration differs depending on the depth where temperature is measured (Graf *et al.*, 2008; Pavelka *et al.*, 2007). The reason for the change in regression slope with lag length can be seen clearly by inspecting the trigonometric expression for an ellipse. As adapted from Beltrami (1996),

two sine waves that are offset by a phase lag give the equation of an ellipse when superimposed perpendicularly:

$$R = R_A \frac{T}{T_A} \cos\delta + R_A \sqrt{\left(1 - \frac{T^2}{T_A}\right)} \sin\delta$$

where R_A and T_A are the amplitudes of respiration rate and temperature, respectively, R and T are instantaneous respiration rate and temperature, respectively, and δ is the phase lag (expressed in radians).

One should note that for the simulations shown in Figures 3.2 and 3.3, soil respiration did not form a perfect sine wave because it was simulated with an exponential response to soil temperature, with disproportionally greater responses at high temperatures than at low temperatures. This produced the curvilinearity observable in the ellipses in Figure 2. The simplified case of two perfect sine waves, however, is instructive for demonstrating that lag length determines the principle axes of an ellipse. When δ is a full period (equivalent to a 0 or 24 hour lag), the expression of an ellipse simplifies to a straight line with positive slope. For a ½ period (12 hours) the expression simplifies to a straight line with negative slope. For phase lags of ¼ period (6hrs) the result will be a horizontal ellipse. It is possible to observe any of these orientations within a soil profile depending on the depth of soil temperature measurements.

Because the apparent temperature sensitivity of surface flux varies with temperature measurement depth, an important question emerges: at what depth should soil temperature be measured to provide the best estimates of the true respiration

temperature sensitivity? Unfortunately, there is no simple answer to this question because, as the following simulations show, the relationship between surface flux and temperature at any depth is not constant and varies with environmental conditions. Furthermore, because surface flux is an integrated response to temperature across the production profile, no single discrete soil depth can consistently provide a measure of the average temperature forcing soil respiration. Even at depths where there is no time lag between temperature and surface flux, fitting a regression often will not produce a reasonable estimate of respiration temperature sensitivity. For example, in Figure 2, surface flux is nearly synchronized with 5cm soil temperature and little hysteresis is apparent, so it may be tempting to fit an exponential curve directly to these data and calculate a Q_{10} value. However, the apparent Q_{10} that would be calculated from this analysis would be 1.53, which is substantially smaller than the actual Q_{10} (2.0) that was used to parameterize the model, shown in grey.

Although CO_2 production is concentrated close to the soil surface in our model simulations, production occurs throughout the soil, and it is necessary to consider temperatures across the whole production profile to understand how respiration responds to temperature, rather than at a single depth. Furthermore, surface flux is not only a response to current soil temperatures, but also to past soil temperatures, because of the time required for CO_2 produced at depth to diffuse to the soil surface.

Despite these complexities, for practical purposes soil temperature measurements in field studies are often restricted to one or a few discrete soil depths. In

our study we tried to strengthen conceptual links between processes that take place across the entire soil production profile, and patterns that may be observed in field data, by discussing lag times using an arbitrary reference depth of 10cm for soil temperature. Also, because our simulations employ an exponential relationship between temperature and CO_2 production, the time offsets between daily maximum respiration and temperature differ slightly from the time offsets between minimum values. For simplicity we only report lag times between maxima, noting when trends differ for lag times between minima.

Sensitivity of lag time to thermal diffusivity

Thermal diffusivity (D_T) influences the speed with which changes in air temperature propagate through soil, and the depth to which diel variations in air temperature are detectable (Figure 3). D_T increases with air-filled pore space, and therefore varies both with soil texture and moisture. As D_T was increased in the model, changes in air temperature propagated through soil more quickly, which shortened lags between soil temperatures and surface flux. Variations in D_T had a larger effect on lag time then any other single factor we examined, although the effect was non-linear (Figure 3.4A). Lag times varied six-fold for values of D_T within the range of 1 to 10^{-7} m^2s^{-1}, which is the approximate range for mineral soils experiencing normal field moisture levels (Ochsner *et al.*, 2001). Lag times increased substantially for lower D_T values in the range of $1\text{-}10^{-8}$ m^2s^{-1}, which corresponds with the range for organic soils

(Hillel, 1998). Under field conditions, D_T would be expected to increase as a result of soil drying. Soil drying would therefore cause an increase in lag time, with the largest increases expected for soils with porous textures or profiles with well-developed organic horizons.

Sensitivity to CO_2 diffusivity and production depth

In contrast to D_T**,** large changes in simulated D_{CO2} had a relatively small effect on lag time (Figure 3.4A), but D_{CO2} nevertheless had impacts that are essential for interpreting temperature-respiration relationships. The impacts of D_{CO2} are best understood by first considering what happened to CO_2 concentrations within the soil profile as we changed D_{CO2}. As D_{CO2} was increased in the model, lag times between CO_2 concentration and temperature measured at the same depth became smaller (Figure 3.5A). This is because CO_2 diffusion from soil becomes less restricted with increasing D_{CO2}, and the rates at which CO_2 is produced in soil and diffuses out become more closely balanced. The ability of soil to store CO_2 is reduced, and as a result, changes in CO_2 production, as occur in response to temperature, have a greater and more immediate impact on CO_2 concentrations within the soil profile (Riveros-Iregui *et al.*, 2007). Increasing D_{CO2} allows changes in soil temperature to more rapidly alter soil CO_2 concentrations.

In comparison, increasing D_{CO2} did not consistently decrease lag times between surface flux and soil temperature. The effects of D_{CO2} on lag times varied depending on

both the distribution of CO_2 production and the depth of the reference temperature. For a soil profile in which production is concentrated near the surface and decreases exponentially with depth (Figure 3.5B), the phase of the surface flux sine wave shifted closer to the waves of near-surface temperatures as D_{CO2} increased, but shifted farther away from the waves of deep soil temperatures. In other words, if soil temperature was measured near the surface lag times decreased, but if soil temperature was measured deeper in the soil (e.g. 10cm) lag times increased. For example, Figure 3.4A shows lag times between surface flux and soil temperature at 10cm increasing with D_{CO2}, a result that may seem counter-intuitive unless one understands that in these simulations 72% of production occurred above 10cm, so respiration was most heavily influenced by more shallow temperatures. In contrast, when CO_2 production was uniformly distributed throughout the soil, a greater proportion of CO_2 came from deep soil layers (Figure 3.5C), so increasing D_{CO2} caused the phase of the surface flux sine wave to shift closer to deep soil temperatures and to shift farther from air and near-surface temperature. As D_{CO2} increased, CO_2 storage within the profile decreased, permitting CO_2 produced at depth to have a more immediate impact on surface flux rates.

Similar reasoning helps to explain the sensitivity of lag time to variations in production depth when D_{CO2} was held constant. Figure 3.4A shows changes in the depth of CO_2 production with respect to the exponential folding depth, d_p, where a higher d_p indicates production is spread more evenly across the soil profile and a lower d_p indicates production is confined more to the shallow subsurface. Changes in production

within the shallow subsurface (e.g. an increase in d_p from 5cm to 10cm) had greater impacts on lag time than changes in production deeper within the soil (e.g. an increase in d_p from 60cm to 70cm), because most diel variability in soil temperature occurred at shallow depths. Even at very high D_T, diel temperature oscillations occurred primarily within the top few centimeters of soil. For example, for the maximum D_T plotted in Figure 3.4A (D_T= 9^{-7} m^2s^{-1}), temperature amplitude decreases to approximately one-third by 16cm depth. CO_2 production deep in the soil profile varied little throughout the day because it experienced a relatively constant temperature environment, so increasing production from deep soil did little to shift diel respiration oscillations.

As has been noted by Chen *et al.* (2009), production depth also has important impacts on the diel variation of soil respiration rates. Production profiles that are weighted towards shallow soil depths have greater diel variability than profiles with deep production, reflecting the greater temperature variability in shallow soil. This is important for interpreting surface flux-temperature relationships because surface flux from a profile with substantial deep production will appear to be fairly insensitive to soil temperature measured at an arbitrary shallow depth (e.g.10cm), when in fact temperature variation is small in deeper soils where much of CO_2 production originates.

Sensitivity to air temperature amplitude, Q10, and basal respiration rate

The principles described above lay a foundation for understanding the impacts of many other variables on respiration-temperature lags. Variables that cause non-

uniform changes in temperature across the soil profile, or non-uniformity in how respiration responds to temperatures across the soil profile, will tend to impact lag times. Here we provide several more examples.

As the diel amplitude of air temperature (A_0) was increased in the model, shallow soil depths experienced bigger variations in temperature than deep soil layers, since diel oscillations damped with depth. Furthermore, high temperatures had a greater affect on CO_2 production than low temperatures, due to the exponential function used to model the response of CO_2 production to temperature. As a consequence of these non-uniform dynamics, as A_0 was increased, the combination of higher temperature maxima at shallow soil depths and greater sensitivity of production to these high temperatures tended to shift maximum daily surface flux closer to maximum daily temperatures at shallow soil depths. Lag times between surface flux and shallow soil temperatures decreased with larger values of A_0, while lag times between surface flux and deeper soil temperatures (e.g. 10cm) increased (Figure 3.4B). In contrast, lag times between minimum surface flux and minimum soil temperature tended to exhibit the reverse trend (results not shown). Shallow soil layers experienced more extreme minimum values with increasing values of A_0, and contributed proportionately less CO_2 to surface flux at temperature minimums.

Based on this reasoning, we might also expect that increasing the sensitivity of CO_2 production to temperature would have similar effects, causing daily peak surface flux to become more closely synchronized with near-surface temperatures, and daily

minimum flux to become more closely synchronized with deep soil temperatures. We expected that if we increased Q_{10}, the phase lag between peak surface flux and 10cm temperature would increase as surface flux became more sensitive to the maximum temperatures of near-surface soil layers. Our simulations supported this prediction in part; however, an increase in Q_{10} did not produce a monotonic increase in lag time (Figures 3.4B & 3.6). Lag time initially decreased between Q_{10} values 1-1.4, before increasing slightly between Q_{10} values 1.4-3. For Q_{10} values close to 1 (production has little temperature sensitivity), surface flux exhibited a small amount of temperature sensitivity due to temperature dependence of the D_{CO2} parameter. At fairly low Q_{10} values, however, these small changes in D_{CO2} were obscured by temperature-dependent changes in production.

In contrast to changes in air-temperature amplitude and Q_{10}, which had non-uniform effects on soil temperatures and production rates across the soil profile, increases in the basal CO_2 production rate did not influence lag times (Figure 3.4B). Changing basal production rate alone did not alter the distribution of CO_2 production profile, and therefore did not alter the proportional contribution from each soil layer to surface flux.

Effects of soil moisture

To model the effects of soil moisture on lag time, we allowed both D_T and D_{CO2} to vary simultaneously as functions of air-filled porosity (Figure 3.7A and B). D_T and

CO_2 have different relationships with soil moisture: heat propagates more quickly through water than through air-filled pore spaces, whereas CO_2 propagates more quickly through air-filled pores than through water. As simulated soil moisture was decreased, increases in D_{CO2} and decreases in D_T both led to an increase in lag time for 10cm soil temperature (Figure 3.7A), for the reasons explained above. This modeled trend is consistent with field observations in several studies. Under oak canopies, Tang *et al*. (2005) observed increasing lag times between surface flux and soil temperature at 8cm depth as soils dried, although they attributed the lag to the influence of tree photosynthesis on respiration of the rhizosphere rather than to gas and temperature transport processes (discussed more below). Our results showed that as soil moisture decreased and lag times between surface flux and soil temperatures increased, the resulting hysteresis patterns became more elliptical and less linear (Figure 3.7B). This phenomenon has been observed in mixed conifer forests (Vargas & Allen, 2008b) and shrub ecosystems (Carbone *et al.*, 2008). In both of these field studies, periods of most pronounced diel hysteresis coincided with the driest parts of the growing season.

The results from the field studies mentioned above seem to contrast with findings of Riveros-Iregui *et al*. (2007), who observed less pronounced hysteresis between soil CO_2 concentrations and temperature at 20cm depth as soil dried. However, as explained earlier, lag times between soil temperature and CO_2 concentration at the same depth behave differently than surface flux, tending to decrease with higher vales of D_{CO2}. The decreased lag time between CO_2 concentration and temperature at the

same depth results in more linear and less elliptical hysteresis relationships. In addition, similar patterns can occur as a result of soil moisture effects on biological activity and CO_2 production. As soil dries and production declines, the magnitude and diel range of surface flux and subsurface concentrations decrease, and hysteresis can appear to become less pronounced over time.

To demonstrate the potential impacts of moisture on biological activity, we added an additional level of complexity to the moisture simulation by decreasing basal CO_2 production rate as a linear function of soil dryness (Figures 3.7C and D). As the diel amplitude of surface flux decreased, hysteresis appeared to become more linear and horizontal (Figure 7D); however, this was a result of the magnitude and daily range of respiration changing rather than a change in the principle axes of the ellipses. Lag times, which control the shape and orientation of hysteresis loops, remained unaffected by altered production rates (Figure 3.7C). As mentioned above, simulated changes in basal production rate alone did not affect lag times unless the distribution of production was also changed.

These examples demonstrate the difficulty of teasing apart moisture-dependent biological and physical processes that are potential drivers of diel respiration patterns. For example, it would be logical to interpret an increase in lag time between surface flux and soil temperature as the soil dries as a product of substrate limitations (Carbone *et al.*, 2008). Substrate limitations are indeed coupled with soil moisture, since low moisture can reduce canopy production and allocation of photosynthate below ground

(Irvine *et al.*, 2002; Irvine *et al.*, 2005), and also reduce diffusion of carbon substrates through soil (Davidson *et al.*, 2006a). But increasing lag times can also result from moisture influences on D_T and D_{CO2} (Fig 3.7a), so it is unlikely that such patterns would be due to substrate limitations alone. Similarly, declines in the amplitude and apparent temperature sensitivity of surface flux with decreasing soil moisture have been attributed to reduced substrate supply, although heat transport effects produce similar results (Fig 3.7b).

Numerical simulations provide a theoretical limit to the impact of soil physical processes on lag times. We found that phase lags between surface flux and a reference temperature at 10cm depth are between 1-3.5 hours for mineral soils across a wide range of soil physical and environmental conditions (Figures 3.4 & 3.7). Lag times greater then this may be indicative of other biological factors influencing soil respiration. For example, Tang *et al*. (2005), found an approximately four hour lag between soil surface flux and temperature at 8cm depth under an oak tree canopy, and no lag in an adjacent area of dead annual grasses. This large difference in lag times is unlikely to be a result of physical processes alone, since soil temperature data indicate D_T was similar in the two locations. As Tang *et al*. concluded, photosynthetic carbon supply may have influenced the different diel patterns in these two locations.

Diel variation in atmospheric CO_2

Concentrations of atmospheric CO_2 within and near plant canopies often vary on a diel basis, due to plant gas exchange taking up CO_2 during the day and releasing CO_2 at night. We simulated diel oscillations in atmospheric CO_2 as a sinusoidal wave with a daily range of 50ppm. Data from the HJ Andrews Experimental Forest indicated that daily minimum CO_2 concentration at the soil surface may be lagged from maximum temperature by as much as +/- 5 hours, so we hypothesized that diel changes in atmospheric CO_2 could modify surface flux and contribute to diel hysteresis between surface flux and temperature. Our simulations suggested, however, that atmospheric CO_2 has a very small effect on flux rates compared with effects of temperature variation. When air and soil temperature were held constant, varying atmospheric CO_2 alone changed surface flux rates by less than 0.5% (Figure 3.8A). In contrast, when atmospheric CO_2 was held constant and air temperature was allowed to vary daily by 15ºC, even a very small Q_{10} value of 1.2 resulted in surface flux rates changing by 6.8% daily. CO_2 production requires little temperature sensitivity to swamp the effects of atmospheric CO_2 variations, when moderate daily temperature variations occur.

To further test the hypothesis that diel changes in atmospheric CO_2 could modify surface flux, we modeled a time series in which minimum CO_2 occurred 3 hours before or after peak air temperature (Figure 3.8B). With Q_{10} equal to 2, modeled surface flux rates varied by approximately 50%, much greater than the effect of atmospheric CO_2 alone. We could not detect any effect of varying atmospheric CO_2 on lag time or

diel hysteresis. Atmospheric CO_2 had only a small effect on surface flux rates because CO_2 flux was driven by concentration gradients between the atmosphere and soil that were much greater then diel variations in atmospheric CO_2.

Changing substrate supply

Several lines of evidence have indicated close links between canopy carbon supply and soil respiration rates, including phloem girdling studies (Högberg *et al.*, 2001; Tedeschi *et al.*, 2006), studies across natural gradients of root abundance (Tang *et al.*, 2005), lag analyses between canopy variables and soil respired $\delta^{13}CO_2$ (Ekblad *et al.*, 2005; Fessenden & Ehleringer, 2003; Kodoma *et al.*, 2008; McDowell *et al.*, 2004), and isotopic labeling studies of photosynthate (Bahn *et al.*, 2009; Högberg *et al.*, 2008). We simulated potential impacts of diel variations in subsurface photosynthate supply on hysteresis in the respiration versus temperature relationship. We modeled diel variation in photosynthate supply as a simple linear function of PAR, increasing basal soil CO_2 production rate from 1.5μmol m^{-2} s^{-1} at night to 3μmol m^{-2} s^{-1} in response to peak PAR (Figure 9A). Since phloem transport may delay the supply of carbon substrates belowground, we simulated a range of time offsets between peak PAR and peak subsurface photosynthate supply (6-26 hours). Some studies have suggested lag times of less then a day (Tang *et al.*, 2005), while others have suggested lags ranging 1-8 days (Högberg *et al.*, 2001; McDowell *et al.*, 2004); however, for illustrative purposes we focused on potential short-term responses to photosynthesis over the course of a single

day. We modeled day length as 12 hours, with increases in air temperature beginning at dawn.

Diel variations in substrate supply substantially modified surface flux and produced hysteresis relationships with complex shapes (Figure 3.9B). Although the shapes were quite variable depending on the timing of peak substrate supply, there are some consistencies among the curves that may be useful for interpreting field data. The hysteresis loops are consistently flatter on the bottom, corresponding with periods when PAR-dependent substrate supply ceased and respiration responded only to soil temperature. Modeling also suggested that for large time offsets between substrate supply and soil temperature, soil respiration can exhibit double peaks over the course of the day, peaking once in response to maximum carbon supply and again in response to maximum temperature (Fig 3.9A). Carbone *et al*. (2008) observed daily double peaks in field measurements of shrub and grassland ecosystems, particularly during parts of the growing season when soil respiration was most active. Such asymmetrical diel patterns cannot be accounted for by temperature alone and are due to influences from more then one factor.

CONCLUSIONS

Diel phase lags between surface flux and soil temperature can result entirely from heat and CO_2 transport processes, and drivers other then temperature are not required to explain the existence of diel hysteresis. Under field conditions, however,

soil respiration does likely exhibit diel responses to factors other then temperature (Bahn *et al.*, 2009; Carbone *et al.*, 2008; Tang *et al.*, 2005). Responses to environmental influences other than temperature, such as changes in substrate supply, modify lag times and hysteresis patterns to varying degrees. One way of detecting the influence of secondary environmental factors is from asymmetrical hysteresis patterns. Asymmetrical hysteresis can indicate processes such as photosynthesis that are limited to a portion of the day only.

Lag times and hysteresis patterns are sensitive to a number of environmental factors, and changes in environment can substantially alter respiration hysteresis patterns on a day-to-day basis as well as over longer seasonal time spans. Changes in air temperature amplitude and photosynthate supply, and rapid changes in soil moisture caused by rain events, can all cause significant changes in respiration hysteresis patterns from one day to the next. Gradual soil drying over seasonal time spans can lead to increasingly elliptical hysteresis patterns on a seasonal time scale.

Because the relationship between surface flux and temperature at any depth is not constant, there is no consistent depth where soil temperature should be measured in order to determine the temperature sensitivity of soil respiration. Fitting regressions of surface flux and soil temperature at a single depth can produce Q_{10} values substantially different from the “true” temperature sensitivity used to parameterize the model. Owing to the greater diel variability in soil temperature close to the surface, diel oscillations in surface flux will generally be most in phase with soil temperatures within a few

centimeters of the surface. When soil temperature is measured at deeper depths, phase lags between surface flux and soil temperature will tend to increase with depth. We found that theoretical phase lags between surface flux and a reference temperature at 10cm depth are between 1-3.5 hours across a wide range of soil physical and environmental conditions (Figs 3.4 and 3.7). The exception to this is highly porous or organic soils, or soils with thick O-horizons, which can have considerably longer phase lags, particularly under dry conditions. For mineral soils, however, phase lags greater than 3.5 hours may indicate the influence of additional factors on soil respiration rates other than temperature alone.

The mechanistic soil flux model used in this study can be extended to simulate field studies, provided soil heat transport is dominated by conduction and CO_2 transport is dominated by diffusion. This model can provide an approach to tease apart influences of temperature from other factors that have diel periodicity. Detailed environmental data and soil physical parameters are required to drive the model; however, such data are becoming increasingly available as soil flux measurements become more widespread. At a minimum, by measuring both air and soil temperature, or still better, measuring soil temperature at more then one depth, one can calculate soil thermal diffusivity to obtain a rough estimate of theoretical lags between soil temperature and surface flux. Phase lags between temperatures measured at several depths can be used to constrain D_T (Beltrami, 1996), which influences expected lag times more then any other single factor we examined. Even without more detailed information on other parameters, such

as the depth of CO_2 production or gas diffusivity, an estimate of thermal diffusivity can provide a rough approximation of expected lag times (e.g. Fig 3.4). Such estimates may be particularly helpful for researchers comparing diel hysteresis patterns under different soil moisture conditions. If heat and gas transport processes are not considered, phase lags between soil respiration and temperature may be misinterpreted.

ACKNOWLEDGEMENTS

Surface flux data shown in Figure 1 and soil physical parameters were measured at the HJ Andrews Experimental Forest, which is funded by the National Science Foundation's Long-Term Ecological Research Program (DEB 08-23380), US Forest Service Pacific Northwest Research Station, and Oregon State University. Thanks to Shane Easter for help with field measurements, and Carlos Sierra for helpful feedback on this manuscript.

REFERENCES

Bahn M, Schmitt M, Siegwolf R, Richter A, Brüggemann N (2009) Does photosynthesis affect grassland soil-respired CO_2 and its carbon isotopie composition on a diurnal timescale? *New Phytologist,* **182**, 451-460.

Beltrami H (1996) Active Layer Distortion of Annual Air/Soil Thermal Orbits. *Permafrost and Periglacial Processes,* **7**, 101-110.

Carbone MS, Vargas R (2008) Automated soil respiration measurements: new information, opportunities and challenges. *New Phytologist,* **177**, 295-297.

Carbone MS, Winston GC, Trumbore SE (2008) Soil respiration in perennial grass and shrub ecosystems: Linking environmental controls with plant and microbial sources on seasonal and diel timescales. *Journal of Geophysical Research,* **113**.

Chen JM, Huang SE, Ju W, Gaumont-Guay D, Black TA (2009) Daily heterotrophic respiration model considering the diurnal temperature variability in the soil. *Journal of Geophysical Research,* **114**.

Davidson EA, Janssens IA, Luo Y (2006a) On the variability of respiration in terrestrial ecosystems: moving beyond Q_{10}. *Global Change Biology*, **12**, 154-164.

Davidson EA, Savage KE, Trumbore SE, Borken W (2006b) Vertical partitioning of CO2 production within a temperate forest soil. *Global Change Biology*, **12**, 944-956.

Ekblad A, Boström B, Holm A, Comstdet D (2005) Forest soil respiration rate and $\delta^{13}C$ is regulated by recent above ground weather conditions. *Oecologia,* **143**, 136-142.

Fessenden JE, Ehleringer JR (2003) Temporal variation in $\delta^{13}C$ of ecosystem respiration in the Pacific Northwest: links to moisture stress. *Oecologia,* **136**, 129-136.

Gaumont-Guay D, Black A, McCaughey H, Barr AG, Krishnan P, Jassal RS, Nesic Z (2009) Soil CO2 efflux in contrasting boreal deciduous and coniferous stands and its contribution to the ecosystem carbon balance. *Global Change Biology*.

Graf A, Weihermüller L, Huisman JA, Herbst M, Bauer J, Vereecken H (2008) Measurement depth effects on the apparent temperature sensitivity of soil respiration in field studies. *Biogeosciences,* **5**, 1175-1188.

Hillel D (1998) *Environmental Soil Physics,* San Diego, Academic Press.

Högberg P, Högberg MN, Göttlicher SG *et al.* (2008) High temporal resolution tracing of photosynthate carbon from the tree canopy to forest soil microorganisms. *New Phytologist,* **177**, 220-228.

Högberg P, Nordgern A, Buchmann N *et al.* (2001) Large-scale forest girdling shows that current photosynthesis drives soil respiration. *Nature,* **411**, 789-792.

Irvine J, Law BE, Anthoni P, Meinzer FC (2002) Water Limtations to Carbon Exchange in Old-Growth and Young Ponderosa Pine Stands. *Tree Physiology,* **22**, 189-196.

Irvine J, Law BE, Kurpius MR (2005) Coupling of canopy gas exchange with root and rhizosphere respiration in a semi-arid forest. *Biogeochemistry,* **73**, 271.

Jassal RS, Black TA, Cai T, Morgenstern K, Li Z, Gaumont-Guay D, Nesic Z (2007) Components of ecosystem respiration and an estimate of net primary productivity of an intermediate-aged Douglas-fir stand. *Agricultural and Forest Meteorology,* **144**, 44-57.

Kodoma N, Barnard RL, Salmon Y *et al.* (2008) Temporal dynamics of the carbon isotope composition in a *Pinus sylvestris* stand: from newly assimilated organic carbon to respired carbon dioxide. *Oecologia,* **156**, 737-750.

McDowell NG, Bowling DR, Bond BJ, Irvine J, Law BE, Anthoni P, Ehleringer JR (2004) Response of the carbon isotopic content of ecosystem, leaf, and soil respiration to meteorological and physiological driving factors in a *Pinus ponderosa* ecosystem. *Global Biogeochemical Cycles,* **18**.

Moldrup P, Olesen T, Schjonning P, Yamaguchi T, Rolston DE (2000) Predicting the Gas Diffusion Coefficient in Undisturbed Soil from Soil Water Characteristics *Soil Sci. Soc. Am. J.,* **64**, 94-100.

Nickerson N, Risk D (2009a) Physical Controls on the Isotopic Composition of Soil Respired CO_2. *Journal of Geophysical Research,* **114**, doi:10.1029/2008JG000766.

Ochsner TE, Horton R, Ren T (2001) A New Perspective on Soil Thermal Properties. *Soil Science Society of America Journal,* **65**, 1641-1647.

Pavelka M, Acosta M, Marek MV, Kutsch W, Janous D (2007) Dependence of the Q_{10} values on the depth on the the soil temperature measuring point. *Plant and Soil*.

Pumpanen J, Ilvesniemi H, Hari P (2003) A Process-Based Model for Predicting Soil Carbon Dioxide Efflux and Concentration. *Soil Sci Soc Am J,* **67**, 402-413.

Pypker T, Hauck M, Sulzman EW *et al.* (2008) Towards using $\delta^{13}C$ of ecosystem respiration to monitor canopy physiology in complex terrain. *Oecologia,* **158**, 399-410.

Risk D, Kellman L, Beltrami H (2002a) Carbon dioxide in soil profiles: production and temperature dependence. *Geophysical Research Letters,* **29**.

Riveros-Iregui DA, Emanuel RE, Muth DJ *et al.* (2007) Diurnal hysteresis between soil CO_2 and soil temperature is controlled by soil water content. *Geophysical Research Letters,* **34**.

Ryan MG, Law BE (2005) Interpreting, measuring, and modeling soil respiration. *Biogeochemistry,* **73**, 3.

Smerdon JE, Beltrami H, Creelman C, Stevens MB (2009) Characterizing land-surface processes: A quantitative analysis using air-ground thermal orbits. *Journal of Geophysical Research,* **114**.

Tang J, Baldocchi DD, Xu L (2005) Tree photosynthesis modulates soil respiration on a diurnal time scale. *Global Change Biology*, **11**, 1298-1304.

Tedeschi V, Rey A, Manca G, Valentini R, Jarviss PG, Borghetti M (2006) Soil respiration in a Mediterranean oak forest at different developmental stages after coppicing. *Global Change Biology*, **12**, 110-121.

Trumbore SE (2006) Carbon respired by terrestrial ecosystems--recent progress and challenges. *Global Change Biology*, **12**, 141-153.

Vargas R, Allen MF (2008) Environmental controls and the influence of vegetation type, fine roots and rhizomorphs on diel and seasonal variation in soil respiration. *New Phytologist*.

Figure 3.1. (A) Diel soil respiration hysteresis from HJ Andrews Experimental Forest over a four day period (soil moisture 0.35-0.33 v/v at 8cm depth). Hysteresis is counterclockwise for all days. (B) Corresponding time series for 5cm soil temperature (black line) and surface flux (black circles). Observations were measured hourly.

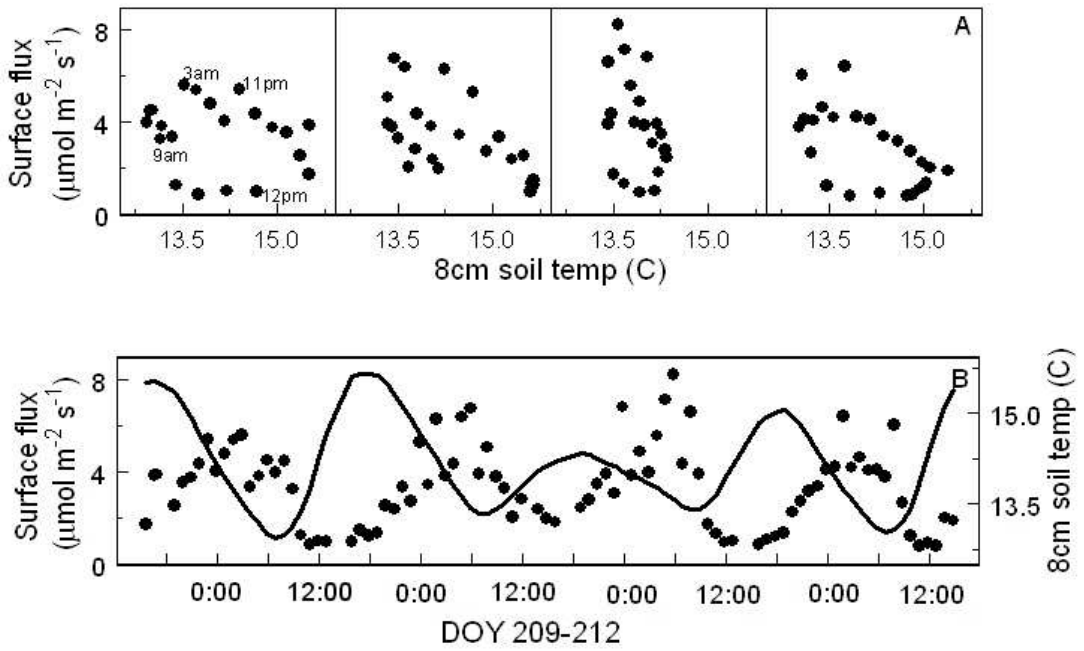

Figure 3.2. Diel hysteresis between surface CO_2 flux and soil temperature at several depths, $D_t = 5\times10^{-7}$ m^2s^{-1} (same data as bottom panel of Figure 3). Solid points show time = 12 hours, and arrows indicate the direction of hysteresis over time. Grey lines show the fitted values that would produce an apparent Q_{10} of 2.

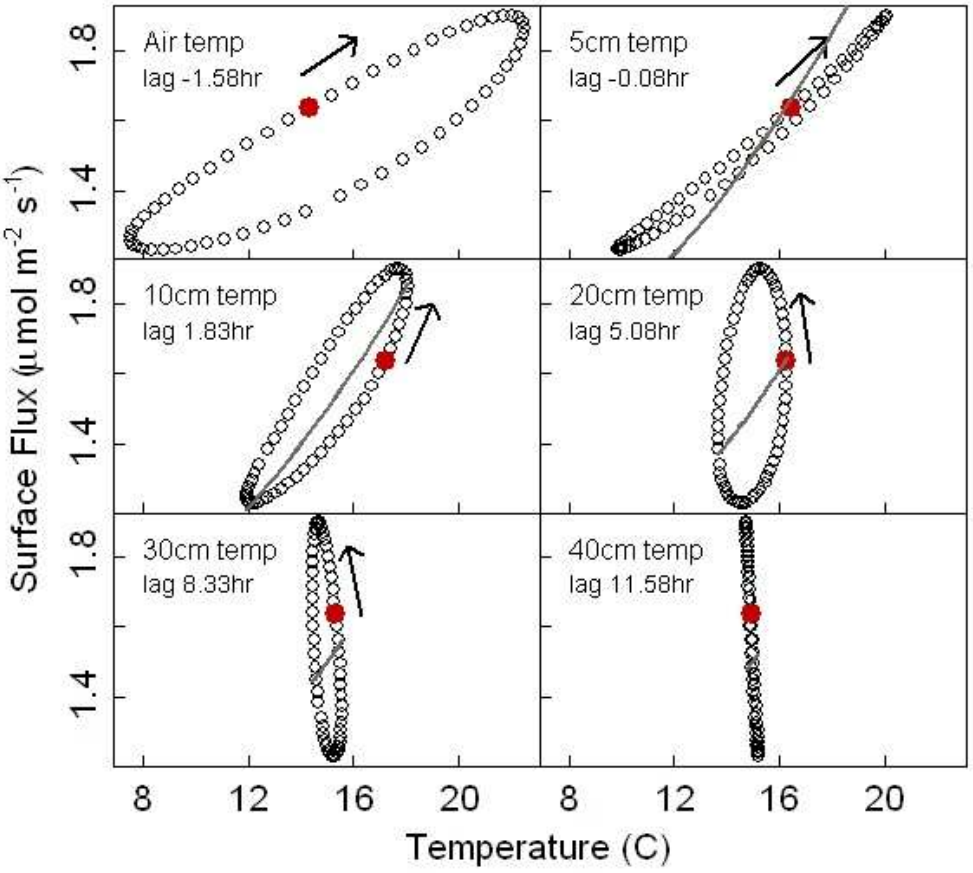

Figure 3.3. Effect of thermal diffusivity on surface CO_2 flux (grey) and soil temperature (black) at the soil surface (solid), 10cm (dotted), 20cm (dot-dashed), and 30cm (dashed). See Table 1 for values of other input parameters.

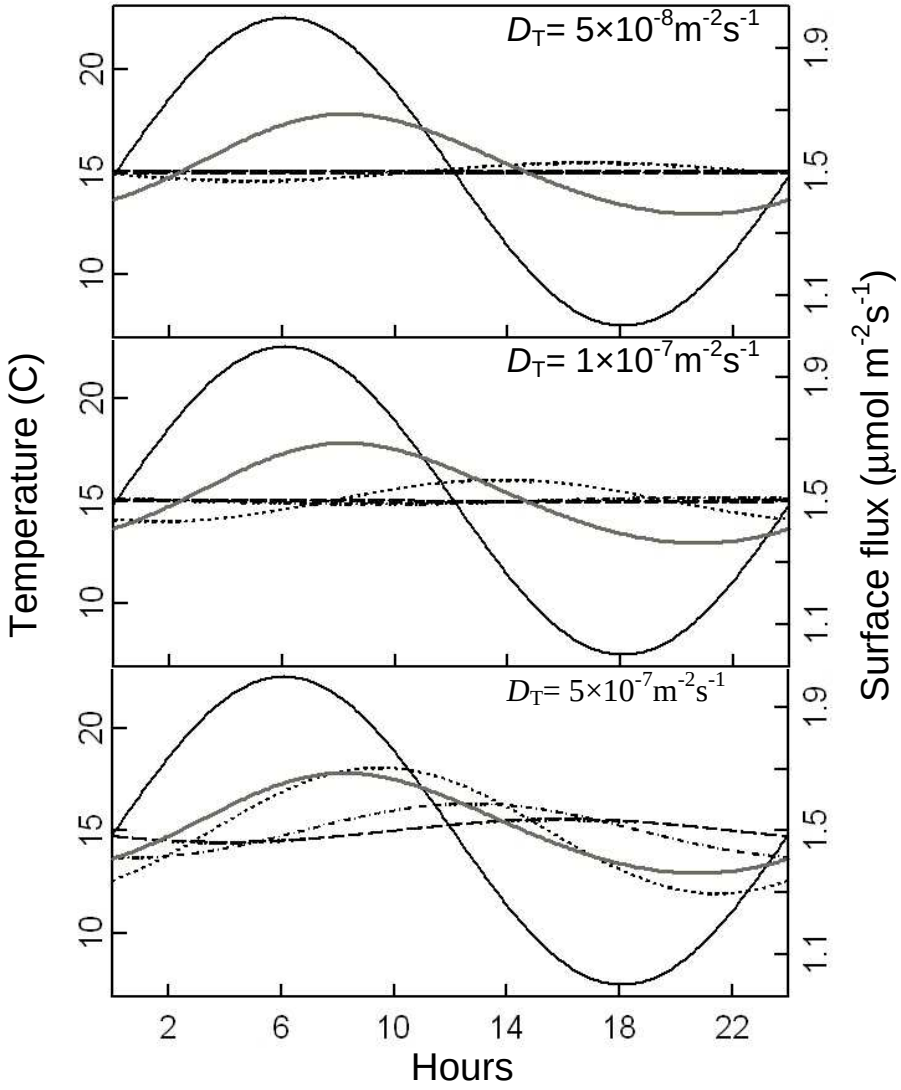

Figure 3.4. Sensitivity of lag time (between maximum surface flux and maximum 10cm temperature) to soil and environmental parameters. (A) Thermal diffusivity, D_T (●); CO_2 diffusivity, D_{CO2} (◊); and exponential folding depth for CO_2 production, d_p (▲). (B) Basal total CO_2 production, Γ_0 (○); Q_{10} temperature sensitivity (×); and diel air temperature amplitude, A_0 (▼).

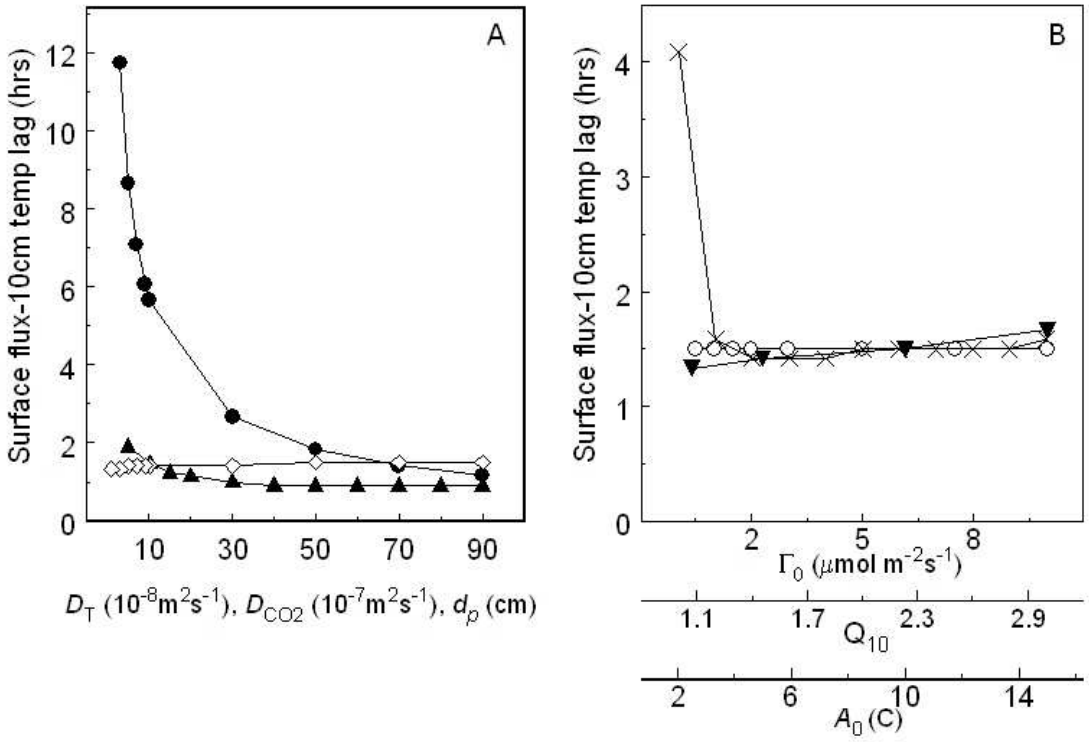

Figure 3.5. Effect of CO_2 diffusivity on concentration and surface flux lags. (A) 10cm soil CO_2 (grey lines) lagged from temperature at the same depth (dashed black) and atmospheric temperature (solid black), for several levels of D_{CO2}. $D_{CO2} = 1\times10^{-7}$ (solid dark grey), 5×10^{-7} (dashed dark grey), 1×10^{-6} (solid light grey), 5×10^{-6} (dashed light grey). CO_2 is normalized by maximum daily concentration to show all diffusivity levels on the same scale. (B) Same as A except grey lines represent surface CO_2 flux. (C) Same as B except CO_2 production is uniformly distributed, rather then decreasing exponentially with soil depth.

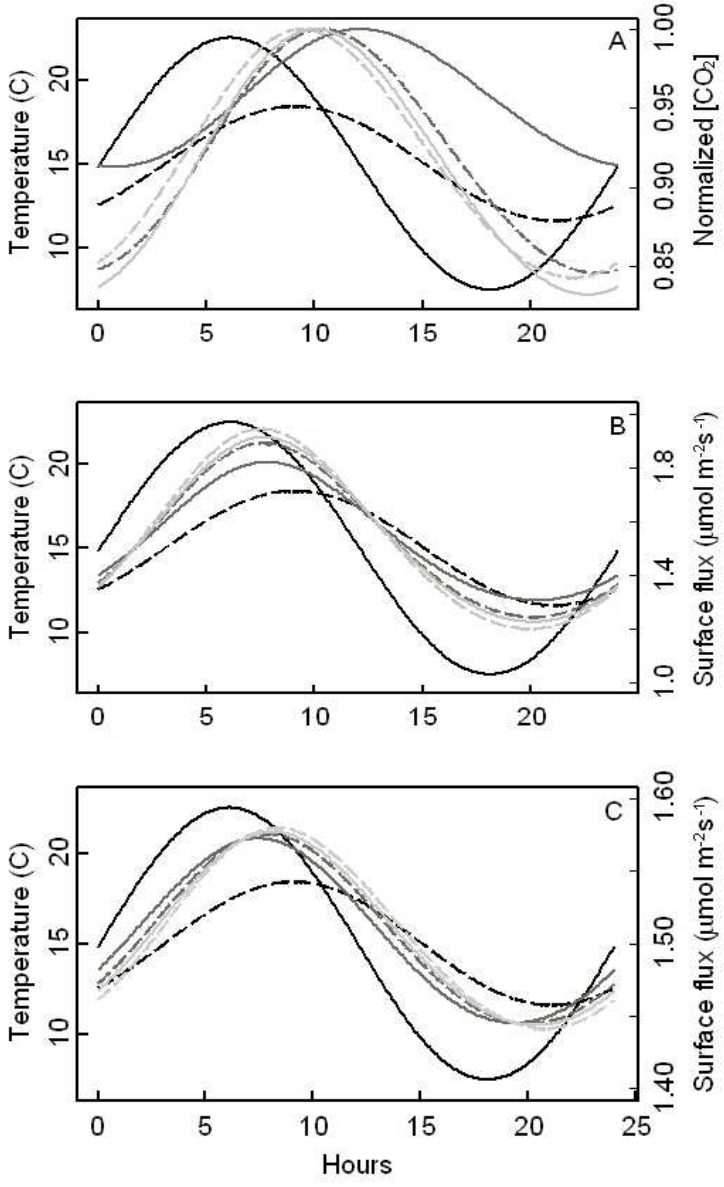

Figure 3.6. Effect of Q_{10} on lag time. Air temperature (black), 10cm soil temperature (dashed black), and surface CO_2 flux for various Q_{10} values (grey lines). Q_{10} values from dark to light grey: 1, 1.2,1.4, 2, 2.4.

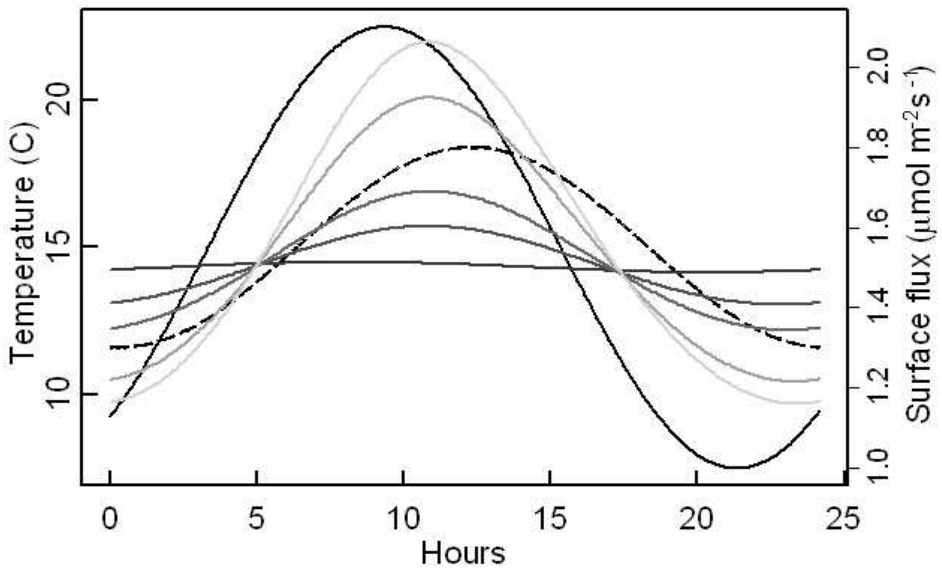

Figure 3.7. Effects of soil moisture of soil physical properties, lag times, and hysteresis patterns. (A) Effect of moisture on thermal diffusivity (●), CO_2 diffusivity (▲), and the lag time between surface flux and 10cm soil temperature (■) for a uniform sandy-loam soil. (B) Surface flux hysteresis for moisture-dependent conditions shown in A. From lightest to darkest: 5,15,25,35,45, and 55% air-filled porosity. (C) Changes in total basal CO_2 production (■) were added to simulations, but had no effect on lag times (▼). (D) Corresponding surface flux hysteresis. From lightest to darkest: 5-55% air-filled porosity, as in B.

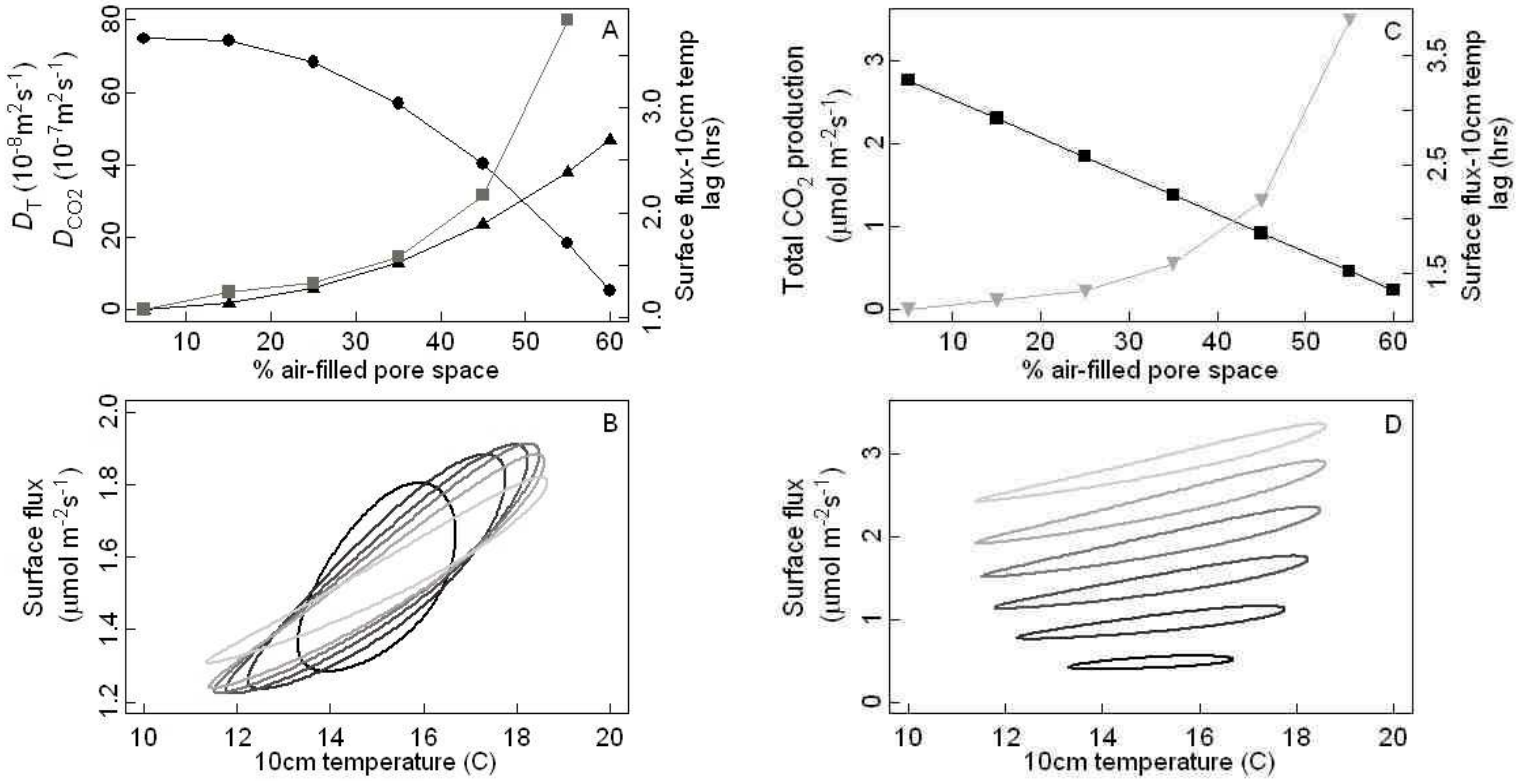

Figure 3.8. Effect of varying atmospheric CO_2 concentrations on surface flux rates. (A) Diurnal changes in atmospheric CO_2 (dashed black), with air and soil temperatures (grey lines) held constant at 15ºC. (B) Air temperature (dashed grey) was allowed to vary simultaneously with atmospheric CO_2 (dashed black) In this example atmospheric CO_2 reached a minimum 3 hours before peak air temperature. Soil temperature at 10cm is shown in solid grey, and surface flux is shown in solid black.

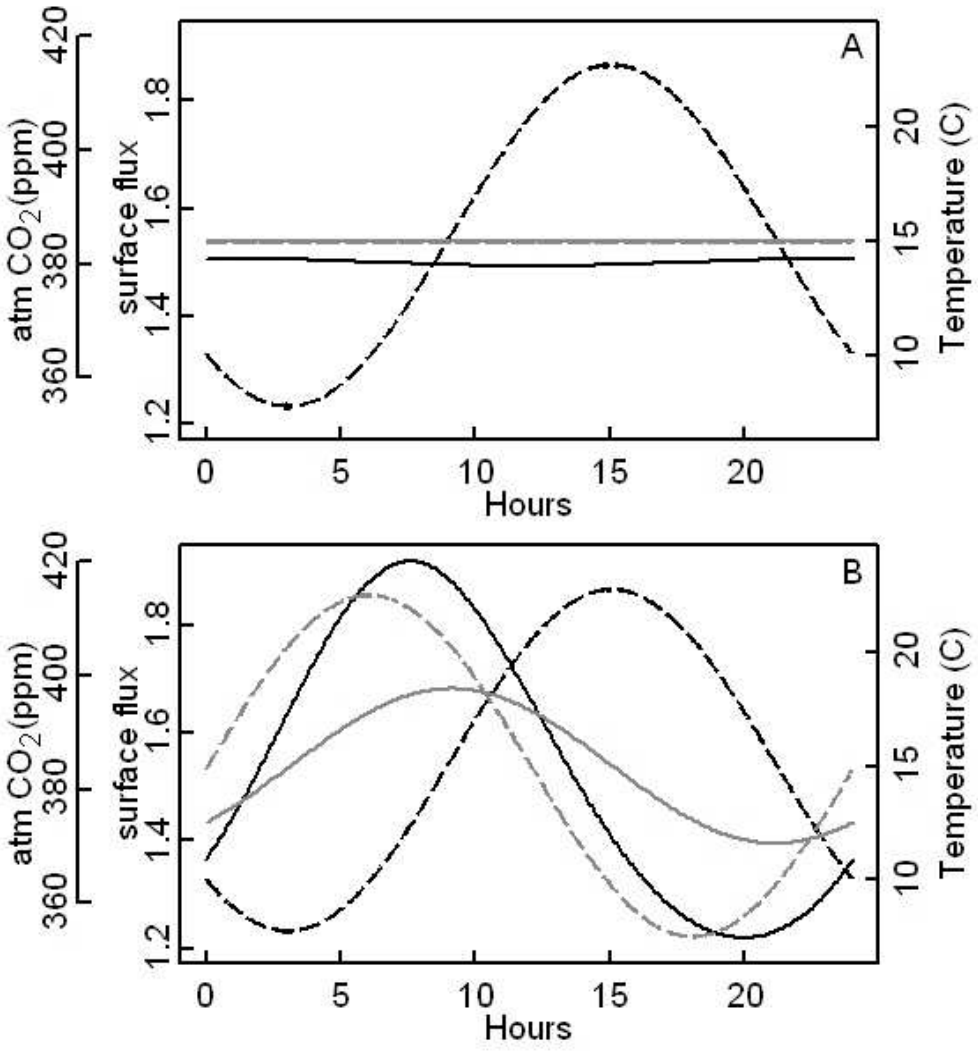

Figure 3.9. Potential responses of soil respiration to diel changes in photosynthate supply. (A) Diel changes in PAR (dashed black), air temperature (dashed grey), 10cm soil temperature (solid grey), and surface CO_2 flux (solid black). In this example subsurface carbon supply peaked 16hr after PAR. (B) Hysteresis between surface flux and 10cm soil temperature for various offsets between peak PAR and peak subsurface carbon supply: 6hr offset (solid grey), 11hr offset (dashed grey), 16hr offset (solid black, same as in A), and 26hr offset (dashed black).

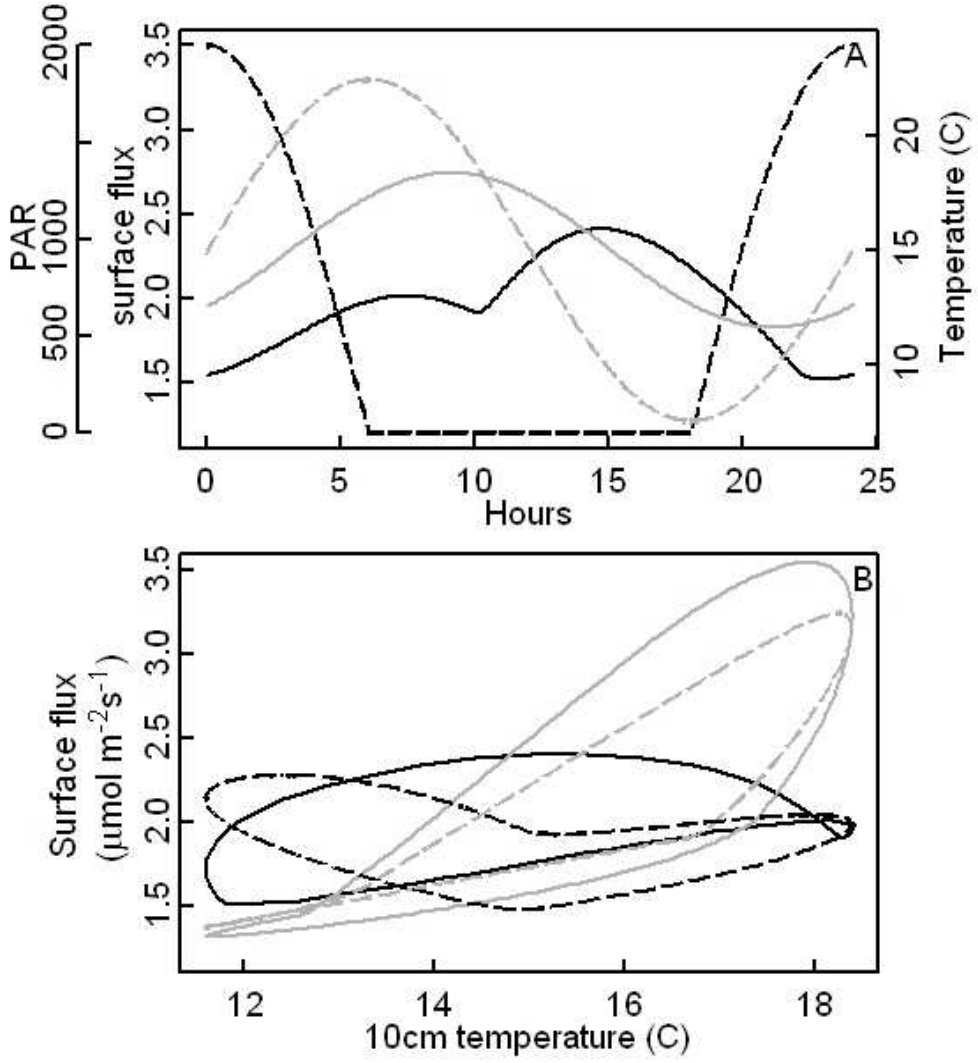

CHAPTER FOUR: SOIL MOISTURE EFFECTS ON THE CARBON ISOTOPIC COMPOSITION OF SOIL RESPIRATION

Claire L. Phillips, Nick Nickerson, David Risk, Zachary Kayler, Chris Andersen, Alan Mix, Barbara J. Bond

Prepared for *Rapid Communications in Mass Spectrometry*
111 River Street
Hoboken, NJ 07030

ABSTRACT

The carbon isotopic composition ($\delta^{13}C$) of recent photosynthates is known to depend on plant water-stress, caused either by low soil moisture or low atmospheric humidity. Similarly, a number of studies have shown correlations between $\delta^{13}C$ of soil-respired CO_2 and recent air humidity, which suggests a possible link between the $\delta^{13}C$ of recent photosynthates and soil $\delta^{13}CO_2$ dynamics. However, direct causality has not been demonstrated, and recent work suggests soil $\delta^{13}CO_2$ dynamics over time may be independent of the $\delta^{13}C$ of respiratory substrates. Using a combination of greenhouse experiments and modeling, we examined how moisture impacts soil-respired $\delta^{13}CO_2$, and tested whether moisture impacts could result from 1) changes in $\delta^{13}CO_2$ of soil microbial respiration, or 2) CO_2 gas-transport effects, in contrast to the $\delta^{13}C$ of recent photosynthates. In a first experiment we grew Douglas-fir seedlings under high and low moisture conditions and found soil-respired $\delta^{13}CO_2$ was 4.7‰ more enriched in the low moisture treatment; however, using an isotopologue gas diffusion model to simulate the sampling conditions, we found these results were likely influenced by gas transport effects. In a second experiment we tested moisture effects on microbially-respired $\delta^{13}CO_2$, using sealed soil chambers to limit gas-transport related fractionation. Microbial soil respiration did not change isotopically across a large moisture range, and could not explain moisture impacts on total soil-respired $\delta^{13}CO_2$. Although we cannot rule out the potential influence of recent photosynthates on soil-respired $\delta^{13}CO_2$, our calculations indicated that the maximum expected difference in $\delta^{13}CO_2$ from high- and

low-moisture seedlings was smaller than our measured difference, and was also smaller than theoretical diffusive fractionation. We conclude that it is possible to obtain a biologically reasonable relationship between moisture and soil-respired $\delta^{13}CO_2$ from purely physical effects.

INTRODUCTION

Soil respiration is often the largest flux of CO_2 from terrestrial ecosystems (Gaumont-Guay *et al.*, 2009; Jassal *et al.*, 2007; Ryan & Law, 2005), and there is great interest in employing carbon isotopes to identify the sources and drivers of soil CO_2 fluxes (Boutton, 1996; Bowling *et al.*, 2008b). A number of isotope studies have suggested that supply of recently-assimilated photosynthates has a substantial influence of soil respiration (Ekblad *et al.*, 2005; Ekblad & Högberg, 2001; Fessenden & Ehleringer, 2003; McDowell *et al.*, 2004). In these studies, the isotopic composition of soil respiration was shown to vary with recent atmospheric humidity in a similar way as photosynthetic discrimination is known to respond (Brugnoli *et al.*, 1988). Correlations between soil respiration and recent humidity conditions have been interpreted as indirect evidence that plant photosynthates are rapidly transported below ground and consumed, so the isotopic composition of soil respiration reflects the recent moisture status of plants.

However, a causal relationship between plant moisture status and soil $\delta^{13}C$ flux has not been demonstrated directly, and several recent studies have cast doubts on

whether plant moisture status has a substantial influence on soil $\delta^{13}CO_2$. Both in plants (Bowling *et al.*, 2008b; Maunoury *et al.*, 2007; Werner *et al.*, 2009) and in soil (Nickerson & Risk, 2009a; Nickerson & Risk, 2009c) complex temporal dynamics of respired $\delta^{13}CO_2$ have been observed that are independent of substrate $\delta^{13}C$. In this study we performed a greenhouse experiment to test explicitly whether moisture conditions impact soil-respired $\delta^{13}CO_2$, and tested two possible alternatives to photosynthetic discrimination to explain variability in soil-respired $\delta^{13}CO_2$ in response to soil moisture. Our goal was not to challenge the importance of photosynthesis as a driver of soil respiration, but to develop correct interpretations of soil-respired $\delta^{13}CO_2$ so that such measurements can be more useful to ecosystems carbon studies.

When C_3 plants are moisture limited, either due to low soil moisture, or to high transpiration demands, they discriminate less against the heavy $^{13}CO_2$ isotopolgue during photosynthesis, and assimilate carbon that is enriched in ^{13}C compared to non-water-stressed plants (Brugnoli *et al.*, 1988; Flanagan & Ehleringer, 1998; Pate & Arthur, 1998). The sensitivity of photosynthetic discrimination to plant moisture status is explained by the theoretical model first proposed by Farquhar *et al*. (1982). The Farquhar model describes photosynthetic discrimination for C_3 plants as a function of stomatal openness, expressed as the ratio of CO_2 inside and outside the leaf. An indication that the Farquhar model of photosynthetic discrimination may help to explain $\delta^{13}C$ variation in carbon pools beyond leaves came from the study by Pate and Arthur (1998), which showed variation of up to 8‰ in the $\delta^{13}C$ of phloem sugars corresponding with seasonal patterns of plant water stress.

A number of more recent studies, however, have shown that on timescales of hours to days, plant-respired $\delta^{13}CO_2$ is independent of putative respiratory substrates, which raises some questions about the predictive ability of the Farquhar model for describing plant-respired $\delta^{13}CO_2$ on short timescales (reviewed by Bowling *et al.*, 2008b). Both Werner *et al*. (2009) and Hymus *et al*. (2005) have shown that large diurnal changes exceeding 7‰ occur in leaf-respired $\delta^{13}CO_2$, while the $\delta^{13}C$ of carbohydrate substrates remains relatively constant. Similarly, Gessler *et al*. (2007) found that day-to-day variations in root-respired $\delta^{13}CO_2$ were not significantly correlated with water-soluble root $\delta^{13}C$.

In addition to root respiration, soil respiration is composed of microbial respiration. Another potential problem with linking soil-respired $\delta^{13}CO_2$ to plant processes is that the impact of moisture on microbial-respired $\delta^{13}CO_2$ needs be assessed. We are unaware of any previous studies that have explicitly examined day-to-day or seasonal isotope dynamics of heterotrophic soil fluxes.

Perhaps the biggest challenge to previous interpretations of soil-respired $\delta^{13}CO_2$ is the methodological sampling issues that recent modeling has demonstrated (Nickerson & Risk, 2009a; Risk & Kellman, 2008). A large number of field studies have employed various types of soil surface chambers to sample respired $\delta^{13}CO_2$, and models of soil gas diffusion indicate that surface chambers alter CO_2 concentration gradients between the soil and atmosphere, creating non-steady-state conditions that change the $\delta^{13}CO_2$ of surface flux during measurements. Furthermore, the magnitude of

the disturbance created by chambers and the time required for re-equilibrium depends on soil gas diffusivity, which varies with soil moisture conditions. With most surface chamber measurement techniques, low moisture soils produce $\delta^{13}CO_2$ measurements that are more biased towards enriched values than high moisture soils (Nickerson & Risk, 2009b). These results from numerical simulations open the possibility that previous correlations between moisture and soil-respired $\delta^{13}CO_2$ may have resulted from fractionation related to soil gas transport, in contrast to biogenic causes.

Several lines of evidence other than natural abundance isotope measurements have also indicated close links between canopy carbon supply and soil respiration rates, and we do not dispute the likely importance of photosynthesis as a driver of soil respiration. These include phloem girdling studies (Högberg *et al.*, 2001; Tedeschi *et al.*, 2006), studies across natural gradients of root abundance (Tang *et al.*, 2005), and isotopic labeling studies of photosynthate (Bahn *et al.*, 2009; Högberg *et al.*, 2008). Although the conclusions reached using natural abundance carbon isotopes are corroborated by other studies, it is not clear whether the conclusions of natural abundance studies were reached for the correct reasons. Natural abundance measurements hold important potential for examining canopy-soil linkages because they cause minimal disturbance and are increasingly affordable, but their full utility can only be realized if the processes that cause discrimination along plant-soil pathways are known. In contrast to photosynthetic discrimination, which has been thoroughly described and is mechanistically well-understood, far less is known about fractionation

that occurs during post-photosynthetic processing, and whether this fractionation is moisture-dependent.

In this study we performed two greenhouse experiments to examine mechanisms for moisture-related changes in soil-respired $\delta^{13}CO_2$. The purpose of the first experiment was to test in a controlled setting the hypothesis that moisture conditions that are stressful to plants cause $\delta^{13}C$ enrichment of soil respiration, by growing Douglas-fir seedlings in soil columns at high and low moisture levels. Because we used a surface chamber to measure soil-respired $\delta^{13}C$, at a later date we also employed an isotopologue gas diffusion model (Nickerson & Risk, 2009a) to test the secondary hypothesis that moisture-related differences in our measurements were caused by transport-related fractionation. In the second experiment we tested the hypothesis that $\delta^{13}C$ of heterotrophic soil respiration does not vary with moisture. If moisture effects on soil respired $\delta^{13}CO_2$ are due to plant moisture stress, then in the absence of roots respired $\delta^{13}CO_2$ should remain static across a range of soil moistures. We incubated root-free soils in sealed chambers to minimize transport-related fractionation, and also validated this sampling approach with an isotopologue diffusion model.

MATERIALS AND METHODS

Soil description

For both greenhouse experiments, soil columns (15 cm ID x 38 cm height, non-transparent PVC pipe) were filled with a 1:1 mixture of perlite and cobbley silt-loam

soil collected from the HJ Andrews Experimental Forest in the western Oregon Cascade Range. The soil is derived from alluvium of volcanic origin, part of the Quentin series, and the dominate vegetation is mature Douglas-fir dominated forest (Brown, 1974). Soil was removed from the O, A, and B1 horizons to 15cm depth, homogenized, and large roots and rocks were removed by sieving to 2cm. Soil was mixed with horticultural perlite to reduce compaction during prolonged watering. Perlite is an inert, neutral, amorphous volcanic glass that is heated until it expands, forming granules with a closed cell interior structure. In a pretest, we verified that perlite does not release detectable amounts of CO_2. We filled three replicate 12mL Exetainer^{TM} vials (Labco, UK) with moistened perlite, flushed the air space overnight with CO_2 free air, and then allowed the perlite to incubate for ~8 hours before analyzing CO_2 concentration in the headspace. Soil columns were supported by 1mm fiberglass mesh on the bottom to facilitate drainage, and had 3 cm headspace at the top. The dry bulk density was approximately 0.5 g cm^{-3}, and effective porosity was 59%.

Experiment 1: Impact of stressful moisture conditions on total soil-respired $\delta^{13}CO_2$

Ten Douglas-fir seedlings (each two-years old) from Weber Forest Nursery in Olympia, Washington, were planted in soil columns in April 2006, and watered for three months in a sheltered outdoor area at Oregon State University to become established. In July the columns were moved to a greenhouse and randomly selected for either a high- or low-moisture treatment. Columns in the high-moisture treatment were

watered to field capacity every evening with tap water, and columns in the low-moisture treatment were allowed to dry over five weeks.

To monitor physiological water stress, stomatal conductance and photosynthesis were measured on seedlings mid-morning once per week. Foliar gas exchange measurements were performed with a Licor-6400 using a conifer leaf chamber at ambient light conditions. Leaf areas (one-sided) were measured following harvest by scanning the needles in a flat bed digital scanner and calculating the needle areas with ImageJ software (http://rsbweb.nih.gov/ij/). Soil moisture was also measured continuously with CS-610 TDR moisture probes (Campbell Scientific, Logan, Utah), using calibration coefficients we determined by comparing sensor voltage with volumetric water content of the packed soil columns (determined as gravimetric water content × bulk density). Air temperature in the greenhouse ranged approximately 21-30ºC.

We measured soil respiration weekly throughout the equilibration period and just prior to isotope sampling. A miniature soil respiration chamber was constructed to fit inside the planted soil columns and connect to a Licor 6400. This miniature soil chamber was constructed of a non-transparent PVC end cap (5.15cm ID), and had the same features as the LiCor 6400-19 soil chamber, including an E-type thermocouple, pressure release vent, and a rim with a closed-cell foam gasket to interface with soil collars. The standard LI-6400 soil chamber automatic program was used to measure respiration, with the chamber mixing fan on the low speed setting. Accuracy of the

custom soil chamber plus collar was validated by a series of comparisons with a Licor 6400-19 in unplanted soil columns (regression slope = 1.00 ± 0.03, R^2 = 0.99, n = 9).

Isotope samples were collected using a smaller version of the chamber system described by Ekblad and Högberg (2001). Soil collars were capped with a PVC endcap (total volume 178cm^3) fitted with a Swagelok stainless steel union holding an acetyl-butyl septa. A series of four gas samples were taken from the chamber headspace, at three minute intervals for high moisture soils and five minute intervals for low-moisture soils, with the goal of capturing CO_2 levels spanning at least 200ppm. A two end-member mixing model, or Keeling plot, was used to calculate $\delta^{13}C$ of soil respiration. The $\delta^{13}C$ values of air samples from the chamber headspace were plotted against their corresponding 1/[CO_2] values, and ordinary least squares regression was used to extrapolate the Keeling intercept (Pypker *et al.*, 2008).

Experiment 2: Impact of soil moisture on heterotrophic soil-respired $\delta^{13}CO_2$

Nine soil columns were packed with perlite-amended soil to the conditions described above. To achieve a range of soil moistures, all the columns were initially watered and were kept moist by saturating the bottom 2cm in a shallow pan of water to permit capillary draw. Each week, for a total of five weeks, 1-2 pots were set aside to commence drying. Soil respired CO_2 was sampled for C isotope analysis from all the soil columns at the end of this period, with water content ranging 10-35%. Water contents were determined gravimetrically and converted to volumetric water contents by multiplying by bulk density. Soil respiration was also measured prior to isotope

sampling using a Licor 6400 gas exchange system with a 6400-19 soil chamber (Lincoln, Nebraska).

To sample soil respired $\delta^{13}C$, we sealed the soil columns by capping the top and bottom with PVC end caps and sealing the edges with silicone vacuum grease, creating a 700ml headspace. The columns were incubated overnight for a total of 22 hours to allow soil-derived CO_2 to build up to high concentrations, and for gas in the soil pores and chamber headspace to come to isotopic equilibrium The headspace was vented to an airlock during the incubation period to allow pressure venting, and was switched with a 3-way valve to a syringe needle during sampling.

Because these soils did not become as dry as the soil columns with plants experiment 2, at a later date we also incubated smaller quantities of air-dry soils directly in 12mL Exetainer vials. Three replicate 5g samples of air-dry soil were sealed in Exetainer vials, and flushed with CO_2-free air overnight to purge the airspace (approximately 6mL). Because of low production rates, these soils were incubated for 72 hours to allow CO_2 concentrations to reach similar concentrations as the soil column incubations. We simulated the large soil columns with a gas diffusion model (details follow) to quantify residual isotopic disequilibrium following the incubation period, and to ensure comparable results between the two incubations techniques.

Sampling and analysis of $\delta^{13}CO_2$

In both experiments, gas samples were collected from the headspace of the soil chambers into 12mL Exetainer vials pre-flushed with N_2. A handpump connected to a

3-way valve was used to evacuate Exetainers and immediately take a sample. Because evacuation was incomplete, we sampled standard gases with the handpump and calculated concentration dilution factors to account for residual N_2. Dilution averaged 9.38% (std dev = 0.83%) over the course of all the experiments. After sampling, vials were capped with silicone adhesive and analyzed within 24-72 h using a Finnigan/MAT DeltaPlus XL isotope ratio mass spectrometer interfaced to a GasBench II automated headspace sampler. For the air dried soils incubated in Exetainers, headspace $\delta^{13}C$ and CO_2 were measured directly on the Gas Bench II, similar to the procedure described by Crow et al. (2006).

In the first experiment, samples were analyzed at the Institute for Stable Isotope Research Facility (ISIRF) at the Environmental Protection Agency Western Ecology Division. In the second experiment, samples were analyzed at the College of Oceanic and Atmospheric Science (COAS), Oregon State University. The same instrument models were used at both locations. The combined standard uncertainties of the measurements, which include sampling and instrument uncertainties, were determined based on replicate analyses to be 0.4‰ PDB and 2.51% of CO_2 concentration for the ISIRF instrument, and 0.13‰ PDB and 3.75% of CO_2 concentration for the COAS instrument (NIST guidelines, Taylor & Kuyatt, 1994).

Modeling simulations: Fractionation during gas transport and sampling

To assess how sampling conditions affected measured $\delta^{13}C$ values, we simulated the diffusive processes in each experiment with an isotopologue diffusion model. We

simulated the surface chamber used in the first experiment with a 3-dimensional (3-D) version of the model to account for feedbacks between the chamber and the surrounding soil surface. Details of the 3-D model and experimental validations are described by Nickerson and Risk (2009a). We used a 1-D version of the model (Nickerson & Risk, 2009c) for the sealed soil columns in the second experiment. The performance of the 1-D model was validated by comparing modeled and observed values of chamber headspace $\delta^{13}C$ and CO_2 during incubation. Briefly, both versions of the model calculated fluxes of $^{12}CO_2$ and $^{13}CO_2$ using Fick's First law with isotopolgue-specific gas diffusivites. The modeled environment assumes a well-mixed atmospheric boundary layer and a soil profile divided into 100 uniform layers (1-D) or cells (3-D). The model allows gas exchange between neighboring soil layers or cells following concentration gradients.

A constant atmospheric upper boundary layer was set at 380ppm and -10‰ (also a lower atmospheric boundary layer in the small chamber experiment representing the screened bottom of the soil column). The modeled soil profile consisted of solids and water- and air-filled pore space. Water content and air-filled porosity were assumed to be uniform throughout the profile, and were parameterized for each soil column based on measured water contents. Air-filled pore space was used to calculate effective gas diffusivity with the Millington-Quirk relationship (McCarthy & Johnson, 1995). We also independently calculated effective diffusivity of the perlite-amended soil across a range of moisture levels and found close agreement with the Millington-Quirk relationship (regression slope = 0.96, $R^2 = 0.76$, n = 9).

Production of CO_2 was assumed to be equal throughout the soil profile, and total production for each soil column was estimated as the measured surface flux rate, multiplied by two to account for equal fluxes from the top and bottom of the soil column. Model runs were initialized with open tops and bottoms until the soil CO_2 and $\delta^{13}C$ profiles stabilized, and then boundary conditions were modified to model the presence of sampling chambers.

RESULTS

Experiment 1: Impact of stressful moisture conditions on total soil-respired $\delta^{13}CO_2$

Mid-morning stomatal conductance measurements indicated that low-moisture seedlings experienced physiological stress by the 4th week of soil drying (Figure 4.1). In the high moisture treatment, stomatal conductance showed expected increases and decreases over time in response to natural light conditions. In the low-moisture treatment stomatal conductance decreased monotonically over time, from an initial value of 0.12mmol H_2O m^{-2} s^{-1}, similar to the high-moisture treatment, to 0.02mmol H_2O m^{-2} s^{-1} by week four (Figure 4.1). At the end of week five when isotope samples were collected, soil moisture levels averaged 5.6% (v/v) in the low moisture treatment and 39.4% (v/v) in the high moisture treatment.

Keeling intercepts calculated from surface chamber $\delta^{13}C$ and CO_2 data were 4.7‰ higher in the low-moisture treatment (-20.0 ± 2.4‰) as compared with the high-moisture treatment (-24.7 ± 1.3‰), shown in Figure 4.2 ($p=0.0004$, Welch's t-test). However, because surface chambers were used, these raw Keeling intercepts are likely

to have some non-linear artifacts that must be corrected to obtain the true isotopic signature of soil respiration. To evaluate correct Keeling intercepts we used the 3-D gas diffusion model to simulate the time evolution of both CO_2 concentrations and $\delta^{13}C$ signatures within the chamber headspace. The model was parameterized with measured chamber surface area and volume, soil physical properties (pore space, diffusivity, depth) and CO_2 efflux rates.

We compared measured and modeled values of CO_2 concentration and $\delta^{13}C$ from the sampling chamber over time (Figure 4.3), and found the measured values leveled off more rapidly than predicted by the gas diffusion model. We first assessed whether this disparity could be due to uncertainty in our production measurements, by varying production rate in the model while holding other parameters constant. Model results showed that production had a large effect on the final concentration and $\delta^{13}C$ of the equilibrated chamber, but did not fully account for the speed of chamber equilibration observed in direct measurements. The large disparity between measured and modeled rates of change indicated the soil columns had higher effective diffusivities than expected.

We next examined what level of effective diffusivity would best match the measured data by varying diffusivity in the model, and assessing the best fit between measured and modeled data with Pearson's correlation coefficient. The fit consistently improved as we increased diffusivity in the model, and the "true" diffusivity appeared to exceed the range of values that would be reasonable for soil. Furthermore, the highest diffusivity level fit data from low-moisture and high-moisture soils almost equally well

(average R^2 was 0.987 vs 0.996 for low and high moisture, respectively), suggesting that CO_2 transport in our soil columns was far less sensitive to soil moisture then would be expected under diffusion-dominated conditions. A logical explanation of the high apparent diffusivity and the lack of sensitivity to moisture is that advection occurred during the sampling process. Extraction of the four 12mL air samples used to construct the Keeling plots would have displaced approximately 27% of the chamber headspace volume, thereby drawing CO_2 into the chamber from the soil profile. Although we are unable to confirm that advection occurred without differential pressure data, there are isotopic signals of advection present in our data set, which we discuss later.

Experiment 2: Impact of soil moisture on heterotrophic soil-respired $\delta^{13}CO_2$

To test the impact of microbial respiration on soil $\delta^{13}CO_2$ moisture dynamics, we incubated soils without plants overnight at different moisture levels in sealed soil columns. After 22 hours of incubation, headspace concentration ranged 1.1-2.0% CO_2 and $\delta^{13}C$ averaged -27.3 ± 0.2‰ (Figure 4.4, open circles). We also incubated smaller amounts of air-dried soils in Exetainer vials, which reached an average of 1.2 ± 0.2% CO_2 and ¯29.0 ± 0.4‰ $\delta^{13}C$ after 72 hours of incubation (Figure 4.4, triangles). Despite similar CO_2 concentrations, the soil columns had higher (more enriched) $\delta^{13}C$ signatures than the small Exetainer vials. We hypothesized this difference was a result of incomplete diffusive equilibration due to the relatively large volumes of the soil columns.

To test this hypothesis we parameterized the 1-D isotopologue model for each soil column using measured water contents and flux rates. The true values for soil $\delta^{13}C$ were unknown and were initially estimated as -28‰ across all moisture levels, and then reiterated at -28.4‰ to better match measured chamber values. Figure 4.5 shows the performance of the model at predicting chamber $\delta^{13}C$ and CO_2 after 22 hours of incubation. For concentration, the slope of the modeled versus measured CO_2 is not significantly different from one across a large range of post-incubation concentrations (95% CI=0.748-1.66, R^2=0.82). Measured chamber $\delta^{13}C$ values following the incubation period were similar for all moisture levels, varying by less then measurement uncertainty of ± 0.4‰. Modeling a single soil $\delta^{13}C$ value of -28.4‰ across all moisture levels predicted experimental chamber values to within ¯0.48 - 0.3‰.

Model simulations confirmed our hypothesis; the chamber headspace $\delta^{13}C$ was still more enriched than soil-respired $\delta^{13}C$ after the incubation period due to incomplete diffusive equilibration, by 1.0-1.3‰. When we subtracted the residual enrichment of each soil column from measured chamber $\delta^{13}C$ values, we found no significant difference between $\delta^{13}C$ values from the soil columns and Exetainer vials (Figure 4.4, closed symbols). A slight linear trend towards lighter $\delta^{13}C$ at low moisture was found, but the slope was not significantly different from zero (95% CI=-0.002-0.148).

DISCUSSION

The first goal of this study was to evaluate whether low moisture conditions that are stressful to plants cause enrichment of soil-respired $\delta^{13}CO_2$. In Experiment 1, we measured an average difference in soil-respired $\delta^{13}CO_2$ of 4.7‰ between moisture-sufficient and moisture-limited seedlings. Our second goal was to determine whether the treatment difference had biological origins or was due to sampling approach. Modeling of surface chambers under diffusive conditions (Nickerson and Risk 2009b) has indicated that soil moisture can substantially impact measured $\delta^{13}C$ because of greater non-linearity in the Keeling plot at low moisture levels. However, our sampling approach of repeatedly filling Exetainers from a soil surface chamber did not appear to be purely diffusive, and may have been impacted by advection. In the following discussion, we further evaluate the potential impacts of these advective sampling conditions on Keeling plot measurements.

In Experiment 2, our goal was to determine the influence of moisture on soil microbial-respired CO_2, and we were able to show clearly that enrichment of soil respiration under low moisture did not occur in the absence of roots. We found good agreement between the isotopologue gas diffusion model and our measurements using sealed soil columns. After modeling and correcting for the residual difference between soil-respired and headspace $\delta^{13}CO_2$ when soil columns were sampled, we found close agreement between samples from the large soil columns and the Exetainer vials. Across

a large range of soil moisture conditions we found no significant differences in $\delta^{13}CO_2$ of heterotrophic respiration.

Impacts of advection on measured $\delta^{13}C$

Under diffusive conditions, numerical simulations by Risk and Kellman (2008) and Nickerson and Risk (2009b) have shown that surface chambers disrupt concentration gradients between the soil and atmosphere, and cause the $\delta^{13}C$ of surface flux to change as the system approaches a new equilibrium. Both theoretical evidence (Nickerson & Risk, 2009a) and experimental evidence (Kayler *et al.*, 2008) have further demonstrated that the CO_2 concentrations and $\delta^{13}C$ signatures of surface chambers equilibrate to soil values at the depth where chambers are inserted. Pulses of advective transport, which draw soil gas into the surface chamber, are likely to increase the speed with which chambers approach and equilibrate with soil profile $\delta^{13}C$ and CO_2. The progressive enrichment of CO_2 fluxes entering the soil chamber over time produces Keeling intercepts that are biased towards enriched values.

In addition to advancing the equilibration between the chamber and soil, advection will also alter $\delta^{13}C$ of soil fluxes by drawing gas from soil pores that is more enriched than biological respiration, due to diffusive fractionation and atmospheric invasion. Soil pore CO_2 is more enriched than biological respiration by a minimum of 4.4‰ under steady-state conditions (Cerling *et al.*, 1991). Drawing this isotopically heavy CO_2 should considerably enrich the $\delta^{13}CO_2$ of fluxes entering the chamber headspace.

Advective sampling conditions can help to explain why the high and low moisture treatments had relatively enriched Keeling intercepts compared to both the closed incubation experiment, and the expected $\delta^{13}C$ values for C_3 plant-derived substrates (Dawson *et al.*, 2002). Under moist conditions, we expected $\delta^{13}C$ of total soil respiration to be similar to the average value obtained in Experiment 2 (-28.4‰). Instead, measured Keeling intercepts in Experiment 1 were considerably more enriched, averaging -24.7 and -20.0‰ for high and low moisture treatments, respectively.

The significant difference between high and low moisture treatments may be a result of differing enrichment of the isotopic profiles from which CO_2 is drawn into the surface chambers. As explained by Cerling *et al*. (1991), soils with low moisture (high diffusivity) experience greater atmospheric invasion than comparable soils with high moisture, and therefore have lower CO_2 concentrations and more enriched $\delta^{13}C$ values throughout the soil profile. In dry soils, low rates of biological CO_2 production further exacerbate atmospheric incursion into soil profiles. Advective sampling should therefore draw more enriched air from a dry soil than from a moist soil.

A reasonable response to this explanation might be that Keeling plots should be able to un-mix atmospheric and soil $\delta^{13}C$ end-members contributing to chamber CO_2. To apply Keeling plots correctly, however, the $\delta^{13}C$ of the air mixture in a surface chamber must approach the $\delta^{13}C$ of soil-produced CO_2 over time as concentrations increase in the chamber. In the advective case, as samples are drawn into the surface chamber, the $\delta^{13}C$ of the chamber approaches the $\delta^{13}C$ of the soil profile, which is a mixture of both atmospheric and soil-produced CO_2. The contributions of atmospheric

air to the soil profile make CO_2 within the profile more enriched, and therefore make Keeling intercepts more enriched than soil-produced CO_2. Furthermore, a dry soil profile containing more atmospheric air will produce a more enriched Keeling intercept than a moist soil.

Although the model does not explicitly model advective transport, our reasoning argues that the difference between Keeling intercepts at high and low moisture was due at least in part to CO_2 transport effects. The greater enrichment of CO_2 in dry soil profiles, and the failure of Keeling plots to un-mix atmospheric and soil $\delta^{13}C$ end-members under advective conditions, likely contributed to measured differences between the high and low-moisture treatments.

Interpreting surface chamber data

The failure of Keeling plots to un-mix atmospheric and soil $\delta^{13}C$ end-members is not isolated to advective conditions, but occurs anytime the $\delta^{13}C$ of flux entering a surface chamber changes over time. In general, surface chambers violate the assumptions of Keeling plot analysis by disturbing soil-atmosphere concentration gradients and altering the $\delta^{13}C$ of fluxes entering the chamber (Nickerson & Risk, 2009b). Furthermore, the magnitude of the disturbance depends on the moisture and diffusivity of the soil. A wide variety of designs have been employed to sample soil-respired CO_2 for $\delta^{13}C$ analysis, including three basic types of surface chambers: static chambers (Ekblad & Högberg, 2000; Kayler *et al.*, 2008; Mora & Raich, 2007), closed-

loop flow-through chambers (Buchmann & Ehleringer, 1997; Susfalk *et al.*, 2002), and open-loop flow-through chambers (Midwood *et al.*, 2008; Millard *et al.*, 2008; Miller *et al.*, 1999; Subke *et al.*, 2009). Few studies have rigorously tested these approaches (Midwood *et al.*, 2008; Nickerson & Risk, 2009b), and in cases where techniques are validated or compared to one another, soil moisture is not usually considered as a modulating factor (Gessler *et al.*, 2007; Kayler *et al.*, 2008; Ohlsson *et al.*, 2005).

The 1-D and 3-D isotopologue gas diffusion models presented here provide an option for validating sampling techniques, as well as interpreting existing data. As demonstrated in the second experiment with closed chambers, simulations are particularly useful for comparing results under different soil moisture levels. Models can also be used to assess the effects of sampling time, sample volume, and other variables. Chamber time-series data that has been collected for Keeling plot analysis can also be analyzed to determine the actual $\delta^{13}C$ of soil-produced CO_2.

Similarity between transport-related fractionation and photosynthetic discrimination

Sampling-related fractionation with surface chambers can impact Keeling intercepts to a similar extent and in the same direction as expected due to photosynthetic discrimination, which increases the likelihood that purely physical effects can be mistaken for biologically reasonable patterns. As reported elsewhere, and shown here for simulations we performed for the small chamber design used in the first experiment (Figure 4.6), under diffusive conditions Keeling intercepts become more enriched as soils become drier (Nickerson and Risk, 2009b). Under extreme sampling conditions,

with a long 45-minute measurement period and very dry soil, simulations produced Keeling intercepts biased by almost 4‰.

We compared the potential bias from transport-related effects to the expected impacts from photosynthetic discrimination, calculating theoretical $\delta^{13}C$ values for soil respiration from the planted soil columns used in Experiment 1. The photosynthetic discrimination of the seedlings was estimated using the model from Farquhar *et al*. (1989):

$$\Delta = a + [b - a][C_i / C_a]$$

where Δ is total discrimination due to photosynthesis, a is the fractionation due to diffusion in air (4.4‰), b is the net fractionation caused by carboxylation (27‰), and C_i and C_a are leaf internal CO_2 and ambient CO_2 concentration, respectively, which were both determined from foliar gas exchange measurements. We calculated Δ for each plant using mid-morning C_i and C_a values measured during week 5 of the moisture treatments. The $\delta^{13}C$ of photosynthate was assumed to equal the average daytime CO_2 in the greenhouse (estimated as -10‰) minus photosynthetic discrimination, Δ.

Theoretical values for $\delta^{13}C$ of soil respiration were calculated based on several simplifying assumptions. First, we assumed that $\delta^{13}C$ of heterotrophic respiration remained static at -28.4‰ (the average value from the heterotrophic incubation experiment) and did not vary with soil moisture. Second, we assumed that $\delta^{13}C$ of autotrophic soil respiration had the same isotopic composition as photosynthate calculated with the Farquhar model. We estimated heterotrophic respiration rates from

the root-free soils used in Experiment 2, and estimated autotrophic respiration rate by difference for planted and root-free soils with similar moisture content (rates were also normalized to 25ºC for comparison). We used these autotrophic and heterotrophic respiration rates and isotope values in a two-member mixing equation to calculate expected $\delta^{13}C$ of total soil respiration for each soil column.

As shown in Figure 4.7, the expected difference in soil-respired $\delta^{13}CO_2$ due to photosynthetic discrimination was 3.8‰ between the high and low-moisture treatments. The difference in autotrophic soil respiration predicted by Farquhar *et al.*'s model was approximately 8‰, but this autotrophic signal was diluted by heterotrophic fluxes that we assumed would remain isotopically static across moisture levels. The predicted difference in soil-respired $\delta^{13}CO_2$ due to photosynthetic discrimination was smaller than the difference in our Keeling intercepts measurements (4.7‰). Furthermore, even though we compared plants at high and extremely low moisture levels, the predicted difference in Keeling intercepts was within the range of bias that can occur from using surface chambers, even without advection (Figure 4.6).

The predicted difference due to photosynthetic discrimination was also smaller than theoretical diffusive fractionation (4.4‰), which reinforces the need to examine physical effects on measured soil $\delta^{13}CO_2$, not only associated with sampling, but also related to wind and other environmental factors (Bowling *et al.*, 2008a; Nickerson & Risk, 2009c). The magnitude to which wind or other variables affect soil-respired $\delta^{13}CO_2$ may depend on soil moisture content (Nickerson & Risk, 2009c). Therefore, it is

particularly important to scrutinize more closely soil $\delta^{13}CO_2$ measurements made across varying soil moistures, which may be susceptible to spurious correlations.

CONCLUSIONS

In this study we tested whether soil-respired $\delta^{13}CO_2$ is impacted by soil moisture, and whether the effects of moisture could be explained by microbial or gas transport-related fractionation. We demonstrated that heterotrophic respiration does not vary with moisture and cannot explain moisture effects on soil-respired $\delta^{13}CO_2$. When plants were present, we measured different Keeling intercepts at high and low-moisture levels, and modeling suggests these measured values were likely influenced by gas transport processes. Although we cannot rule out potential impacts from photosynthetic discrimination, we further demonstrated that the maximum difference in soil-respired $\delta^{13}CO_2$ we could expect from changes in $\delta^{13}C$ of recent photosynthates was smaller than our measured difference, and was also smaller than the theoretical value associated with gas diffusion. This indicates that it may be difficult to detect the impacts of photosynthetic discrimination on soil-respired $\delta^{13}CO_2$ because of gas transport-related fractionation, and that it is quite possible to obtain a biologically reasonable relationship between moisture and soil-respired $\delta^{13}CO_2$ from purely physical effects.

ACKNOWLEDGEMENTS

With great fondness and appreciation we acknowledge the memory of Elizabeth W. Sulzman, whose efforts to understand soil isofluxes helped stimulate this inquiry. We thank William Rugh and Renee J. Brooks from the Environmental Protection Agency Integrated Stable Isotope Research Facility, for their support in analyzing samples from the second greenhouse experiment. Andrew Ross from the OSU / COAS Stable Isotope Mass Spectrometer Facility helped analyze samples for the first greenhouse experiment. Model computation was performed on the Atlantic Computational Excellence Network (ACEnet). Funding was provided in part by the National Science Foundation (Grants DEB-0132737 and DEB-0416060). C. Phillips received funding from the Richardson Family Fellowship and travel assistance from Richard and Doris Waring.

REFERENCES

Bahn M, Schmitt M, Siegwolf R, Richter A, Brüggemann N (2009) Does photosynthesis affect grassland soil-respired CO_2 and its carbon isotope composition on a diurnal timescale? *New Phytologist,* **182**, 451-460.

Boutton TW (1996) Stable carbon isotope ratios of soil oganic matter and their use as indicators of vegetation and climate changes. In: *Mass Spectrometry of Soils.* (eds Boutton Tw, Yamasaki Si) pp Page. New York, Marcel Dekker.

Bowling DR, Massman WJ, Schaeffer SM, Burns SP, Monson RK, Williams MW (2008a) Biological and physical influences on the carbon isotope content of CO_2 in a subsalpine forest snowpack, Niwot Ridge, Colorado. *Biogeochemistry*.

Bowling DR, Pataki DE, Randerson JT (2008b) Carbon isotopes in terrestrial ecosystem pools and CO_2 fluxes. *New Phytologist,* **178**.

Brown RB (1974) Genesis of some soils in the central western Cascades of Oregon. Unpublished M.S. Thesis M.S. Thesis, Oregon State University, Corvallis, OR, 172 pp.

Brugnoli E, Hubick KT, von Caemmerer S, Wong SC, Garquhar GD (1988) Correlation between the carbon isotope discrimination in leaf starch and sugars of C_3 plants

and the ratio of intercellular and atmospheric partial pressures of carbon dioxide. *Plant Physiology,* **88**, 1418-1424.

Buchmann N, Ehleringer JR (1997) CO_2 concentration profiles, and carbon and oxygen isotopes in C_3 and C_4 crop canopies. *Agricultural and Forest Meteorology,* **89**, 45-58.

Cerling T, Solomon DK, Quade J, Bowman JR (1991) On the isotopic composition of carbon in soil carbon dioxide. *Geochimica et Cosmochimica Acta*, 3403-3405.

Crow SE, Sulzman EW, Rugh WD, Bowden RD, Lajtha K (2006) Isotopic analysis of respired CO_2 during decomposition of separated soil organic matter pools. *Soil Biology & Biochemistry*, **38**, 3279-3291.

Dawson TE, Mambelli S, Plamboeck AH, Templer PH, Tu KP (2002) Stable Isotopes on Plant Ecology. *Annual Review of Ecology and Systematics*, 507-559.

Ekblad A, Boström B, Holm A, Comstdet D (2005) Forest soil respiration rate and $\delta^{13}C$ is regulated by recent above ground weather conditions. *Oecologia,* **143**, 136-142.

Ekblad A, Högberg P (2000) Analysis of $\delta^{13}C$ of CO_2 distinguishes between microbial respiration of added C_4-sucrose and other soil respiration in a C_3-ecosystem. *Plant and Soil,* **219**, 197-209.

Ekblad A, Högberg P (2001) Natural abundance of ^{13}C in CO_2 respired from forest soils reveals speed of link between tree photosynthesis and root respiration. *Oecologia,* **127**, 305-308.

Farquhar GD, Ehleringer JR, Hubick KT (1989) Carbon isotope discrimination and photosynthesis. *Annual Review of Plant Physiology and Plant Molecular Biology,* **40**, 503-537.

Fessenden JE, Ehleringer JR (2003) Temporal variation in $\delta^{13}C$ of ecosystem respiration in the Pacific Northwest: links to moisture stress. *Oecologia,* **136**, 129-136.

Flanagan LB, Ehleringer JR (1998) Ecosystem-atmosphere CO2 exchange: interpreting signals of change using stable isotope ratios. *Trends in Ecology and Evolution,* **13**, 10-14.

Gaumont-Guay D, Black A, McCaughey H, Barr AG, Krishnan P, Jassal RS, Nesic Z (2009) Soil CO2 efflux in contrasting boreal deciduous and coniferous stands and its contribution to the ecosystem carbon balance. *Global Change Biology*.

Gessler A, Keitel C, Kodoma N *et al.* (2007) $\delta^{13}C$ of organic matter transported form the leaves to the roots in *Eucalyptus delegatensis*: short-term variations and relation to respired CO_2. *Functional Plant Biology,* **34**, 692-706.

Högberg P, Högberg MN, Göttlicher SG *et al.* (2008) High temporal resolution tracing of photosynthate carbon from the tree canopy to forest soil microorganisms. *New Phytologist*, **177**, 220-228.

Högberg P, Nordgern A, Buchmann N *et al.* (2001) Large-scale forest girdling shows that current photosynthesis drives soil respiration. *Nature,* **411**, 789-792.

Hymus GJ, Maseyk K, Valentini R, Yakir D (2005) Large daily variation in ^{13}C-enrichment of leaf-respired CO_2 in two *Quercus* forest canopies. *New Phytologist*, **167**, 377-384.

Jassal RS, Black TA, Cai T, Morgenstern K, Li Z, Gaumont-Guay D, Nesic Z (2007) Components of ecosystem respiration and an estimate of net primary productivity of an intermediate-aged Douglas-fir stand. *Agricultural and Forest Meteorology*, **144**, 44-57.

Kayler Z, Sulzman EW, Marshall JD, Mix AC, Rugh WD, Bond BJ (2008) A laboratory comparison of two methods used to estimate the isotopic composition of soil $\delta^{13}CO_2$ efflux at steady state. *Rapid Communications in Mass Spectrometry*, **22**, 2533-2538.

Maunoury F, Berveiller D, Lelarge C, Pontailler J-Y, Vanbostal L, Damesin C (2007) Seasonal, daily and diurnal variations in the stable carbon isotope composition of carbon dioxide respired by tree trunks in a deciduous oak forest. *Oecologia*, **151**, 268-279.

McCarthy KA, Johnson RL (1995) Measurement of trichloroethylene diffusion as a function of moisture-content in sections of gravity-drained soil columns. *Journal of Environmental Quality*, **24**, 49-55.

McDowell NG, Bowling DR, Bond BJ, Irvine J, Law BE, Anthoni P, Ehleringer JR (2004) Response of the carbon isotopic content of ecosystem, leaf, and soil respiration to meteorological and physiological driving factors in a *Pinus ponderosa* ecosystem. *Global Biogeochemical Cycles*, **18**.

Midwood AJ, Thornton B, Millard P (2008) Measuring the ^{13}C content of soil-respired CO_2 using a novel open chamber system. *Rapid Communications in Mass Spectrometry*, **22**, 2073-2081.

Millard P, Midwood AJ, Hunt JE, Whitehead D, Boutton TW (2008) Partitioning soil surface CO_2 efflux into autotrophic and heterotrophic components, using natural gradients in soil $\delta^{13}C$ in an undisturnbed savannah soil. *Soil Biology & Biochemistry*, **40**, 1575-1582.

Miller JB, Yaki D, White JWC, Tans PP (1999) Measurement of $^{18}O/^{16}O$ in the soil-atmosphere CO_2 flux. *Global Biogeochemical Cycles*, **13**, 761-774.

Mora G, Raich JW (2007) Carbon-isotopic composition of soil-respirated carbon dioxide in static closed chambers at equilibrium. *Rapid Communications in Mass Spectrometry*, **21**, 1866-1870.

Nickerson N, Risk D (2009a) Keeling plots are non-linear in non-steady state diffusive environments. *Geophysical Research Letters*, **36**, doi:10.1029/2008GL036945.

Nickerson N, Risk D (2009b) A numerical evaluation of chamber methodologies used in measuring the $\delta^{13}C$ of soil respiration. *Rapid Communications in Mass Spectrometry*, **23**, 2802-2810.

Nickerson N, Risk D (2009c) Physical Controls on the Isotopic Composition of Soil Respired CO_2. *Journal of Geophysical Research*, **114**, doi:10.1029/2008JG000766.

Ohlsson KEA, Singh B, Holm S, Nordgren A, Lövdahl L, Högberg P (2005) Uncertainties in static closed chamber measurements of the carbon isotopic ratio of soil-respired CO2. *Soil Biology and Biochemistry,* **37**, 2273-2276.

Pate J, Arthur D (1998) $\delta^{13}C$ analysis of phloem sap carbon: novel means of evaluating seasonal water stress and interpreting carbon isotope signatures of foliage and trunk wood of *Eucalyptus globulus*. *Oecologia,* **117**, 301-311.

Pypker T, Hauck M, Sulzman EW *et al.* (2008) Towards using $\delta^{13}C$ of ecosystem respiration to monitor canopy physiology in complex terrain. *Oecologia,* **158**, 399-410.

Risk D, Kellman L (2008) Isotopic fractionation in non-equilibrium diffusive environments. *Geophysical Research Letters,* **35**, L02403-02406.

Ryan MG, Law BE (2005) Interpreting, measuring, and modeling soil respiration. *Biogeochemistry,* **73**, 3.

Subke J-A, Vallack HW, Magnusson T, Keel SG, Metcalfe DB, Högberg P, Ineson P (2009) Short-term dynamics of abiotic and biotic soil $^{13}CO_2$ effluxes after *in situ* $^{13}CO_2$ pulse labelling of a boreal pine forest. *New Phytologist,* **183**, 349-357.

Susfalk RB, Cheng W, Johnson DW, Walker RF, Verburg P, Fu S (2002) Lateral diffusion and atmospheric CO_2 mixing compromise estimates of rhizosphere respiration in a forest soil. *Canadian Journal of Forest Research*, **32**, 1005-1015.

Tang J, Baldocchi DD, Xu L (2005) Tree photosynthesis modulates soil respiration on a diurnal time scale. *Global Change Biology*, **11**, 1298-1304.

Taylor BN, Kuyatt CE (1994) NIST Technical Note 1297: Guidelines for Evaluating and Expressing the Uncertainty of NIST Measurement Results. *National Institute of Standards and Technology, US Dept of Commerce, Technology Administration*.

Tedeschi V, Rey A, Manca G, Valentini R, Jarviss PG, Borghetti M (2006) Soil respiration in a Mediterranean oak forest at different developmental stages after coppicing. *Global Change Biology*, **12**, 110-121.

Werner C, Wegener F, Unger S, Nogués S, Priault P (2009) Short-term dynamics of isotopic composition of leaf-respired CO_2 upon darkening: measurements and implications. *Rapid Communications in Mass Spectrometry,* **23**, 2428-2438.

Figure 4.1. Mean mid-morning stomatal conductance under natural light over the course of moisture treatments. Error bars are 95% confidence intervals.

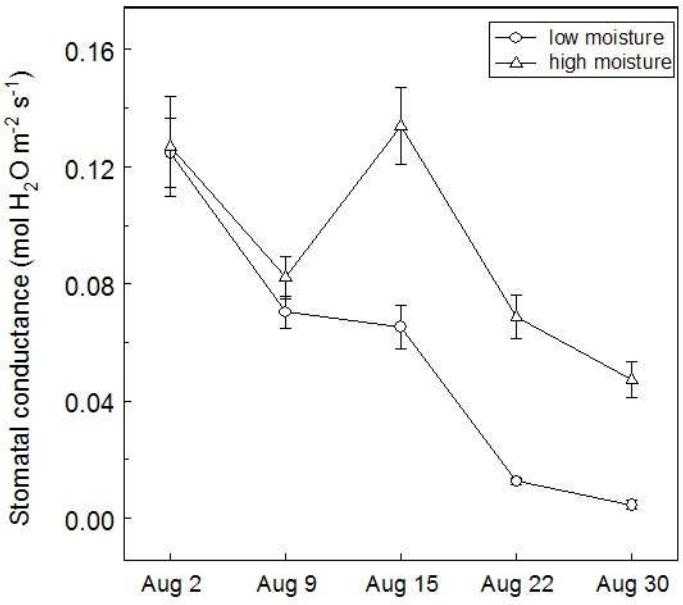

Figure 4.2. Keeling intercepts at high and low moisture levels for total soil respiration with Douglas-fir seedling roots. Error bars are SE for the intercepts of linear least squares regressions.

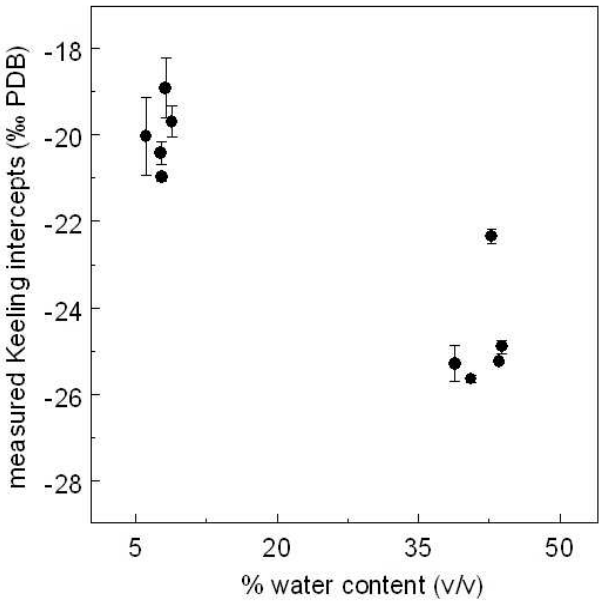

Figure 4.3. Measured and modeled $\delta^{13}C$ and CO_2 for a small soil chamber. Black circles and black line are measured and modeled $\delta^{13}C$, respectively. Grey triangles and grey line are measured and modeled CO_2 concentration, respectively. Water content was 6% (v/v) and respiration rate was 1.2μmol CO_2 $m^{-2}s^{-1}$.

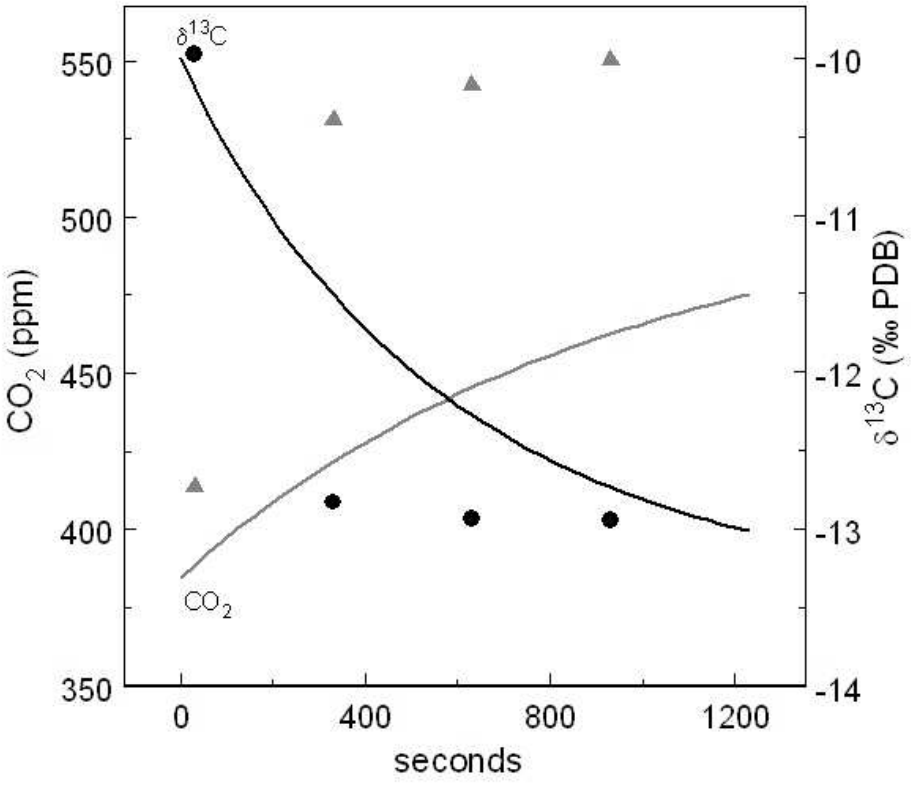

Figure 4.4. Heterotrophic soil respiration $\delta^{13}C$ across a range of soil moistures. Measured $\delta^{13}C$ of large chamber headspace (○), measurements adjusted by modeled estimates of residual headspace enrichment (●), and measured $\delta^{13}C$ of small vial headspace (▲). Slope of regression is not statistically different from zero (slope=0.02, p=0.06). Error bars are mass spectrometer measurement uncertainty (0.4‰).

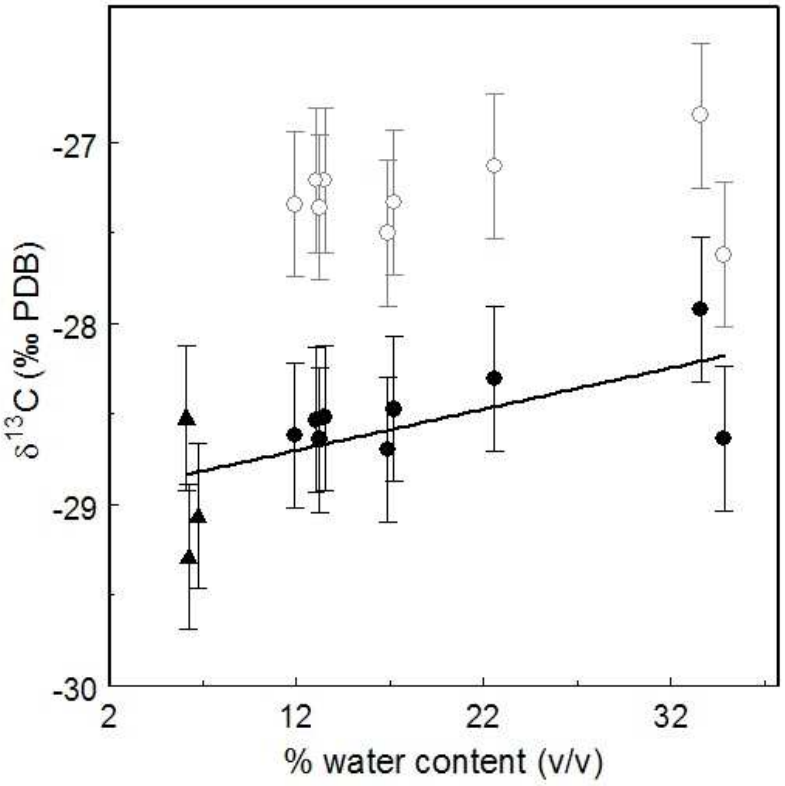

Figure 4.5. Modeled versus measured chamber headspace $\delta^{13}C$ (top) and CO_2 concentration (bottom), for a 22-hr incubation period. Horizontal bars are mass spectrometer uncertainties for $\delta^{13}C$ (± 0.4‰) and CO_2 concentration (± 2.5%), respectively. Vertical error bars represent model output for ± 25% of the CO_2 production rate measured prior to sealing the pots, to account for uncertain fluctuations in temperature during the incubation period. Darkest to lightest colors indicate highest to lowest soil moisture.

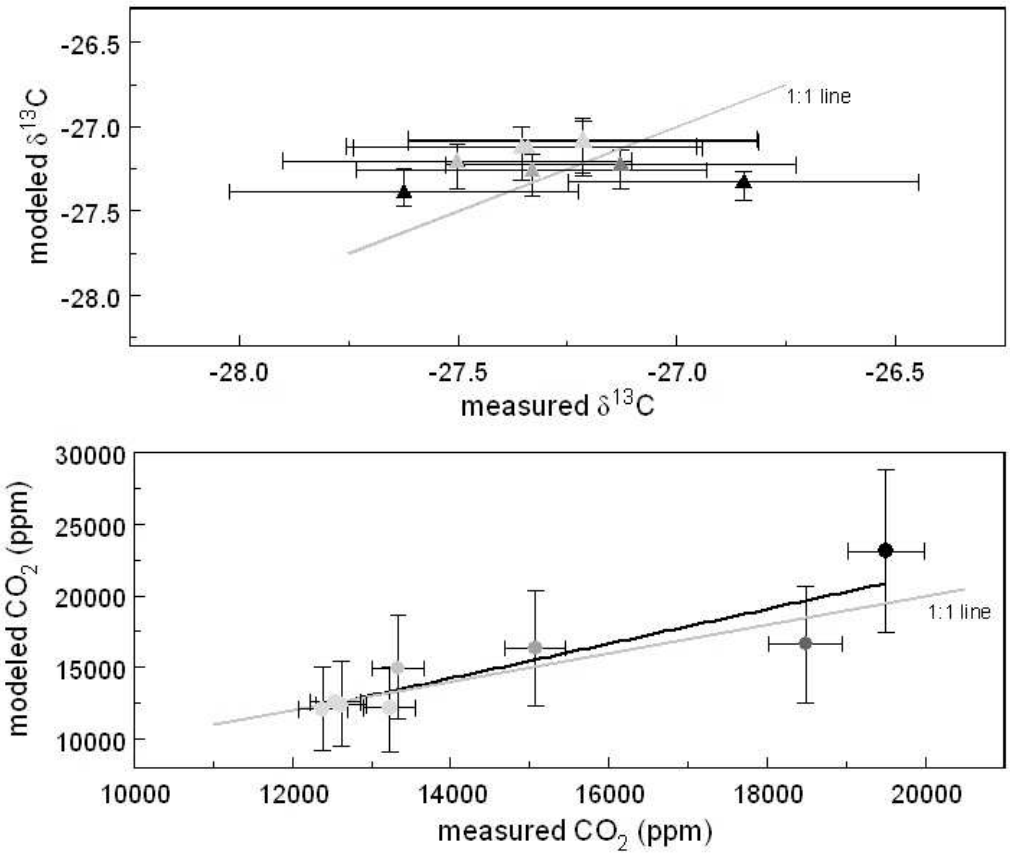

Figure 4.6. Modeled Keeling intercepts for 3 levels of soil respiration (μmol m^{-2} s^{-1}) and a range of water contents. Circles are Keeling intercepts fitted to 4 points spaced 15 minutes apart, and triangles are fitted to 4 points spaced 5 minutes apart. Error bars are standard errors for intercepts of least squares regressions.

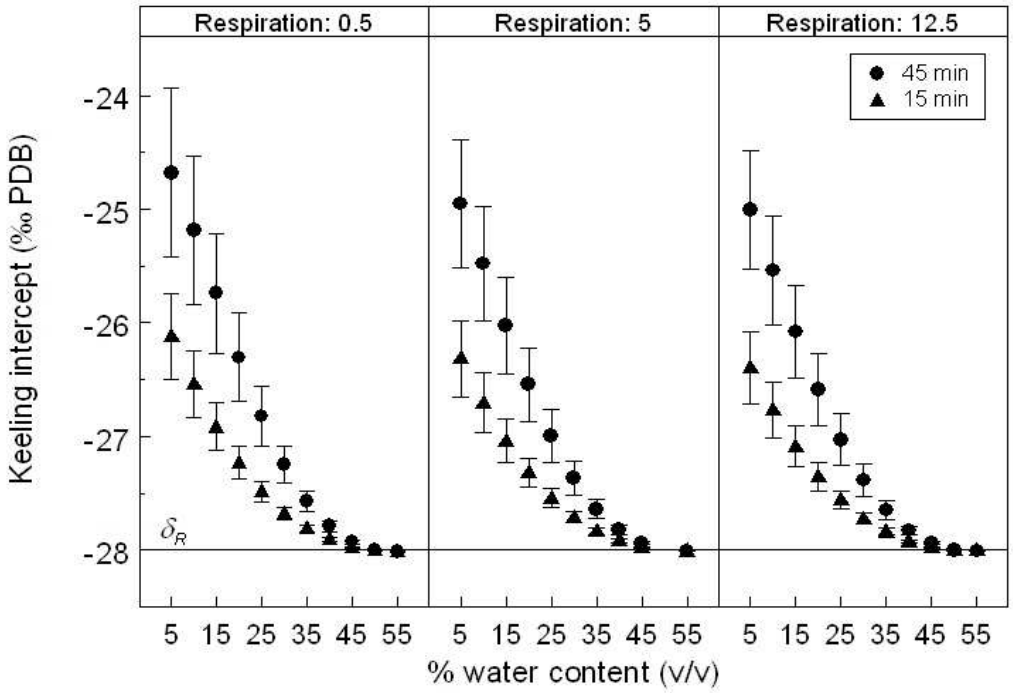

Figure 4.7. Theoretical soil-respired $\delta^{13}CO_2$ using the Farquhar model to calculate $\delta^{13}C$ of autotrophic contributions. Heterotrophic $\delta^{13}C$ was held constant (-28.4‰), autotrophic $\delta^{13}C$was modeled from foliar gas exchange measurements and the Farquhar *et al*. model, and $\delta^{13}C$ of total soil respiration was calculated from heterotrophic and autotrophic end-members using a 2-member mixing equation. Relative contributions of autotrophic and heterotrophic sources were determined from respiration rates measured from intact and root-free soils.

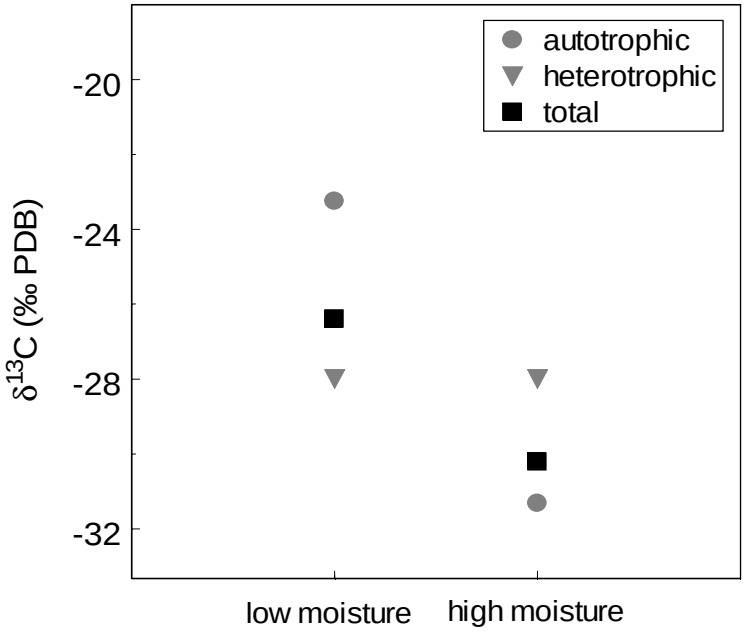

CHAPTER FIVE: GENERAL CONCLUSIONS

The studies presented above collectively demonstrate that soil gas transport has important influences on respiration dynamics under varying moisture and temperature conditions. In the first study I showed that the seasonal contributions of EcM mats to total soil respiration may vary in part due to impacts of soil moisture on gas diffusivity. I found that fluxes from deep soil horizons decreased with higher moisture in the fall and winter, which may have helped to increase the relative contributions of soil biota concentrated near the soil surface. In the second study, I showed that diel hysteresis patterns between soil respiration and soil temperature can be explained entirely by CO_2 and heat transport processes. Although biological influences such as diel changes in photosynthate supply can modify these patterns, they are not necessary to explain the existence of hysteresis. Finally, in the third study I showed that soil moisture effects on the $\delta^{13}C$ of soil respiration were likely caused in part by gas transport effects.

The common conclusion from these studies, that soil physics plays an important role in respiration dynamics, should come as no surprise. Analagous ecophysiology studies of plant gas exchange (aboveground) have led to mathematical descriptions of the impacts of CO_2 diffusion, water availability, heat and energy balance on rates of photosynthesis and respiration (Nobel, 1991). In light of the more sophisticated understanding already developed for plant respiration, perhaps more surprising is the fact that physical descriptions of soil respiration have not been developed farther already. However, as shown in this dissertation, in many cases physical responses to

environmental drivers produce similar soil respiration dynamics as would be expected for biological responses. Gas transport responses to temperature and moisture often are not readily evident unless soil CO_2 profiles are explicitly examined in addition to soil surface fluxes.

A next step in developing more mechanistic descriptions of soil respiration would be to build both conceptual and numerical models of soil respiration that are more spatially realistic. In many soil respiration studies, CO_2 fluxes are only measured at the soil surface, and environmental variables such as moisture and temperature are measured at one or a few discreet depths within the soil. Without also knowing how CO_2 production is distributed in the soil, there may be significant mismatch between sensor locations and depths where CO_2 production originates. As an analogy, a plant ecophysiologist would not compare photosynthesis rates at the very top of a forest canopy to light levels or temperatures half way through the canopy, because it is widely appreciated that steep environmental gradients exist within plant canopies. Similarly, soil profiles exhibit steep environmental gradients, as well as gradients in soil physical properties and biological activity, with changes often occurring across distances of centimeters. Too often these gradients are ignored, and measurements at arbitrary depths are used to represent the whole production profile, or soils are treated with only very coarse spatial representations (e.g. Biome-BGC contains a rooting zone, and a sub-rooting zone).

In these studies, by comparing interpretations of soil respiration with and without accounting for gas transport, I argue that soil physical effects can often be

overlooked, and that ignoring gas transport processes can lead to incorrect assessments of how moisture, temperature, and other forcing factors influence soil respiration.

Nobel PS (1991) *Physicochemical and Environmental Plant Physiology*, San Diego, CA, Academic Press.

CONSOLIDATED BIBLIOGRAPHY

Aerts R (2002) The role of various types of mycorrhizal fungi in nutrient cycling and plant competition. In: *Mycorrhizal Ecology*. (eds Van Der Heijden Mga, Sanders Ir) pp Page. Berlin, Springer-Verlag.

Agerer R (2001) Exploration types of ectomycorrhizae. A proposal to classify ectomycorrhizal mycelial systems according to their patterns of differentiation and putative ecological importance. *Mycorrhiza,* **11**, 107-114.

Bahn M, Schmitt M, Siegwolf R, Richter A, Brüggemann N (2009) Does photosynthesis affect grassland soil-respired CO_2 and its carbon isotope composition on a diurnal timescale? *New Phytologist,* **182**, 451-460.

Beltrami H (1996) Active Layer Distortion of Annual Air/Soil Thermal Orbits. *Permafrost and Periglacial Processes,* **7**, 101-110.

Bhupinderpal-Singh A, Nordgren A, Ottosson Löfvenius M, Högberg MN, Mellander P-E, Högberg P (2003) Tree root and soil heterotrophic respiration as revealed by girdling of boreal Scots pine forest: extending observations beyond the first year. *Plant, Cell, and Environment,* **26**, 1287-1296.

Blanchard JH (2008) Episodic dynamics of microbial communities associated with the birth and death of ectomycorrhizal mats in old-growth Douglas-fir stands. Unpublished M.S. Oregon State University, Corvallis, 52 pp.

Bond-Lamberty B, Wang C, Gower ST (2004) A Global Relationship Between the Heterotrophic and Autotrophic Components of Soil Respiration? *Global Change Biology*, **10**, 1756-1766.

Boutton TW (1996) Stable carbon isotope ratios of soil oganic matter and their use as indicators of vegetation and climate changes. In: *Mass Spectrometry of Soils.* (eds Boutton Tw, Yamasaki Si) pp Page. New York, Marcel Dekker.

Bowling DR, Massman WJ, Schaeffer SM, Burns SP, Monson RK, Williams MW (2008a) Biological and physical influences on the carbon isotope content of CO_2 in a subsalpine forest snowpack, Niwot Ridge, Colorado. *Biogeochemistry*.

Bowling DR, Pataki DE, Randerson JT (2008b) Carbon isotopes in terrestrial ecosystem pools and CO_2 fluxes. *New Phytologist,* **178**.

Brown RB (1974) Genesis of some soils in the central western Cascades of Oregon. Unpublished M.S. Thesis M.S. Thesis, Oregon State University, Corvallis, OR, 172 pp.

Brugnoli E, Hubick KT, von Caemmerer S, Wong SC, Garquhar GD (1988) Correlation between the carbon isotope discrimination in leaf starch and sugars of C_3 plants and the ratio of intercellular and atmospheric partial pressures of carbon dioxide. *Plant Physiology,* **88**, 1418-1424.

Buchmann N, Ehleringer JR (1997) CO_2 concentration profiles, and carbon and oxygen isotopes in C_3 and C_4 crop canopies. *Agricultural and Forest Meteorology,* **89**, 45-58.

Cairney JWG, Chambers SM (eds) (1999) *Ectomycorrhizal Fungi: Key Genera in Profile*, Berlin, Springer.

Campbell JL, Sun OJ, Law BE (2004) Supply-Side Controls on Soil Respiration Among Oregon Forests *Global Change Biology,* **10**, 1857-1869.

Carbone MS, Czimczik CI, McDuffee KE, Trumbore SE (2007) Allocation and residence time of photosynthetic products in a boreal forest using a low-level ^{14}C pulse-chase labeling technique. *Global Change Biology,* **13**, 466-477.

Carbone MS, Vargas R (2008) Automated soil respiration measurements: new information, opportunities and challenges. *New Phytologist,* **177**, 295-297.

Carbone MS, Winston GC, Trumbore SE (2008) Soil respiration in perennial grass and shrub ecosystems: Linking environmental controls with plant and microbial sources on seasonal and diel timescales. *Journal of Geophysical Research,* **113**.

Castellano MA (1988) The taxonomy of the genus *Hysterangium* (Basidiomycotina, Hysterangiaceae) with notes on its ecology. Unpublished Ph.D. Oregon State University, Corvallis, OR, 238 pp.

Cerling T, Solomon DK, Quade J, Bowman JR (1991) On the isotopic composition of carbon in soil carbon dioxide. *Geochimica et Cosmochimica Acta*, 3403-3405.

Chen JM, Huang SE, Ju W, Gaumont-Guay D, Black TA (2009) Daily heterotrophic respiration model considering the diurnal temperature variability in the soil. *Journal of Geophysical Research,* **114**.

Cheng W, Johnson DW, Fu S (2003) Rhizosphere effects on decomposition: controls of plant species, phenology, and fertilization. *Soil Science Society of America Journal,* **67**, 1418–1427.

Cromack K, Fichter BL, Moldenke AM, Entry JA, Ingham ER (1988) Interactions between soil animals and ectomycorrhizal fungal mats. *Agriculture, Ecosystems & Environment*, **24**, 161-168.

Cromack K, Sollins P, Graustein WC *et al.* (1979) Calcium oxalate accumulation and soil weathering in mats of the hypogeous fungus *Hysterangium crassum*. *Soil Biology & Biochemistry*, **11**, 463-468.

Crow SE, Sulzman EW, Rugh WD, Bowden RD, Lajtha K (2006) Isotopic analysis of respired CO_2 during decomposition of separated soil organic matter pools. *Soil Biology & Biochemistry*, **38**, 3279-3291.

Davidson EA, Janssens IA, Luo Y (2006a) On the variability of respiration in terrestrial ecosystems: moving beyond Q_{10}. *Global Change Biology,* **12**, 154-164.

Davidson EA, Savage KE, Trumbore SE, Borken W (2006b) Vertical partitioning of CO2 production within a temperate forest soil. *Global Change Biology*, **12**, 944-956.

Davidson EA, Trumbore SE (1995) Gas diffusivity and production of CO_2 in deep soils of the eastern Amazon. *Tellus B,* **47**, 550-565.

Dawson TE, Mambelli S, Plamboeck AH, Templer PH, Tu KP (2002) Stable Isotopes on Plant Ecology. *Annual Review of Ecology and Systematics*, 507-559.

Dijkstra FA, Cheng W (2007) Interactions between soil and tree roots accelerate long-term soil carbon decomposition. *Ecology Letters,* **10**, 1046-1053.

Dixon JJ (2003) Applying GIS to soil-geomorphic landscape mapping in the Lookout Creek valley, Western Cascades, Oregon. Unpublished M.S. Oregon State University, Corvallis.

Dunham SM, Larsson K-H, Spatafora JW (2007) Diversity and community structure of mat-forming ectomycorrhizal fungi in old growth and rotation age Douglas-fir forests fo the HJ Andrews Experimental Forest, Oregon, USA. *Mycorrhiza,* **17**, 633-645.

Ekblad A, Boström B, Holm A, Comstdet D (2005) Forest soil respiration rate and $\delta^{13}C$ is regulated by recent above ground weather conditions. *Oecologia,* **143**, 136-142.

Ekblad A, Högberg P (2000) Analysis of $\delta^{13}C$ of CO_2 distinguishes between microbial respiration of added C_4-sucrose and other soil respiration in a C_3-ecosystem. *Plant and Soil,* **219**, 197-209.

Ekblad A, Högberg P (2001) Natural abundance of ^{13}C in CO_2 respired from forest soils reveals speed of link between tree photosynthesis and root respiration. *Oecologia,* **127**, 305-308.

Entry JA, Rose CL, Cromack K (1991) Litter decomposition and nutrient release in ectomycorrhizal mat soils of a Douglas fir ecosystem. *Soil Biology & Biochemistry*, **23**, 285-290.

Erland S, Taylor AFS (2002) Diveristy of ecto-mycorrhizal fungal communities in relation to the abiotic environment. In: *Mycorrhizal Ecology.* (eds Van Der Heijden Mga, Sanders Ir) pp Page. Berlin, Springer-Verlag.

Fahey T, Tierney G, Fitzhugh R, Wilson G, Siccama T (2005) Soil respiration and soil carbon balance in a northern hardwood forest ecosystem. *Canadian Journal of Forest Research*, **35**, 244-253.

Farquhar GD, Ehleringer JR, Hubick KT (1989) Carbon isotope discrimination and photosynthesis. *Annual Review of Plant Physiology and Plant Molecular Biology*, **40**, 503-537.

Fessenden JE, Ehleringer JR (2003) Temporal variation in $\delta^{13}C$ of ecosystem respiration in the Pacific Northwest: links to moisture stress. *Oecologia,* **136**, 129-136.

Flanagan LB, Ehleringer JR (1998) Ecosystem-atmosphere CO2 exchange: interpreting signals of change using stable isotope ratios. *Trends in Ecology and Evolution,* **13**, 10-14.

Garbaye J (1994) Helper bacteria: a new dimension to the mycorrhizal symbiosis. *New Phytologist*, **128**, 197-210.

Gaumont-Guay D, Black A, McCaughey H, Barr AG, Krishnan P, Jassal RS, Nesic Z (2009) Soil CO2 efflux in contrasting boreal deciduous and coniferous stands and its contribution to the ecosystem carbon balance. *Global Change Biology*.

Gessler A, Keitel C, Kodoma N *et al.* (2007) $\delta^{13}C$ of organic matter transported form the leaves to the roots in *Eucalyptus delegatensis*: short-term variations and relation to respired CO_2. *Functional Plant Biology*, **34**, 692-706.

Goodman DM, Trofymow JA (1998) Distribution of ectomycorrhizas in micro-habitats in mature and old-growth stands of douglas-fir on southeastern Vancouver Island. *Soil Biology & Biochemistry*, **30**, 2127-2138.

Graf A, Weihermüller L, Huisman JA, Herbst M, Bauer J, Vereecken H (2008) Measurement depth effects on the apparent temperature sensitivity of soil respiration in field studies. *Biogeosciences*, **5**, 1175-1188.

Griffiths RP, Baham JE, Caldwell BA (1994) Soil solution chemistry of ectomycorrhizal mats in forest soil. *Soil Biology & Biochemistry*, **26**, 331-337.

Griffiths RP, Bradshaw GA, Marks B, Lienkaemper GW (1996) Spatial distribution of ectomycorrhizal mats in coniferous forests of the Pacific Northwest, USA. *Plant and Soil*, **180**, 147-158.

Griffiths RP, Caldwell BA (1992) Mycorrhizal mat communities in forest soils. In: *Mycorrhizae in ecosystems*. (eds Read Dj, Lewis Dh, Fitter Ah, Alexander Ij) pp Page. Cambridge, Cambridge University Press.

Griffiths RP, Caldwell BA, Cromack Jr K, Morita RY (1990) Douglas-fir forest soils colonized by ectomycorrhizal mats. I. Seasonal variation in nitrogen chemistry and nitrogen cycle transformation rates. *Canadian Journal of Forest Research*, **20**, 211-218.

Griffiths RP, Chadwick AC, Robatzek M, Schauer K, Schaffroth KA (1995) Association of ectomycorrhizal mats with Pacific yew and other understory trees in coniferous forests. *Plant and Soil*, **173**, 343-347.

Heinemeyer A, Hartley IP, Evans SP, Carreira de la Fuentes JA, Ineson P (2007) Forest soil CO_2 flux: uncovering the contribution and environmental responses of ectomycorrhizas. *Global Change Biology*, **13**, 1786-1797.

Heinemeyer A, Ineson P, Ostle N, Fitter AH (2006) Respiration of the External Mycelium in the Arbuscular Mycorrhizal Symbiosis Shows Strong Dependence on Recent Photosynthates and Acclimation to Temperature. *New Phytologist*, **171**, 159-170.

Hibbard KA, Law BE, Reichstein M, Sulzman J (2005) An analysis of soil respiration across northern hemisphere temperate ecosystems. *Biogeochemistry*, **73**, 29.

Hillel D (1998) *Environmental Soil Physics*, San Diego, Academic Press.

Hobbie EA (2006) Carbon Allocation to Ectomycorrhizal Fungi Correlates with Belowground Allocation in Culture Studies. *Ecology*, **87**, 563-569.

Hodge A, Alexander IJ, Gooday GW (1995) Chitinolytic activities of *Eucalyptus pilularis* and *Pinus sylvestris* root systems challenged with mycorrhizal and pathogenic fungi. *New Phytologist*, **131**, 255-261.

Hoffland E, Kuyper TW, Wallander H *et al.* (2004) The role of fungi in weathering. *Frontiers in Ecology and the Environment*, **2**, 258-264.

Högberg MN, Högberg P (2002) Extramatrical Ectomycorrhizal Mycelium Contributes One-Third of Microbial Biomass and Produces, Together with Associated Roots, Half the Dissolved Organic Carbon in a Forest Soil. *New Phytologist*, **154**, 791-795.

Högberg P, Högberg MN, Göttlicher SG *et al.* (2008) High temporal resolution tracing of photosynthate carbon from the tree canopy to forest soil microorganisms. *New Phytologist*, **177**, 220-228.

Högberg P, Nordgern A, Buchmann N *et al.* (2001) Large-scale forest girdling shows that current photosynthesis drives soil respiration. *Nature*, **411**, 789-792.

Hymus GJ, Maseyk K, Valentini R, Yakir D (2005) Large daily variation in ^{13}C-enrichment of leaf-respired CO_2 in two *Quercus* forest canopies. *New Phytologist*, **167**, 377-384.

Ingham ER, Griffiths RP, Cromack K, Entry JA (1991) Comparison of Direct vs Fumigation Incubation Microbial Biomass Estimates from Ectomycorrhizal Mat and Non-mat Soils. *Soil Biology and Biochemistry*, **23**, 465-471.

Irvine J, Law B, Martin J, Vickers D (2008) Interannual variation in soil CO_2 efflux and the response of root respiration to climate and canopy gas exchange in mature ponderosa pine. *Global Change Biology*, **14**, 2848-2859.

Irvine J, Law BE, Anthoni P, Meinzer FC (2002) Water Limtations to Carbon Exchange in Old-Growth and Young Ponderosa Pine Stands. *Tree Physiology*, **22**, 189-196.

Irvine J, Law BE, Kurpius MR (2005) Coupling of canopy gas exchange with root and rhizosphere respiration in a semi-arid forest. *Biogeochemistry*, **73**, 271.

Jassal RS, Black TA, Cai T, Morgenstern K, Li Z, Gaumont-Guay D, Nesic Z (2007) Components of ecosystem respiration and an estimate of net primary productivity of an intermediate-aged Douglas-fir stand. *Agricultural and Forest Meteorology*, **144**, 44-57.

Kayler Z, Sulzman EW, Marshall JD, Mix AC, Rugh WD, Bond BJ (2008) A laboratory comparison of two methods used to estimate the isotopic composition of soil $\delta^{13}CO_2$ efflux at steady state. *Rapid Communications in Mass Spectrometry*, **22**, 2533-2538.

Kodoma N, Barnard RL, Salmon Y *et al.* (2008) Temporal dynamics of the carbon isotope composition in a *Pinus sylvestris* stand: from newly assimilated organic carbon to respired carbon dioxide. *Oecologia*, **156**, 737-750.

Law BE, Ryan MG, Anthoni PM (1999) Seasonal and annual respiration of a ponderosa pine ecosystem. *Global Change Biology*, **5**, 169-182.

Martin JG, Bolstad PV (2005) Annual soil respiration in broadleaf forests of northern Wisconsin: influence of moisture and site biological, chemical, and physical characteristics. *Biogeochemistry*, **73**, 149.

Massman WJ, Frank JM (2006) Advective transport of CO2 in permeable media induced by atmospheric pressure fluctuations: 2. Observational evidence under snowpacks. *J. Geophys. Res.*, **111**.

Maunoury F, Berveiller D, Lelarge C, Pontailler J-Y, Vanbostal L, Damesin C (2007) Seasonal, daily and diurnal variations in the stable carbon isotope composition of carbon dioxide respired by tree trunks in a deciduous oak forest. *Oecologia*, **151**, 268-279.

McCarthy KA, Johnson RL (1995) Measurement of trichloroethylene diffusion as a function of moisture-content in sections of gravity-drained soil columns. *Journal of Environmental Quality*, **24**, 49-55.

McDowell NG, Bowling DR, Bond BJ, Irvine J, Law BE, Anthoni P, Ehleringer JR (2004) Response of the carbon isotopic content of ecosystem, leaf, and soil respiration to meteorological and physiological driving factors in a *Pinus ponderosa* ecosystem. *Global Biogeochemical Cycles*, **18**.

Midwood AJ, Thornton B, Millard P (2008) Measuring the ^{13}C content of soil-respired CO_2 using a novel open chamber system. *Rapid Communications in Mass Spectrometry*, **22**, 2073-2081.

Millard P, Midwood AJ, Hunt JE, Whitehead D, Boutton TW (2008) Partitioning soil surface CO_2 efflux into autotrophic and heterotrophic components, using natural gradients in soil $\delta^{13}C$ in an undisturnbed savannah soil. *Soil Biology & Biochemistry*, **40**, 1575-1582.

Miller JB, Yaki D, White JWC, Tans PP (1999) Measurement of $^{18}O/^{16}O$ in the soil-atmosphere CO_2 flux. *Global Biogeochemical Cycles*, **13**, 761-774.

Miller M, Palojarvi A, Rangger A, Reeslev M, Kjoller A (1998) The Use of Fluorogenic Substrates To Measure Fungal Presence and Activity in Soil. *Appl. Environ. Microbiol.*, **64**, 613-617.

Mitchell SR, Beven KJ, Freer JE (in press) Multiple sources of predictive uncertainty in modeled estimates of net ecosystem CO_2 exchange. *Ecological Modeling*.

Moldrup P, Olesen T, Schjonning P, Yamaguchi T, Rolston DE (2000) Predicting the Gas Diffusion Coefficient in Undisturbed Soil from Soil Water Characteristics *Soil Sci. Soc. Am. J.*, **64**, 94-100.

Moldrup P, Olesen T, Yamaguchi T, SchjÃ¸nning P, Rolston DE (1999) Modeling Diffusion and Reaction in Soils: Ix. the Buckingham-Burdine-Campbell Equation for Gas Diffusivity in Undisturbed Soil. *Soil Science*, **164**, 542-551.

Mora G, Raich JW (2007) Carbon-isotopic composition of soil-respirated carbon dioxide in static closed chambers at equilibrium. *Rapid Communications in Mass Spectrometry*, **21**, 1866-1870.

Nickerson N, Risk D (2009a) Keeling plots are non-linear in non-steady state diffusive environments. *Geophysical Research Letters*, **36**, doi:10.1029/2008GL036945.

Nickerson N, Risk D (2009b) A numerical evaluation of chamber methodologies used in measuring the $\delta^{13}C$ of soil respiration. *Rapid Communications in Mass Spectrometry*, **23**, 2802-2810.

Nickerson N, Risk D (2009c) Physical Controls on the Isotopic Composition of Soil Respired CO_2. *Journal of Geophysical Research*, **114**, doi:10.1029/2008JG000766.

Ochsner TE, Horton R, Ren T (2001) A New Perspective on Soil Thermal Properties. *Soil Science Society of America Journal*, **65**, 1641-1647.

Ohlsson KEA, Singh B, Holm S, Nordgren A, Lövdahl L, Högberg P (2005) Uncertainties in static closed chamber measurements of the carbon isotopic ratio of soil-respired CO2. *Soil Biology and Biochemistry*, **37**, 2273-2276.

Olsson PA, KJakobsen I, Wallander H (2002) Foraging and resource allocation strategies of mycorrhizal fungi in a patchy environment. In: *Mycorrhizal Ecology.* (eds Van Der Heijden Mga, Sanders Ir) pp Page. Berlin, Spring-Verlag.

Parham JA, Deng SP (2000) Detection, quantification and characterization of glucosaminidase activity in soil. *Soil Biology & Biochemistry,* **32**, 1183-1190.

Pate J, Arthur D (1998) $\delta^{13}C$ analysis of phloem sap carbon: novel means of evaluating seasonal water stress and interpreting carbon isotope signatures of foliage and trunk wood of *Eucalyptus globulus*. *Oecologia,* **117**, 301-311.

Pavelka M, Acosta M, Marek MV, Kutsch W, Janous D (2007) Dependence of the Q_{10} values on the depth on the the soil temperature measuring point. *Plant and Soil*.

Poulenard J, Podwojewski P, Herbillon AJ (2003) Characteristics of non-allophanic Andisols with hydric properies from the Ecudarian páramos. *Geoderma,* **117**, 267-281.

Pumpanen J, Ilvesniemi H, Hari P (2003) A Process-Based Model for Predicting Soil Carbon Dioxide Efflux and Concentration. *Soil Sci Soc Am J,* **67**, 402-413.

Pypker T, Hauck M, Sulzman EW *et al.* (2008) Towards using $\delta^{13}C$ of ecosystem respiration to monitor canopy physiology in complex terrain. *Oecologia,* **158**, 399-410.

Read DJ, Leake JR, Perez-Moreno J (2004) Mycorrhizal fungi as drivers of ecosystem processes in heathland and boreal forest biomes. *Canadian Journal of Botany,* **82**, 1243-1263.

Read DJ, Perez-Moreno J (2003) Mycorrhizas and Nutrient Cycling in Ecosystems--A Journey Towards Relevance? *New Phytologist,* **157**, 475-492.

Reid CPP, Kidd FA, Ekwebelam SA (1983) Nitrogen nutrition, photosynthesis and carbon allocation in ectomycorrhizal pine. *Plant and Soil,* **71**, 415-432.

Risk D, Kellman L (2008) Isotopic fractionation in non-equilibrium diffusive environments. *Geophysical Research Letters,* **35**, L02403-02406.

Risk D, Kellman L, Beltrami H (2002) Carbon dioxide in soil profiles: production and temperature dependence. *Geophysical Research Letters,* **29**.

Riveros-Iregui DA, Emanuel RE, Muth DJ *et al.* (2007) Diurnal hysteresis between soil CO_2 and soil temperature is controlled by soil water content. *Geophysical Research Letters,* **34**.

Rustad LE, Campbell JL, Marion GM *et al.* (2001) A meta-analysis of the response of soil respiraiton, net nitrogen mineralization, and aboveground plant growth to expeirmental ecosystem warming. *Oecologia,* **126**, 543-562.

Ryan MG, Binkley D, Fownes JH, Giardina CP, Senock RS (2004) An experimental test of the causes of forest growth decline with stand age. *Ecological Monographs,* **74**, 393-414.

Ryan MG, Law BE (2005) Interpreting, measuring, and modeling soil respiration. *Biogeochemistry,* **73**, 3.

Rygiewicz PT, Andersen CP (1994) Mycorrhizae alter quality and quantity of carbon allocated below ground. *Nature,* **369**, 58-60.

Savage KE, Davidson EA (2001) Interannual Variation of Soil Respiraiton in Two New England Forests. *Global Biogeochemical Cycles*, **15**, 337-350.

Schimel J, Bennett J (2004) Nitrogen mineralization: challenges of a changing paradigm. *Ecology*, **85**, 591-602.

Schlesinger WH, Andrews JA (2000) Soil respiration and the global carbon cycle. *Biogeochemistry*, **48**, 7-20.

Selosse M-A, Martin F, Le Tacon F (2001) Intraspecific variation in fruiting phenology in an ectomycorrhizal *Lacarria* population under Douglas fir. *Mycological Research*, **105**, 524-531.

Simard SW, Jones MD, Durall DM (2002) Carbon and Nutrient Fluxes Within and Between Mycorrhizal Palnts. In: *Mycorrhizal Ecology*. (eds Van Der Heijden Mga, Sanders Ir) pp Page. Berlin, Springer-Verlag.

Smerdon JE, Beltrami H, Creelman C, Stevens MB (2009) Characterizing land-surface processes: A quantitative analysis using air-ground thermal orbits. *Journal of Geophysical Research*, **114**.

Smith JE, Molina R, Huso MMP, Larsen MJ (2000) Occurrence of *Piloderma* fallax in young, rotation-age, and old-growth stands of Douglas-fir (*Pseudotsuga menziesii*) in the Cascade Range of Oregon, U.S.A. *Canadian Journal of Botany*, **78**, 995-1001.

Staddon PL, Ramsey CB, Ostle N, Ineson P, Fitter AH (2003) Rapid Turnover of Hyphae of Mycorrhizal Fungi Determined by AMS Microanalysis of ^{14}C. *Science*, **300**, 1138-1140.

Subke J-A, Inglima I, Francesca Cotrufo M (2006) Trends and methodological impacts in soil CO_2 efflux partitioning: A metaanalytical review. *Global Change Biology*, **12**, 921-943.

Subke J-A, Vallack HW, Magnusson T, Keel SG, Metcalfe DB, Högberg P, Ineson P (2009) Short-term dynamics of abiotic and biotic soil $^{13}CO_2$ effluxes after *in situ* $^{13}CO_2$ pulse labelling of a boreal pine forest. *New Phytologist*, **183**, 349-357.

Sulzman EW, Brant JB, Bowden RD, Lajtha K (2005) Contribution of aboveground litter, belowground litter, and rhizosphere respiration to total soil CO_2 efflux in an old growth coniferous forest. *Biogeochemistry*, **73**, 231-256.

Susfalk RB, Cheng W, Johnson DW, Walker RF, Verburg P, Fu S (2002) Lateral diffusion and atmospheric CO_2 mixing compromise estimates of rhizosphere respiration in a forest soil. *Canadian Journal of Forest Research*, **32**, 1005-1015.

Talbot JM, Allison SD, Treseder KK (2008) Decomposers in Disguise: Mycorrhizal Fungi as Regulators on Soil C Dynamics in Ecosystems Under Global Change. *Functional Ecology*, **22**, 955-963.

Tang J, Baldocchi DD (2005) Spatial and temporal variation in soil respiration in an oak-grass savanna ecosystem in California and its partitioning into autotrophic and heterotrophic components. *Biogeochemistry*, **73**, 183.

Tang J, Baldocchi DD, Qi Y, Xu L (2003) Assessing soil CO_2 efflux using continuous measurements of CO_2 profiles in soils with small solid-state sensors. *Agricultural and Forest Meteorology*, **118**, 207.

Tang J, Baldocchi DD, Xu L (2005) Tree photosynthesis modulates soil respiration on a diurnal time scale. *Global Change Biology*, **11**, 1298-1304.

Taylor BN, Kuyatt CE (1994) NIST Technical Note 1297: Guidelines for Evaluating and Expressing the Uncertainty of NIST Measurement Results. *National Institute of Standards and Technology, US Dept of Commerce, Technology Administration*.

Tedeschi V, Rey A, Manca G, Valentini R, Jarviss PG, Borghetti M (2006) Soil respiration in a Mediterranean oak forest at different developmental stages after coppicing. *Global Change Biology*, **12**, 110-121.

Treseder KK, Masiello CA, Lansing JL, Allen MF (2004) Species-specific measurements of ectomycorrhizal turnover under N-fertilization: combining isotopic and genetic approaches. *Oecologia*, **138**, 419-425.

Trojanowski J, Haider K, Hüttermann A (1984) Decomposition of ^{14}C-labelled lignin, holocellulose and lignocellulose by mycorrhizal fungi. *Archives of Microbiology*, **139**, 202-206.

Trumbore SE (2006) Carbon respired by terrestrial ecosystems--recent progress and challenges. *Global Change Biology*, **12**, 141-153.

Valentini R, Matteucci G, Dolman AJ (2000) Respiration as the main determinant of carbon balance in European forests. *Nature*, **404**, 861-864.

Vargas R, Allen MF (2008a) Dynamics of Fine Root, Fungal Rhizomorphs, and Soil Respiration in a Mixed Temperate Forest: Integrating Sensors and Observations. *Vadose Zone Journal*, **7**, 1055-1064.

Vargas R, Allen MF (2008b) Environmental controls and the influence of vegetation type, fine roots and rhizomorphs on diel and seasonal variation in soil respiration. *New Phytologist*.

Warmink JA, Nazir R, van Elsas JD (2009) Univeral and species-specific bacterial 'fungiphiles' in the mycospheres of different basidiomycetous fungi. *Environmental Microbiology*, **11**, 300-312.

Werner C, Wegener F, Unger S, Nogués S, Priault P (2009) Short-term dynamics of isotopic composition of leaf-respired CO_2 upon darkening: measurements and implications. *Rapid Communications in Mass Spectrometry*, **23**, 2428-2438.